

ADRENERGIC SIGNALING IN PANCREATIC ISLET  
DEVELOPMENT

by  
Alexis M. Ceasrine

A dissertation submitted to the Johns Hopkins University in conformity with the  
requirements for the degree of Doctor of Philosophy

Baltimore, Maryland  
October 2018

## ABSTRACT

Diabetes mellitus is a disease that has been rapidly increasing in prevalence worldwide, with more than 9% of the world's adult population currently diagnosed, and an additional 4-5% thought to be living with diabetes without a diagnosis. Diabetes is caused by dysregulation of blood glucose homeostasis. A key regulator of blood glucose homeostasis is insulin secretion from  $\beta$ -cells that reside in pancreatic islets of Langerhans. While much is known about the intrinsic factors that control  $\beta$ -cell development, less is known about how the interaction of  $\beta$ -cells with other non-pancreatic cell types controls development and adult function.

Recently, our lab discovered that sympathetic nerves that innervate the pancreas are essential for pancreatic islet development and adult islet function (Borden et al. 2013). These nerves secrete the neurotransmitter norepinephrine, a potent activator of adrenergic signaling. During development, the mouse pancreas expresses all nine of the adrenergic G-protein coupled receptors (GPCRs), including those most responsive to epinephrine, a hormone secreted from the adrenal gland that is distributed throughout the body through the circulatory system. This led us to hypothesize that adrenergic signaling may play a role in instructing endocrine pancreas development, beyond the commonly studied roles in acute, physiological stress responses.

Here, we identify a sex-specific requirement for the  $\beta$ 2-adrenergic receptor (*Adrb2*) in regulating *Vegf-a* production and vascularization during islet development. Loss of *Adrb2* from islet  $\beta$ -cells enhances *Vegf-a* and insulin expression in  $\beta$ -cells, and results in hyper-vascularized islets in neonatal mice, specifically in females. Despite elevated insulin synthesis, adult mutant females, but not males, exhibited glucose intolerance and impaired

glucose-stimulated insulin secretion (GSIS), in part, due to alterations in genes involved in calcium regulation and exocytosis in islets. Metabolic and molecular phenotypes in adult *Adrb2*-deficient mice were fully rescued by the blockade of Vegf-a signaling and correction of islet hyper-vascularization during development. Consistent with a predominant role for *Adrb2* during development, glucose homeostasis was unaffected by adult-specific deletion of *Adrb2*. Together, these findings uncover a negative regulatory pathway that functions in a sex-specific manner during islet formation to control long-term glucose metabolism by restraining excessive vascular growth.

Advisor: Rejji Kuruvilla, Ph.D.

Second Reader: Samer Hattar, Ph.D.

Committee Members: Mark Van Doren, Ph.D.

Samer Hattar, Ph.D.

Michael Parsons, Ph.D.

## PREFACE

Coming into graduate school I didn't know what I wanted to do with a Ph.D., and I didn't truly understand what it would mean to earn one. All I knew is that I had always been good at school, and that a Ph.D. was more school, so I was sure I would be fine. I've never been more wrong about so many things at once! I struggled throughout my Ph.D. more than I have before, and I attribute that to a combination of intellectual and personal challenges far beyond those I imagined I would ever face. I am grateful for the experiences and support that I have had throughout this time. During my time working with Rejji and the others in her lab, I have learned not only a whole host of incredible techniques and skills, but also how to design, perform, analyze, and explain experiments and results to diverse audiences. Rejji brought out the very best in me, whether or not I was up to the challenge, and I appreciate her all the more for it when I think back on how far I've come. She has always been a force to be reckoned with when it comes to promoting her student's best interests, and for that I will always be grateful.

Working in the collaborative environment of the Mouse Tri-Lab has also been incredible to have throughout the course of my Ph.D. The constant exposure to in-depth research vastly outside my own pushed me to dig deeper into a broad range of scientific literature. It also provided a welcoming and enjoyable environment, where I was excited to share my own work without fear of rejection. This environment truly enabled me to stand on my own and be confident in my work. And as I've learned time after time, confidence and a thick skin are requirements for any academic career.

Exploring a subject area somewhat outside the realm of the main focus of the lab can be challenging at times, but I was fortunate enough to learn from a dedicated graduate

student, Jessica Houtz. Jessica brought me ‘up to speed’ faster than I thought possible. She had high expectations for me, but she never let me fail. She was always capable of pushing me just to the limit of my knowledge before stepping in to help, and I am forever grateful to her for what she taught me – not only scientifically but also about mentorship. I was also fortunate to be able to mentor a variety of students, from high schoolers to Ph.D. candidates, each of whom I learned something from.

Another group of people that I need to thank is my thesis committee, Mark Van Doren Samer Hattar, and Mike Parsons. Without their support, I would not have been confident in my abilities. Standing in a room where the combined scientific knowledge far exceeds my age is daunting, to say the least, and I hold the opinions of my committee in high regard. They were always fair and invested in my success; without them I would not be as analytical and dedicated to a career in academia as I am. To all the people who assisted me throughout my Ph.D. journey, I am grateful to have your support, and I thank you for believing in me.

## TABLE OF CONTENTS

<b>ABSTRACT.....</b>	<b>ii</b>
<b>PREFACE.....</b>	<b>iv</b>
<b>TABLE OF CONTENTS.....</b>	<b>vi</b>
<b>LIST OF TABLES.....</b>	<b>viii</b>
<b>LIST OF FIGURES.....</b>	<b>ix</b>
<b>LIST OF ABBREVIATIONS.....</b>	<b>xii</b>
<b>CHAPTER 1: INTRODUCTION.....</b>	<b>1</b>
<b>CHAPTER 2: <math>\beta</math>-ADRENERGIC SIGNALING CONTROLS FEMALE ISLET VASCULARIZATION.....</b>	<b>17</b>
INTRODUCTION.....	18
RESULTS.....	23
DISCUSSION.....	40
METHODS.....	42
<b>CHAPTER 3: NEONATAL <math>\beta</math>-ADRENERGIC SIGNALING IS NECESSARY FOR FEMALE ISLET FUNCTION.....</b>	<b>47</b>
INTRODUCTION.....	48
RESULTS.....	55
DISCUSSION.....	85
METHODS.....	89
<b>CHAPTER 4: DEVELOPMENTAL ADBR2-MEDIATED VASCULAR REPRESSION IS REQUIRED FOR MATURE ISLET FUNCTION.....</b>	<b>97</b>
INTRODUCTION.....	98
RESULTS.....	100
DISCUSSION.....	107
METHODS.....	109

<b>CHAPTER 5: TAMOXIFEN AFFECTS GLUCOSE TOLERANCE IN A SEX, STRAIN, AND DELIVERY DEPENDENT MANNER.....</b>	<b>114</b>
INTRODUCTION.....	115
RESULTS.....	119
DISCUSSION.....	134
METHODS.....	136
<b>CLOSING REMARKS.....</b>	<b>138</b>
<b>REFERENCES.....</b>	<b>144</b>
<b>CURRICULUM VITAE.....</b>	<b>170</b>

## LIST OF TABLES

Table 2. Primer sets used in Chapter 3 (and 4).....	83
---	----



## LIST OF FIGURES

### Chapter 2:

Figure 2.1. Adrenergic receptor expression in the pancreas.....	30
Figure 2.2. Analysis of <i>Adrb2</i> cKO mice at postnatal day 6 (P6) .....	31
Figure 2.3. Female <i>Adrb2</i> cKO mice have increased insulin biosynthesis.....	32
Figure 2.4. Female <i>Adrb2</i> cKO islets have excess vasculature.....	34
Figure 2.5. Analysis of pancreatic structures in <i>Adrb2</i> cKO mice at P6.....	36
Figure 2.6. Islet hyper-vascularization in female <i>Adrb2</i> cKO islets is likely due to excess Vegf-a signaling.....	38

### Chapter 3:

Figure 3.1. Global <i>Adrb2</i> knockout mice have slightly dampened glucose response..	64
Figure 3.2. Global loss of <i>Adrb1</i> does not affect glucose tolerance.....	66
Figure 3.3. Developmental Vegf-a dependent vascular changes persist in <i>Adrb2</i> cKO adults.....	67
Figure 3.4. Glucose tolerance of 2-month old <i>Adrb2</i> cKO mice.....	68
Figure 3.5. Insulin sensitivity is unaffected by pancreatic <i>Adrb2</i> loss.....	70
Figure 3.6. Insulin and glucagon levels in female and male <i>Adrb2</i> cKO mice.....	71
Figure 3.7. Insulin secretion is impaired in female <i>Adrb2</i> cKO mice.....	73
Figure 3.8. Insulin secretion is perturbed downstream of potassium signaling in female <i>Adrb2</i> cKO islets.....	75
Figure 3.9. Defects in calcium signaling in <i>Adrb2</i> cKO islets.....	76

**Chapter 4:**

Figure 4.1. Vegf pathway inactivation ameliorates developmental defects in *Adrb2* cKO mice.....102

Figure 4.2. Developmental Vegf pathway inactivation ameliorates adult functional defects in *Adrb2* cKO mice. ....104

Figure 4.3. Developmental Vegf pathway inactivation ameliorates adult transcriptional defects in *Adrb2* cKO islets. ....106

**Chapter 5:**

Figure 5.1. I.P. Tamoxifen administration does not affect weight in mice.....123

Figure 5.2. I.P. Tamoxifen administration improves glucose tolerance in mice one week after administration.....125

Figure 5.3. I.P. Tamoxifen administration affects blood glucose levels in a strain-dependent manner.....127

Figure 5.4. Improved glucose tolerance in I.P. tamoxifen injected mice persists three weeks after administration.....129

Figure 5.5. Insulin sensitivity is unaffected by I.P. tamoxifen administration.....131

Figure 5.6. Oral tamoxifen administration does not affect glucose tolerance.....132

**Concluding Remarks:**

Figure 6. *Adrb2* limits vascular growth in pancreatic islets during development to control islet function.....142

## LIST OF ABBREVIATIONS

GPCR (G-protein coupled receptor)  
ATP (adenosine triphosphate)  
NADH (nicotinamide adenine dinucleotide)  
NADPH (nicotinamide adenine dinucleotide phosphate)  
FADH<sub>2</sub> (flavin adenine dinucleotide)  
TCA (tricarboxylic acid)  
PDH (pyruvate dehydrogenase)  
ETC (electron transport chain)  
ADP (adenosine diphosphate)  
PPP (pentose phosphate pathway)  
G6P (glucose-6-phosphate)  
1,3 BPG (1,3-bisphosphoglycerate)  
3PG (3-phosphoglycerate)  
F1P (fructose-1-phosphate)  
DHAP (dihydroxyacetone phosphate)  
UDP (uridine diphosphate)  
G1P (glucose-1-phosphate)  
CoA (coenzyme A)  
vLDL (very low-density lipoprotein)  
PEP (phosphoenolpyruvate)  
PLC (phospholipase C)  
PIP2 (phosphatidylinositol 4,5-bisphosphate)  
DAG (diacylglycerol)  
IP3 (inositol triphosphate)  
PKC (protein kinase C)

cAMP (cyclic adenosine monophosphate)  
PKA (protein kinase A)  
Adrb2 ( $\beta$ 2-adrenergic receptor)  
Pdx (Pancreatic and Duodenal Homeobox 1)  
Shh (sonic hedgehog)  
FGF2 (fibroblast growth factor 2)  
Ptf1a (pancreas specific transcription factor 1)  
Hnf6 (hepatocyte nuclear factor 6)  
bHLH (basic helix-loop-helix)  
Ngn3 (neurogenin 3)  
Vegf (vascular endothelial growth factor)  
GSIS (Glucose-stimulated insulin secretion)  
FACS (Fluorescence-Activated Cell Sorting)  
DBH (dolichos biflorus agglutinin)  
SMA (smooth muscle actin)  
TH (Tyrosine Hydroxylase)  
NF (neurofilament)  
WGA (wheat germ agglutinin)  
TEM (transmission electron microscopy)  
VDCC (voltage-dependent  $\text{Ca}^{2+}$  channels)  
RRP (readily releasable pool)  
NGF (nerve growth factor)  
TrkA (tropomyosin receptor kinase A)  
GIP (Gastric Inhibitory Polypeptide/ glucose-dependent insulinotropic polypeptide)  
GLP-1 (Glucagon-Like Peptide-1)  
Epac2 (exchange protein directly activated by cAMP 2)  
NCAM (neural cell adhesion molecule)

Cx36 (connexin36)

SERM (selective estrogen receptor modulator)

TMX (tamoxifen)

# **CHAPTER 1: INTRODUCTION**

Regulation of all metabolic pathways is crucial to an organism's growth and survival. Disruption of even a single pathway results in a disease state. One commonly known metabolic disorder is diabetes mellitus, a condition in which the affected individual can no longer maintain physiological glucose levels. The prevalence of diabetes has been rapidly increasing world-wide, and it is estimated that one in eleven people are currently living with diabetes, but half of the diabetic population is undiagnosed at this point (IDF, 2017). If the prevalence continues to increase at this rate, then by 2040 it is expected that 10% of the world population will be living with diabetes (IDF, 2017). There are three main categories of diabetes, known as type I, type II, and gestational. While a variety of tissues contribute to metabolic homeostasis, the pancreatic islets of Langerhans are key contributors to glucose regulation. Islets only comprise approximately 2-10% of the total pancreatic mass but house a variety of endocrine cell types responsible for the regulated secretion of hormones to precisely balance blood glucose levels. The primary cell type within islets are  $\beta$ -cells, which secrete the hormone insulin. Insulin secretion is stimulated by high glucose conditions and signals to the rest of the body to remove glucose from the bloodstream. Loss of insulin production or secretion, as seen in diabetes, results in uncontrolled high blood sugar levels. Type I diabetes is an autoimmune disorder generally seen in juveniles that results in the targeted destruction of insulin producing  $\beta$ -cells. The causes of type I diabetes are unclear, though it is thought to be a result of both genetic and environmental factors (IDF, 2017). Type II diabetes, the most prevalent form of diabetes, is a result of ineffective insulin production or secretion from  $\beta$ -cells, or the development of insulin resistance after a time of excess insulin presence in the blood. While the causes of type II diabetes are also thought to be a combination of genetic and environmental factors,

there is a strong association with obesity (as a result of an unhealthy diet and lack of exercise). However, not all individuals with type II diabetes are overweight (IDF, 2017). Gestational diabetes only occurs during pregnancy, and often goes away within the first few months after giving birth. Placental hormones cause increased blood glucose levels, and usually enough insulin can be produced to compensate, but not always. Having gestational diabetes does, however, increase the risk of the mother developing type II diabetes later in life (IDF, 2017). Because islets are such a key contributor to glucose homeostasis, and their loss results in metabolic dysregulation, it is critical to understand how they develop.

Untreated diabetes can cause complications that affect nearly every organ in the human body, causing a multitude of symptoms such as cardiovascular disease and blindness (Chowdhury, Shaho and Moolla 2014). Cardiovascular disease results from sustained elevated blood glucose levels, which can result in the thickening and narrowing of blood vessels due to fatty acid deposit and build-up. Blindness results from sorbitol buildup, which causes osmotic changes in retinal tissues leading to the degeneration of lens fibers (Pollreis and Schmidt-Erfurth 2010). However, these symptoms can generally be controlled by medical intervention. The understanding of the defects that result in diabetes led to the present-day treatment of insulin injections, which can alleviate and even prevent the aforementioned conditions. However, this treatment is not ideal, because natural insulin levels oscillate every 3-9 minutes (Goodner et al, 1977; Hussain, 2014), and current insulin pumps are not capable of mimicking that tight regulation. Type I diabetics require insulin therapy for life, but type II diabetics can usually manage their disease with a combination of healthy diet and exercise, with the addition of insulin therapy and medications to lower



their blood sugar if needed. Other therapies being explored include islet transplants, in which islets are collected from a previously healthy donor (or multiple donors) and transplanted into a diabetic patient. Trials have seen preliminary successes, but there are still many problems with this treatment, including failure of transplanted islets to revascularize, and immune rejection of the transplanted tissue. Understanding how diabetes develops, and therefore how pancreatic islets develop, is crucial for our understanding of the disease, so that in the future we can develop more effective therapies and preventative measures.

### **Energy Extraction from Nutritional Fuel Substrates**

All organisms, from unicellular microbes to humans, rely on various metabolic pathways to grow and survive. Cells have adapted complex regulatory networks and specialized enzymes to extract energy from various substrates. Metabolic processes depend on the consumption of nutrients such as glucose, the main energy-providing molecule for the brain, and fatty acids, the main energy-providing molecule for the heart (Berg, Tymoczko and Stryer 2002). The catabolism, or breakdown, of these macromolecules releases high-energy molecules, such as adenosine triphosphate (ATP), nicotinamide adenine dinucleotide (NADH), nicotinamide adenine dinucleotide phosphate (NADPH), and flavin adenine dinucleotide (FADH<sub>2</sub>). These high-energy molecules are used for many crucial cellular processes, such as maintaining ion gradients, moving motor proteins, and powering anabolic reactions, or those that construct molecules from smaller units. Familiarization with the various metabolic pathways involved in energy generation and

expenditure is important for understanding the underlying mechanisms of metabolic diseases.

### *Catabolism of Nutrients - Carbohydrate Metabolism*

The primary source of an organism's nutritional energy is derived from carbohydrates, such as starch, sucrose, and lactose. These molecules provide approximately 4.7 kilocalories per gram (kcal/g) of energy and comprise almost 50% of all calories in the average human diet (Hussain, 2014). These complex carbohydrates must be broken down into monosaccharide constituents, such as glucose, the basic carbohydrate unit, before they can be absorbed by the intestine and metabolized. During a normal 24-hour day, the average human will consume between 1800 and 2000 calories during intermittent cycles of feeding, such as a meal or snack, and fasting, such as six to eight hours of sleep (Hussain, 2014). For a metabolically healthy adult, the average eight-hour fasting blood glucose levels are between 70 and 100 milligrams per deciliter (mg/dL). After a meal, complex carbohydrates will be broken down to glucose, which will enter the blood stream through the intestine, causing blood glucose levels to spike. Two hours after the meal, blood glucose levels will fall to below 140 mg/dL (Hussain, 2014).

### *Glucose – Glycolysis*

The initial increase of blood glucose levels in the body after a meal acts as an extracellular signal that is sensed by pancreatic  $\beta$ -cells. These highly specialized endocrine cells respond to a glucose threshold by secreting a hormone, insulin, into the blood stream. Insulin is subsequently carried to target tissues (such as the liver, adipose tissue, and skeletal muscle), where it promotes glucose uptake into cells through a glucose transporter,

reducing blood glucose levels. Phosphorylation traps glucose within a cell where it is broken down in the cytoplasm from a six-carbon sugar into two molecules of pyruvate through a ten-step process known as glycolysis. The first half of glycolysis requires the input of two ATP molecules, while the second half of glycolysis produces two NADH, and four ATP molecules. This results in a net gain of two ATP, two NADH, and two pyruvate per glucose molecule.

Pyruvate from glycolysis can be further metabolized in a variety of ways depending on the metabolic demands of the specific cell. Under aerobic conditions, pyruvate can enter the tricarboxylic acid (TCA) cycle, which is also known as the citric acid cycle, or the Krebs's cycle. Pyruvate will be transported into the mitochondria where it will be converted to acetyl-CoA via pyruvate dehydrogenase (PDH), producing one NADH per pyruvate (two NADH per glucose molecule). Acetyl-CoA is condensed with oxaloacetate, the last product of the TCA cycle, to form citrate. As citrate is metabolized through the TCA cycle back to oxaloacetate, three NADH, one ATP, and one FADH<sub>2</sub> are produced. This occurs twice per original glucose molecule, giving a total of six NADH, two ATP, and two FADH<sub>2</sub>.

When blood glucose levels fall too low, pyruvate can be used by hepatocytes to create glucose through gluconeogenesis. During times when energy is required immediately, such as exercises that require fast muscle responses during anaerobic conditions, pyruvate will be converted to lactate, via lactate dehydrogenase, in order to replenish cellular NAD<sup>+</sup> supplies. This supply is necessary for glycolysis to continue so that energy may be generated rapidly, without continuing through the TCA cycle and electron transport chain (ETC).

NADH and FADH<sub>2</sub> generated from the TCA cycle move to the ETC, where electrons are transferred through four enzyme complexes found in the inner mitochondrial membrane to O<sub>2</sub>, the final electron acceptor. As the electrons are transferred, complexes I, III, and IV pump protons from the mitochondrial matrix to the intermembrane space. The continual pumping of these protons creates a strong proton gradient that powers the enzyme ATP synthase, which is located in the inner mitochondrial membrane. ATP synthase uses three protons from the gradient to convert adenosine diphosphate (ADP) and free phosphates into ATP. NADH oxidation contributes to the ETC by donating a pair of electrons used in complex I in the ETC. From this, one NADH will generate three ATP molecules. FADH<sub>2</sub> oxidation contributes to the ETC later, at complex II, bypassing complex I, resulting in the production of only two ATP per FADH<sub>2</sub> molecule. In total, one molecule of glucose that is metabolized through glycolysis, pyruvate oxidation, and subsequently the TCA cycle will produce 38 ATP, far more than glycolysis alone.

#### *Glucose – Pentose Phosphate Pathway*

Although the majority of glucose metabolism occurs through glycolysis, other metabolic pathways also utilize glucose. One example of this is the pentose phosphate pathway (PPP), also known as the hexose monophosphate shunt or the phosphogluconate pathway, which exists parallel to glycolysis. Both pathways share intermediates, and both are located in the cytoplasm, allowing for exchange of intermediates between pathways depending on the metabolic needs of the cell. The PPP shunt originates with glucose-6-phosphate (G6P), a glycolytic intermediate. The oxidation of G6P produces the pentose ribulose-5-phosphate. The series of reactions, the oxidative phase of the PPP, are highly regulated and primarily responsible for producing NADPH, which provides reducing

equivalents for biosynthetic reactions (Hussain, 2014; Wamelink, Struys and Jakobs 2008). Some of these biosynthetic reactions take place more frequently in specialized cell types that have a higher need for NADPH. Adipocytes, for example, shunt up to 50% of their glucose through the PPP to obtain enough NADPH for fatty acid and sterol synthesis. Other cell types that have a high demand for NADPH include hepatocytes and erythrocytes, which shunt up to 10% of their glucose through the PPP. In contrast, skeletal muscle cells use ATP for contraction and therefore primarily metabolize glucose through glycolysis, and barely utilize the PPP.

The second part of the PPP is non-oxidative and begins with the isomerization of ribulose-5-phosphate to ribose-5-phosphate. Ribose-5-phosphate is used by rapidly dividing cells, such as skin cells or tumor cells, to synthesize nucleotides and coenzymes (Nelson and Cox 2008). Each G6P molecule that is oxidized by G6P-dehydrogenase to ribulose-5-phosphate (and subsequently isomerized to ribose-5-phosphate), will produce two NADPH, two CO<sub>2</sub>, and two H<sup>+</sup>. This reaction provides both NADPH for biosynthetic reactions and ribose-5-phosphate for nucleotide synthesis. Some cells, such as hepatocytes and adipocytes, which have high levels of fatty acid synthesis, have more of a need for NADPH, and therefore require less ribose-5-phosphate. These cells recycle the ribose-5-phosphate produced in the oxidative phase into G6P, which then re-enters the oxidative phase of the PPP and leads to more NADPH production. Ribose-5-phosphate epimerase can also generate xylulose-5-phosphate in a reversible reaction. Transketolase, an enzyme unique to the PPP, can then catalyze the condensation of xylulose-5-phosphate and ribose-5-phosphate to form glyceraldehyde-3-phosphate, a glycolytic intermediate, and sedoheptulose-7-phosphate. Glyceraldehyde-3-phosphate can enter glycolysis, and both of

these intermediates can be recycled back to G6P (Tozzi et al. 2006). In total, this pathway is not an ATP producing pathway, but the oxidation of each glucose molecule results in a gain of two NADPH.

#### *Glucose – 2,3 Diphosphoglycerate Pathway*

Another metabolic detour from glycolysis is the 2,3 diphosphoglycerate pathway, which is common in red blood cells (erythrocytes). The 2,3 diphosphoglycerate pathway is a single-intermediate detour around the first ATP-producing step of glycolysis, the conversion of 1,3-bisphosphoglycerate (1,3 BPG) to 3-phosphoglycerate (3PG). In the 2,3 diphosphoglycerate pathway, 1,3 BPG is isomerized to 2,3 BPG by diphosphoglycerate isomerase. After isomerization, 2,3 BPG subsequently binds to hemoglobin and reduces its affinity for oxygen. While this mechanism is crucial because it allows for the release of oxygen to tissues, it is important that cells be economic with their use of it. Producing and maintaining a high concentration of 2,3 BPG is energetically expensive, because it involves the loss of an ATP from glycolysis. Therefore, it is unsurprising that cells carefully regulate the production of 2,3 BPG (Bunn 1971).

#### *Alternative Sugars – Sorbitol*

Although glucose is the major carbohydrate unit responsible for energy production throughout the body, other sugars can also be metabolized by certain tissues. One example of this is sorbitol. Because the enzyme kinetics regulating the conversion of glucose to G6P by hexokinase ( $K_m$  0.1mM) are much more favorable than the conversion of glucose to sorbitol by aldose reductase ( $K_m$  150mM) (Nelson and Cox 2008, Gabbay and Tze 1972), sorbitol is rarely made by the human body. In a disease state, however, where an

individual's blood sugar levels are elevated, aldose reductase will reduce glucose to sorbitol at the expense of one NADPH molecule. In tissues that also contain sorbitol dehydrogenase, sorbitol can be further metabolized to fructose by sorbitol dehydrogenase, producing one NADH. Some tissues, such as the retina, have aldose reductase but not sorbitol dehydrogenase. This can lead to a toxic buildup of sorbitol when an individual's blood sugar levels are constantly high, thus causing retinal damage (Guo et al. 2014). In tissues that do have sorbitol dehydrogenase, the further metabolism of sorbitol to fructose can be beneficial, because fructose can be phosphorylated by hexokinase and enter glycolysis.

#### *Alternative Sugars - Fructose*

Fructose has received much attention recently due to its possible contribution to obesity. However, fructose is common in a healthy diet, as it is found in most fruits and some vegetables (Laughlin 2014). Fructose enters the bloodstream from the gut, and the majority of its metabolism takes place in the liver, where it is converted in the cytoplasm to fructose-1-phosphate (F1P) by fructokinase. F1P is subsequently metabolized to dihydroxyacetone phosphate (DHAP), a glycolytic intermediate, and glyceraldehyde by F1P aldolase, thus bypassing the main regulator of glycolysis, phosphofructokinase-1. As such, a fructose-rich diet can lead to metabolic consequences, such as increased glycolysis without regulation (Hussain, 2014, Laughlin 2014). In cells that do not express fructokinase, such as adipocytes, fructose can be converted by hexokinase to fructose-6-phosphate (F6P), which then enters glycolysis.

### *Alternative Sugars – Galactose*

Galactose is another sugar that is regularly metabolized by the body. It is commonly found in the human diet from milk products. Galactose is converted by galactokinase to galactose-1-phosphate. A transferase (galactose-1-phosphate uridyl transferase) removes the phosphate from galactose-1-phosphate and transfers it to uridine diphosphate-glucose (UDP-glucose) while also transferring the UDP from UDP-glucose to galactose. This reaction releases glucose-1-phosphate (G1P) which is converted to G6P by phosphoglucomutase. G6P then enters the glycolytic pathway. An epimerase converts UDP-galactose back to UDP-glucose, ready for the next galactose-phosphate molecule to be metabolized.

### **Pancreas Development and Specification**

In the mouse, pancreatic specification and development begins approximately 8 days after conception (e8). The pancreatic lineage, marked by expression of Pancreatic and Duodenal Homeobox 1 (Pdx1), is derived from the endoderm cell layer, first evidenced by a condensation of the mesenchyme by the dorsal gut tube. Subsequent evagination of the endoderm into this mesenchyme forms the dorsal pancreatic bud. Approximately 12 hours later in, the ventral pancreatic bud begins to form from evagination of the hepatic/biliary bud. While this process is morphologically similar to that of the dorsal pancreas, the molecular mechanisms promoting ventral pancreas development are distinct (Gittes 2009).

The dorsal pancreatic bud, which is initially in contact with the notochord, is marked by an exclusion of sonic hedgehog (Shh) signaling (Apelqvist et al. 1997). This



exclusion is due to activity of the notochord-derived factors Fibroblast Growth Factor 2 (FGF2) and activin  $\beta$ B. Interestingly, exogenous expression of Shh can override the pancreas-inducing effect of activin  $\beta$ B, suggesting that Shh may be an anti-pancreatic factor, rather than just a marker of non-pancreatic endoderm (Edlund 1998; Edlund 1999).

The ventral pancreas forms from ventral endoderm that is never in contact with the notochord. FGF signaling from the cardiac mesenchyme promotes liver differentiation from the ventral endoderm, while lack of cardiac mesenchyme and FGF signaling promotes the default ventral pancreatic fate (Deutsch et al. 2001). Between embryonic days 12 and 13 in the mouse, the dorsal and ventral pancreatic buds fuse as a result of gut rotation and dorsal bud elongation.

While a few endocrine cells are seen early on (e10), endocrine cell determination and proliferation primarily begin after pancreatic bud fusion, in what is termed the secondary transition (Bernardo, Hay and Docherty 2008). The decision to become endocrine or exocrine pancreas is primarily controlled by Notch signaling (Apelqvist et al. 1999). The exocrine pancreas, comprised of ducts and acinar cells, is formed by positive Notch signaling. The acinar cell fate is promoted through Notch-controlled expression of pancreas specific transcription factor 1 (Ptf1a). Ductal cells initially follow the endocrine cell lineage, but Notch activation as well as expression of the transcription factor hepatocyte nuclear factor 6 (Hnf6) in a subset of cells destined for endocrine fate (Pax4 positive) shunts cells into a ductal fate instead of an endocrine one (Greenwood et al. 2007, Murtaugh 2007).

Endocrine cell differentiation is also controlled by Notch signaling, with Notch inhibiting the endocrine promoting basic helix-loop-helix (bHLH) transcription factor

neurogenin 3 (Ngn3). Downregulation of Notch signaling allows for high expression of Ngn3, which promotes a generic endocrine cell fate. Following Ngn3 expression, a variety of transcription factors control the specific lineage of the endocrine cells. There are five endocrine cell types, glucagon expressing  $\alpha$ -cells, insulin expressing  $\beta$ -cells, somatostatin expressing  $\delta$ -cells, ghrelin expressing  $\epsilon$ -cells, and pancreatic polypeptide expressing PP cells. The first endocrine cells to develop are glucagon positive  $\alpha$ -cells.

After the secondary transition period, endocrine cell clusters begin to form near the ductal epithelium (where these lineages are born). There is some debate in the field as to whether islets coalesce from migration of individual endocrine cells, or whether large clusters of endocrine cells are born at the same place, replicate, and then fission occurs to form unique islet clusters (Jo et al. 2011, Herrera et al. 1991). In either case, in mice the resulting islets are organized into a core of insulin producing  $\beta$ -cells surrounded by a mantle of glucagon producing  $\alpha$ -cells. The remaining endocrine cell types are interspersed throughout the periphery of the islet. In humans, developing islets are morphologically similar to mouse islets, but adult human islets lose the mantle of glucagon cells, and all of the endocrine cell types are instead randomly distributed throughout the islet (Cabrera et al, 2006). Despite these noted differences in islet organization between species, it is generally accepted that islet architecture is developmentally programmed to optimize  $\beta$ -cell- $\beta$ -cell interactions as well as  $\beta$ -cell-endothelial cell interactions, and is essential for mature islet insulin secretion (Halban et al. 1982, Steiner et al. 2010). Disruption of the production or secretion of insulin from  $\beta$ -cells, or a loss in effective insulin response in insulin target tissues results in diabetes, a disease affecting millions of people worldwide with rapidly increasing prevalence (Guariguata et al. 2014). Additionally, perturbation of

islet architecture has also been associated with this disease state (Gepts and Lecompte 1981).

### **Tissue-tissue interactions during organogenesis**

#### *Contribution of sympathetic nerves to pancreas development*

Tissue-tissue interactions during development have also been shown to be essential for pancreas development (Lammert et al, 2001; Borden et al, 2013). A previous study from our lab has demonstrated the necessity of sympathetic innervation in endocrine pancreas development (Borden et al. 2013). Loss of sympathetic innervation during development, but not adulthood, results in impaired endocrine cell differentiation and organization. As  $\beta$ -cell maturation and  $\beta$ -cell- $\beta$ -cell contacts are required for effective glucose-stimulated insulin secretion (GSIS), loss of developmental sympathetic innervation also results in ineffective islet function in mature animals. Furthermore, pharmacological blockade of  $\beta$ -adrenergic signaling during development phenocopied the effects seen following sympathetic denervation, suggesting that the role sympathetic neurons play in islet development is through adrenergic signaling.

#### *Contribution of the vasculature to pancreas development*

Another tissue that contributes significantly to pancreas development is the vascular system. A dense vascular network is set up early during neonatal development (Johansson et al., 2006a), and plays an instructive role by promoting endocrine cell fates while inhibiting exocrine cell fates (Magenheim et al., 2011; Pierreux et al., 2010; Sand et al., 2011). As the pancreas matures, the vasculature is skewed towards islets, with vessel

density being approximately five times as concentrated within islets compared to exocrine tissue (Bonner-Weir and Orci 1982, Konstantinova and Lammert 2004, Brissova et al. 2006, Murakami et al. 1997, Vetterlein, Petho and Schmidt 1987). This is due to  $\beta$ -cell secretion of vascular mitogens, particularly vascular endothelial growth factor-A (Vegf-a), which promotes dense intra-islet vascularization (Bergers et al., 2000; Brissova et al., 2006; Christofori et al., 1995; Inoue et al., 2002). During development the primary source of Vegf-a is endocrine precursor cells, though Vegf-a production is thought to be restricted to  $\beta$ -cells during early neonatal stages (Reinert et al, 2014). Recruitment of endothelial cells by Vegf-a is likely through VEGFR-2 (KDR or Flk1), the primary Vegf-a receptor expressed in intra-islet endothelial cells (Brissova et al., 2006; Kim et al., 2011). This recruitment results in a signaling niche between islet  $\beta$ -cells and intra-islet endothelial cells. Signaling from endothelial cells through basement membrane proteins (such as laminins) has been shown to influence  $\beta$ -cell proliferation and insulin biosynthesis (Nikolova et al, 2006). In mice, hypo- or hyper-vascularization of newly formed islets by  $\beta$ -cell-specific deletion (Brissova et al., 2006) or over-expression of Vegf-a (Cai et al., 2012) elicit detrimental effects on  $\beta$ -cell mass, insulin secretion, and glucose tolerance, suggesting that Vegf-a levels in  $\beta$ -cells must be maintained within a narrow range. Inactivation of Vegf-a and subsequent islet hypo-vascularization in adult islets, however, did not perturb islet mass and insulin secretion and elicited only modest elevations in blood glucose (D'Hoker et al., 2013; Reinert et al., 2013). Together, these studies imply that the influence of the intra-islet vasculature and Vegf-a levels on islet morphology and function is predominantly exerted during development. Of note,  $\beta$ -cell maturation, which is loosely defined by the acquisition of mature  $\beta$ -cell markers, such as Glut2, and the loss of immature  $\beta$ -cell

markers, such as Neuropeptide Y (NPY), overlaps with the developmental timing of islet vascularization. This suggests that islet vascularization may contribute to islet maturation. However, the factors modulating the precise control of  $\beta$ -cell Vegf-a expression, and the link between early islet vascular patterning and later metabolic functions, have remained poorly defined.

Here, we identify a pancreas-specific requirement for the  $\beta$ 2-adrenergic receptor (Adrb2) in controlling glucose homeostasis by suppressing Vegf-a production in  $\beta$ -cells and limiting vascular growth in islets during development. Pancreas-specific loss of Adrb2 results in glucose intolerance and impaired glucose-stimulated insulin secretion, only in female mice. The metabolic defects were recapitulated by Adrb2 deletion from neonatal, but not adult,  $\beta$ -cells, supporting a role for  $\beta$ -cell Adrb2 during development. We provide evidence that Adrb2 acts in  $\beta$ -cells to suppress Vegf-a expression and thus restrict islet vascular growth, which in turn, influences insulin synthesis and secretion. Remarkably, developmental blockade of Vegf-a signaling corrects islet hyper-vascularization in neonatal mice and rescues glucose intolerance and insulin secretion defects in adult Adrb2 mutant mice. These findings reveal Adrb2 as a negative regulator that controls islet development and glucose metabolism by influencing bi-directional communication between islet  $\beta$ -cells and the vasculature.

**CHAPTER 2:  $\beta$ 2-ADRENERGIC  
SIGNALING CONTROLS FEMALE  
ISLET VASCULARIZATION**

# INTRODUCTION

## Adrenergic Signaling

Adrenergic receptors are prototypical G-protein coupled receptors (GPCRs) that respond to adrenal gland-derived epinephrine and nerve-derived norepinephrine to mediate a variety of well-documented, acute physiological responses to stress in adult animals. The activation of the adrenergic system and the following physiological responses are commonly referred to as the “fight or flight” response. The purpose of the fight or flight response is to prepare an organism for a physical challenge. As such, many adrenergic functions are metabolic and serve to increase the availability of circulating glucose to provide energy for the organism. Various organs, such as the liver, pancreas, and adipose tissue respond to increased circulating catecholamine levels (by activation of adrenergic receptors) to (1) increase liver gluconeogenesis, (2) inhibit pancreatic insulin secretion, and (3) increase lipolysis.

The adrenergic receptors are clustered into two main groups,  $\alpha$  and  $\beta$ , based on their G-protein coupling. The three  $\beta$ -adrenergic receptors ( $\beta_1$ ,  $\beta_2$ , and  $\beta_3$ ) are canonically coupled to stimulatory G proteins ( $G_s$ ), whereas, the  $\alpha$ -adrenergic receptors are further divided into  $\alpha_1$  ( $\alpha_{1a}$ ,  $\alpha_{1b}$ , and  $\alpha_{1d}$ ) and  $\alpha_2$  ( $\alpha_{2a}$ ,  $\alpha_{2b}$ , and  $\alpha_{2c}$ ) receptors, which couple with  $G_q$  and  $G_i$  proteins, respectively (Molinoff, 1984). Norepinephrine is the primary ligand for the  $\alpha$ -adrenergic receptors, while epinephrine is the primary ligand for the  $\beta$ -adrenergic receptors. Either ligand can, however, signal through the other class, just with lower affinities;  $\beta$ -adrenergic receptors have approximately 100-fold higher affinity for epinephrine versus norepinephrine (Molinoff, 1984).

Canonical  $\alpha$ 1-adrenergic signaling primarily results in contraction of smooth muscle cells (Perez, 2006). This occurs through activation of phospholipase C (PLC) via Gq proteins, resulting in subsequent cleavage of phosphatidylinositol 4,5-bisphosphate (PIP2) into diacylglycerol (DAG) and the temporary intermediate inositol 1,2-cyclic phosphodiester, which is rapidly hydrolyzed to inositol triphosphate (IP3). DAG remains at the membrane where it acts as a second messenger to activate protein kinase C (PKC), while IP3 travels through the cytosol (to the endoplasmic/sarcoplasmic reticulum) to open IP3-dependent calcium channels, thus resulting in increased intracellular calcium levels. This results in a variety of signaling outcomes depending on the cell type, such as further PKC activation or smooth muscle cell contraction (Perez, 2006). PKC activation additionally promotes smooth muscle cell contraction, as well as glycogenolysis and gluconeogenesis, which both serve to increase available glucose as previously described.

Canonical  $\alpha$ 2-adrenergic signaling results in a variety of physiological responses in both the nervous system and peripheral tissues. In the nervous system, activation of  $\alpha$ 2-adrenergic signaling results in negative feedback of norepinephrine secretion in presynaptic sympathetic nerve terminals. This occurs through stimulation of G-protein gated potassium ( $K^+$ ) channels that hyperpolarize the neuron, thus inhibiting secretion (Perez, 2006). In peripheral tissues,  $\alpha$ 2-adrenergic activation results in a variety of metabolic functions, such as decreased insulin secretion from pancreatic  $\beta$ -cells, increased glucagon secretion from pancreatic  $\alpha$ -cells, inhibition of lipolysis in adipose tissue, and inhibition of glycogen breakdown. This occurs through  $G_i$  protein inhibition of the production of the second messenger, cyclic adenosine monophosphate (cAMP). Inhibition of cAMP production occurs when the  $\alpha$ -subunit of a  $G_i$  protein associates with and inhibits



adenylyl cyclase (AC), the enzyme responsible for cAMP production. Protein kinase A (PKA) is the primary target of cAMP, and active PKA phosphorylates a number of downstream targets, such as crucial metabolic enzymes (pyruvate dehydrogenase) and transcription factors (CREB). Inhibition of AC by  $\alpha$ 2-adrenergic activation results in overall inhibition of this pathway.

Canonical  $\beta$ -adrenergic signaling antagonizes the effects of  $\alpha$ 2-adrenergic signaling, resulting in smooth muscle relaxation, blood vessel dilation, lipolysis, insulin secretion from pancreatic  $\beta$ -cells, and glycogenolysis and gluconeogenesis in the liver and skeletal muscle. These functions are achieved through  $\beta$ -adrenergic receptor mediated activation of  $G_s$  proteins. The  $\alpha$ -subunits of  $G_s$  proteins associate with and activate AC, thus increasing the intracellular cAMP content. The second messenger cAMP then activates PKA, which, as mentioned above, phosphorylates a number of downstream targets. Targets of PKA in the liver and skeletal muscle include the activation of glycogen phosphorylase and inhibition of acetyl-CoA carboxylase, which serves to stimulate glycogenolysis. Glycogenesis is inhibited after PKA phosphorylates (and inhibits) glycogen synthase.

Of the  $\beta$ -adrenergic receptors, the mechanisms of action of the  $\beta$ 2-adrenergic receptor (Adrb2) are the most well studied. In contrast with the other  $\beta$ -adrenergic receptors, studies have revealed that the  $\beta$ 2-adrenergic receptor can switch from signaling through a  $G_s$  to a  $G_i$  or  $G_q$  depending on the membrane niche, local availability of the G-proteins, and in a ligand-dependent manner (Wenzel-Seifert and Seifert 2000, Daaka, Luttrell and Lefkowitz 1997). However, the full extent of this switching, and the effects

that switching has on the outcome of  $\beta$ 2-adrenergic receptor signaling are not well understood. One of the most well characterized downstream targets of ADRB2 is the L-type calcium channel, Cav1.2. Activation of ADRB2 via AC and PKA acutely increases Cav1.2 activity in the brain and heart (Hell et al, 1993; Fuller et al, 2010). Additionally, ADRB2 binding to Cav1.2 has been shown to be necessary for Cav1.2 phosphorylation at residue Ser1928, and that this binding is necessary to dissociate ADRB2 from Cav1.2 (Patriarchi et al. 2016). ADRB2 and Cav1.2 additionally form a macromolecular complex with trimeric G proteins, AC, PKA, and the phosphatase PP2A, which dephosphorylates residues in the main PKA activity site (Ser1928) of Cav1.2 (Davare et al. 2001, Hall et al. 2006). Together, these interactions are necessary for both activation of Cav1.2 as well as modulation of this activation through a negative feedback loop. While this has been well characterized in the heart and brain, these interactions have not yet been explored in pancreatic  $\beta$ -cells, even though Cav1.2 is known to be a primary calcium channel required for glucose-stimulated insulin secretion in these cells.

While the acute physiological responses to adrenergic signaling have been well characterized in adult organisms, the potential role for the adrenergic system during development is less well understood. Interestingly, recent evidence has implicated adrenergic signaling, specifically  $\beta$ -adrenergic signaling, in contributing to organogenesis in rat cardiomyocytes (Rybin et al. 2003). In this study, ADRB2 switching between two different G $\alpha$ s proteins (G $\alpha$ <sub>SL</sub> and G $\alpha$ <sub>SS</sub>) occurs during development, and in part contributes to differential cAMP accumulation in response to  $\beta$ 2-adrenergic stimulation in neonatal versus adult cardiomyocytes. Functionally, G $\alpha$ <sub>SS</sub> has been shown to activate AC more effectively than G $\alpha$ <sub>SL</sub>, effecting cAMP production. However, as the composition of the  $\beta\gamma$

subunits of G-proteins have been shown to change dramatically with age, it is likely that the association of  $G\alpha_{SL}$  and  $G\alpha_{SS}$  with different  $\beta\gamma$  subunits additionally affects function (Hansen, Schroering and Robishaw 1995).

Our lab has previously described a role for  $\beta$ -adrenergic signaling in pancreas development. Pharmacological inhibition of  $\beta$ -adrenergic signaling during early development (E18-P6) results in disrupted pancreatic islet morphology during development and impaired glucose tolerance in adult mice (Borden et al. 2013). This approach did not identify the  $\beta$ -adrenergic receptor(s), but single nucleotide polymorphisms (SNPs) in all three  $\beta$ -adrenergic receptors have been correlated with obesity and/or metabolic defects (Masuo et al. 2005, Park, Shin and Lee 2008, Lima et al. 2007). Importantly, of the three  $\beta$ -adrenergic receptors, only *Adrb2* is expressed in  $\beta$ -cells during embryonic pancreas development, while *Adrb1* and *Adrb3* are detected postnatally and at much lower levels (Berger et al. 2015). Furthermore, global deletion of the  $\beta$ 2-adrenergic receptor in mice results in impaired glucose tolerance (Santulli et al. 2012). Combined, this suggests that *Adrb2* may play a role in pancreas development and function. However, the extent of the developmental roles for  $\beta$ -adrenergic signaling are still widely uncharacterized.

# RESULTS

## Expression of Adrenergic Receptors in the Pancreas

Previous work from our lab has shown that developmental  $\beta$ -adrenergic signaling is essential for pancreatic islet development and function (Borden et al, 2013). This was done using pharmacological inhibition of  $\beta$ -adrenergic receptors during late gestation through early postnatal development (E18-P6). Of the three  $\beta$ -adrenergic receptors, *Adrb2* is the most abundantly expressed in  $\beta$ -cells during that developmental window (Berger et al, 2015). Additionally, it was recently demonstrated that global knockout of the  $\beta$ 2-adrenergic receptor (*Adrb2*) specifically resulted in impaired islet function in adult mice (Santulli et al, 2012). Combined, these results suggest that *Adrb2* may be developmentally required for endocrine pancreas development and function.

We first examined the temporal expression of the adrenergic receptors throughout pancreatic development. At birth (postnatal day 0 [P0]) as well as in adulthood, all of the adrenergic receptors are present, at some level, in the whole pancreas. Mature islets, however, express only five of the nine adrenergic receptors, and only two of the three  $\beta$ -adrenergic receptors (Figure 2.1A). Unfortunately, there are no verified antibodies for *Adrb2*, and we were unable to assess cell specificity with immunohistochemistry. Instead, to assess the  $\beta$ -cell expression of the  $\beta$ 2-adrenergic receptor, we used Fluorescence-Activated Cell Sorting (FACS) to isolate a pure  $\beta$ -cell population from a mouse line expressing GFP under the mouse insulin promoter (MIP-GFP) (Hara et al. 2003). RT-PCR from these cells showed robust expression of the  $\beta$ 2-adrenergic receptor (Figure 2.1B). We were also able to collect non GFP-positive cells representing all other pancreatic cell types.

Comparing *Adrb2* levels between GFP-positive  $\beta$ -cells and non- $\beta$ -cells with qPCR revealed *Adrb2* expression to be approximately 75% lower in non- $\beta$ -cells compared to  $\beta$ -cells (Figure 2.1C).

### **Characterization of mice lacking pancreatic *Adrb2***

To address pancreas-specific functions of *Adrb2* during development, we crossed mice carrying a floxed *Adrb2* allele (*Adrb2*<sup>ff</sup> mice) with transgenic *Pdx1-Cre* mice, to delete *Adrb2* in all cells of the pancreatic anlage starting at embryonic stages. *Pdx1-Cre;Adrb2*<sup>ff</sup> mice (henceforth referred to as *Adrb2* cKO mice) were born at expected Mendelian frequencies, had normal body weight at birth, no gross morphological abnormalities, and survived to adulthood. Efficient *Adrb2* deletion was observed from both male and female pancreata isolated from *Adrb2* cKO mice at postnatal day 6 (P6; Figure 2.2A). Importantly, quantitative PCR (qPCR) analysis showed that levels of other  $\alpha$ - and  $\beta$ -adrenergic receptors were unaltered in the absence of *Adrb2*, indicating that *Adrb2* loss did not elicit compensatory changes in the expression of other adrenergic receptor genes (Figure 2.2A). However, we did note that levels of *Adrb2* were approximately 75% lower in control male pancreata compared to control female pancreata (Figure 2.2B). Although in *Pdx1-Cre* transgenic mice, Cre recombinase activity has been reported in the hypothalamic regions (Song et al., 2010), there is little *Adrb2* expression in these areas (Allen Brain Atlas, <http://mouse.brain-map.org/>, Lein et al., 2007). Additionally, the (*Tg(Pdx1-Cre*<sup>Tuv</sup>) transgenic mice that we employed have not been reported to carry a human growth hormone mini-gene, commonly found in several Cre lines, that elicits metabolic defects (Brouwers et al., 2014).

## Female *Adrb2* cKO mice have increased insulin biosynthesis

Immunohistochemistry (IHC) with the islet hormone markers insulin and glucagon revealed that islet shape and cyto-architecture were largely unaffected by pancreatic *Adrb2* loss in neonatal mice, although *Adrb2* cKO mice had a greater distribution of smaller islets at the expense of larger ones, compared to controls (Figure 2.2 C-D). Endocrine cell numbers were unchanged, suggesting that smaller islet size was the result of an organizational change, and not a result of increased cell death or defects in cell proliferation (Figure 2.2 E). However, we noted a striking increase in insulin immunoreactivity specific to female *Adrb2* cKO mice, although both male and female mutant mice showed comparable Cre-mediated depletion (~70% loss) of *Adrb2*. In order to determine when the increased insulin began, we used immunohistochemistry to examine insulin levels during different developmental times, and saw no changes at P0, but a noted increase starting at P2 and continuing at P6 (Figure 2.3 A-C). In agreement with the IHC observations, we noted increased *Ins2* by qPCR starting at P2 and continuing at P6 in female *Adrb2* cKO pancreata, with no changes in P6 male *Adrb2* cKO pancreata (Figure 2.3 D). Intriguingly, control male islets showed higher insulin levels compared to control female islets by IHC (see Figure 2.3 C), and qPCR for *Ins2* showed significantly higher insulin transcript levels in males compared to females (Figure 2.3 E). The enhanced insulin expression in female *Adrb2* cKO  $\beta$ -cells was additionally seen using ultra-structural analyses, which revealed a significant increase in cytoplasmic insulin granule density in *Adrb2* cKO  $\beta$ -cells (Figure 2.3 F-G). Direct stimulation of MIN6 cells, a mouse insulinoma-derived cell line analogous to  $\beta$ -cells, with the *Adrb2* ligands, epinephrine and norepinephrine, as well as an *Adrb2*-specific agonist, salbutamol, did not alter insulin (*Ins2*) transcript levels, arguing against a

*direct* effect of *Adrb2* signaling on regulating insulin biosynthesis in  $\beta$ -cells (Figure 2.3 H). Together, these results suggest a female-specific role for *Adrb2* in controlling insulin expression in neonatal  $\beta$ -cells, likely through an indirect, non-cell-autonomous mechanism.

### **Female *Adrb2* cKO islets have excess vasculature**

Insulin biosynthesis is known to be influenced by paracrine signaling from intra-islet endothelial cells. Thus, we examined the pancreatic vasculature in neonatal *Adrb2* cKO and control mice using IHC for the endothelial-specific protein, PECAM1 (CD31). We observed a pronounced increase in the density of intra-islet endothelial cells in female, but not male, *Adrb2* cKO islets, similar to the observations for insulin levels. The developmental timing was similar to the insulin expression changes, with no differences being observed at P0 (Figure 2.4 A), but changes being observed beginning at P2 and persisting at P6 in female *Adrb2* cKO islets (Figure 2.4 B-D). The vascular abnormality appeared to be restricted to islets, as PECAM1 staining in the exocrine pancreas appeared grossly normal. Because intra-islet endothelial cells are the sole producers of the vascular basement membrane, a specialized extracellular matrix (ECM) consisting of collagen and laminin proteins that offer structural support, influence  $\beta$ -cell proliferation and insulin gene transcription, we also examined immunoreactivity for Collagen IV and Laminin, two abundant markers of the basement membrane. We noted robust increases in both Collagen IV and Laminin-411/511 in female *Adrb2* cKO islets, while male *Adrb2* cKO islets were comparable to same-sex control islets (Figure 2.4 E). To further characterize the effects of *Adrb2* loss on islet micro-vasculature, we used transmission electron microscopy (TEM) to visualize islets in female P6 *Adrb2* cKO and control mice. Intra-islet capillaries are

highly fenestrated to allow for the rapid exchange of nutrients and hormones between islet-cells and the bloodstream. In the absence of *Adrb2*, we found that intra-islet endothelial cell morphologies were dramatically altered, with a thicker basement membrane, fewer fenestrae, and increased caveolae, plasma membrane invaginations that are involved in macromolecule transport across endothelial cells and signaling (Figure 2.4 F-H). These results suggest that *Adrb2* may be important for restricting developmental islet vasculature growth.

### **Loss of pancreatic *Adrb2* does not affect islet innervation, ductal morphology, or large diameter blood vessels**

Because intra-islet capillaries have been proposed to form a scaffold to promote postnatal growth of autonomic fibers, we performed IHC for tyrosine hydroxylase (TH) to visualize sympathetic axon innervation in the neonatal pancreas in the absence of *Adrb2*. We found that despite the pronounced increase in intra-islet endothelial cells, sympathetic innervation in and around *Adrb2* cKO islets was indistinguishable from that in control tissues (Figure 2.5 A-B). We additionally examined other pancreatic structures which are known to contribute to  $\beta$ -cell development. We saw no changes in female or male *Adrb2* cKO large diameter blood vessels or ducts via IHC with smooth muscle actin (SMA) and dolichos biflorus agglutinin (DBA), respectively (Figure 2.5 C-D).



## **Islet hyper-vascularization in female *Adrb2* cKO islets is likely due to excess Vegf-a signaling**

To understand the basis for hyper-vascularized islets in female *Adrb2* cKO pancreata, we performed qPCR analyses to assess expression of the vascular endothelial growth factor family. We observed a marked (3.5-4.7-fold) increase in *Vegf-a*, the primary angiogenic factor produced by  $\beta$ -cells, in female, but not male, *Adrb2* cKO pancreata starting two days after birth. Interestingly, we also noted increased *Vegf-a* levels in male pancreata compared to female pancreata (Figure 2.6 A). We saw no changes in mRNA expression of the other prominent Vegf isoforms, *Vegf-b* and *Vegf-c* (Figure 2.6 B). To determine if the excess *Vegf-a* expression is  $\beta$ -cell specific, we crossed *Adrb2* cKO mice to *MIP-GFP* mice. Purified  $\beta$ -cells isolated by FACS from female P6 *Adrb2* cKO mice showed a striking 8-fold increase in *Vegf-a* transcript levels compared to control  $\beta$ -cells, whereas no differences were observed in non  $\beta$ -cell populations between control and *Adrb2* cKO pancreata (Figure 2.6 C-D). Again, we noted no change in *Vegf-a* levels in male *Adrb2* cKO  $\beta$ -cells, but we did note higher *Vegf-a* levels in male  $\beta$ -cells compared to female  $\beta$ -cells (Figure 2.6 C). In addition, we noted lower *Adrb2* levels in male  $\beta$ -cells compared to female  $\beta$ -cells (Figure 2.6 E). Together, these results suggest that *Vegf-a* expression and intra-islet vasculature are higher in neonatal male islets, which inversely correlate with the lower *Adrb2* expression compared to females. *Adrb2* loss had no effect on *Vegf-a* expression or islet vasculature in neonatal male islets, suggesting that male islets are less susceptible to *Adrb2* loss compared to females.

To address whether *Adrb2* activity directly regulates *Vegf-a* expression, we treated MIN6 cells with salbutamol, epinephrine and norepinephrine. Salbutamol and epinephrine

treatments significantly suppressed *Vegf-a* mRNA levels, while norepinephrine had no effect, likely because norepinephrine has the lowest affinity of the three agonists for ADRB2 (Figure 2.6 F). Furthermore, treatment of juvenile islets with salbutamol also suppressed *Vegf-a* levels (Figure 2.6 F). Together, these findings provide evidence of a sexually dimorphic function for developmental ADRB2 activity in restricting excessive growth of the intra-islet vasculature by limiting Vegf-a production in  $\beta$ -cells.

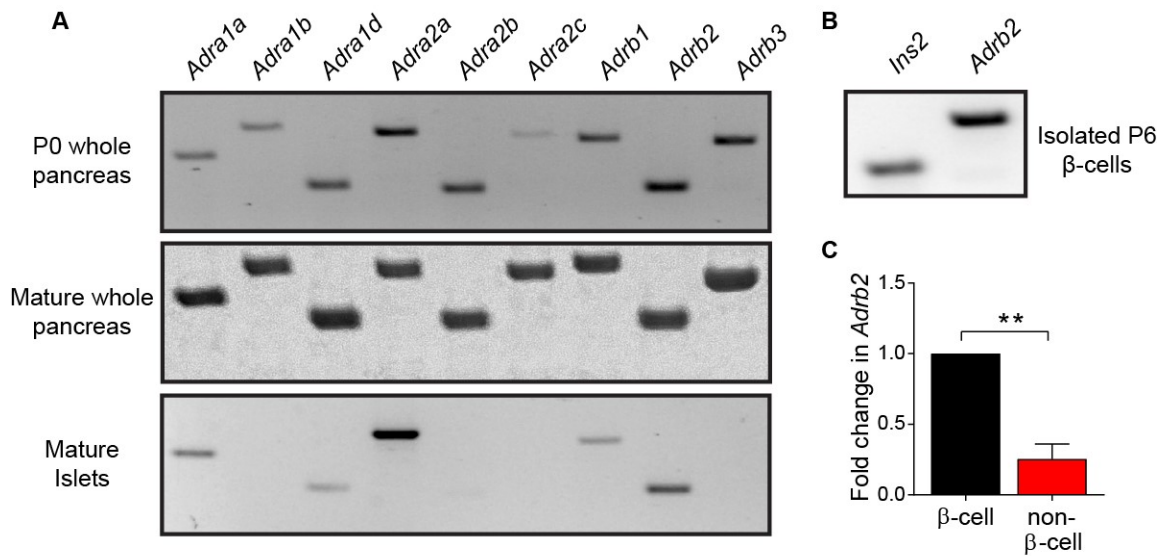


**Figure 2.1. Adrenergic receptor expression in the pancreas.** (A) RT-PCR shows all nine adrenergic receptors are expressed in both neonatal (postnatal day 0) and adult (6 week) pancreata. Isolated islets from adult mice show expression of only five adrenergic receptors, including Adrb2. (B) Adrb2 is expressed in  $\beta$ -cells isolated from neonatal (postnatal day 6) mice. (C) *Adrb2* expression is higher in  $\beta$ -cells than in non- $\beta$ -cells (n=4, \*\*p<0.01 one-sample *t*-test).

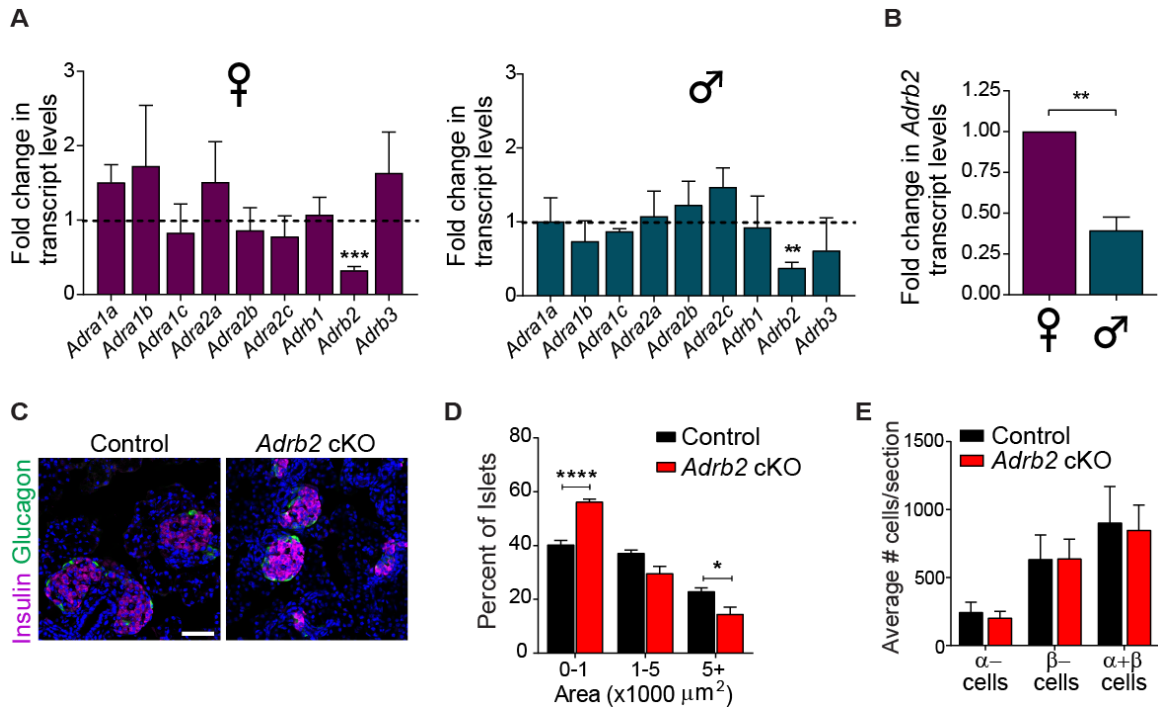


**Figure 2.2. Analysis of *Adrb2* cKO mice at postnatal day 6 (P6).** (A) TaqMan qPCR shows robust deletion of *Adrb2* from *Adrb2* cKO pancreata in both females and males. No compensatory transcriptional changes are seen in either sex (n=3-4 mice/sex/genotype; one sample t-tests \*\*p<0.01, \*\*\*p<0.001). (B) Control males have significantly lower *Adrb2* transcript levels than control females (n=4-6 mice/sex; one sample t-test \*\*p<0.01). (C) IHC for insulin (magenta) and glucagon (green) reveals preserved endocrine cell organization, but smaller islets in *Adrb2* cKO pancreata. Scale bar 50μm. (D) Quantification of islet size shows significantly more small islets, and significantly fewer large islets in *Adrb2* cKO pancreata (n=4-6 mice/genotype; one-way ANOVA \*p<0.05, \*\*\*\*p<0.0001). (E) No changes are seen in endocrine cell number between control and *Adrb2* cKO pancreata, suggesting that smaller islet size is not a result of islet cell death or defects in islet cell proliferation, but rather an organizational change (n=4-6 mice/genotype; one-way ANOVA).

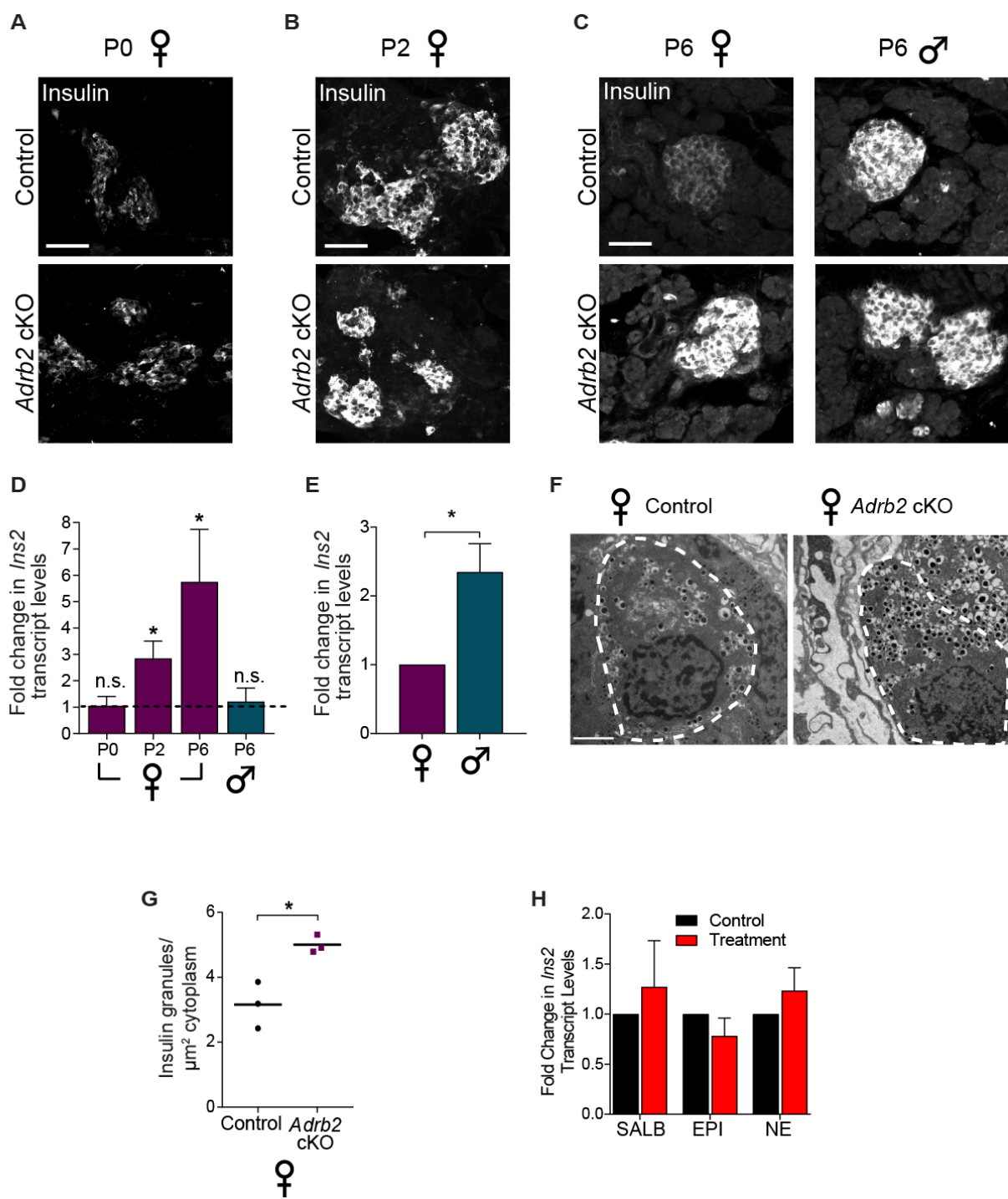


**Figure 2.3. Female *Adrb2* cKO mice have increased insulin biosynthesis.** (A) Immunohistochemistry for insulin reveals no changes in insulin expression at postnatal day 0 (P0). (B) Insulin immunoreactivity is robustly increased in female *Adrb2* cKO islets at P2. (C) Insulin immunoreactivity is increased in female *Adrb2* cKO islets at P6. Insulin is also higher in male controls compared to female controls at P6. No changes are seen between male control islets and male *Adrb2* cKO islets. Scale bars 50 $\mu$ m. (D) Insulin transcript levels are increased in female *Adrb2* cKO pancreata starting at P2 and continue to increase at P6; no changes are seen in male *Adrb2* cKO pancreata at P6 (n=6-10 mice/sex/genotype; one sample t-tests \*p<0.05). (E) Insulin transcript levels are higher in male control pancreata compared to female control pancreata at P6 (n=6-7 mice/sex). (F-G) TEM shows a significant increase in cytoplasmic insulin granule density in female *Adrb2* cKO  $\beta$ -cells at P6 (n=3 mice/genotype; t-test \*p<0.05). Scale bar 2 $\mu$ m. (H) Stimulation of MIN6 cells with adrenergic agonists shows no changes in *Ins2* transcript levels, suggesting increased insulin in female *Adrb2* cKO islets is an indirect effect of *Adrb2* loss (mean  $\pm$  SEM for n=3-4 independent experiments).

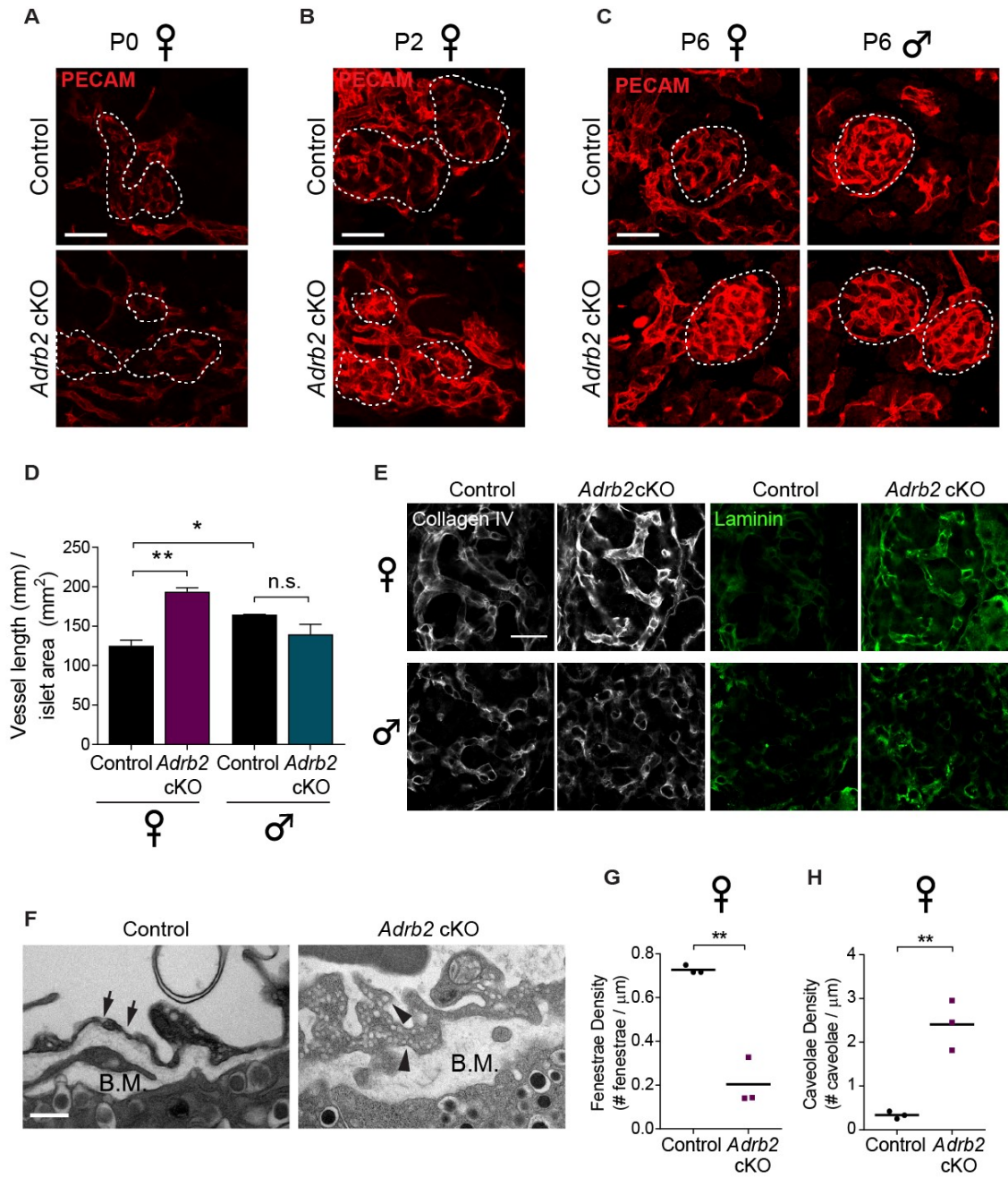


**Figure 2.4. Female *Adrb2* cKO islets have excess vasculature.** (A) Immunohistochemistry for platelet endothelial cell adhesion molecule (PECAM) shows no changes in intra-islet vasculature at P0. (B) PECAM density is increased in female *Adrb2* cKO islets at P2. (C) PECAM density remains increased in female *Adrb2* cKO islet at P6. Male *Adrb2* cKO islets are indistinguishable from male control islets, though male control islets have denser vasculature than female islets. Scale bars 50 $\mu$ m. (D) Quantification of total vessel length (mm) per islet area (mm<sup>2</sup>). Means  $\pm$  SEM for n=3 female and male mice per genotype. \*p<0.05, two-way ANOVA with Bonferroni's post-test. (E) Female *Adrb2* cKO islets have increased immunoreactivity for the basement membrane markers Collagen IV and Laminin. (F-H) TEM shows female *Adrb2* cKO islets have a thicker basement membrane, fewer fenestrae (arrows), and more caveolae (arrowheads) compared to control females (n=3 mice/genotype; *t*-tests \*p<0.05, \*\*p<0.01). Scale bar 500nm.



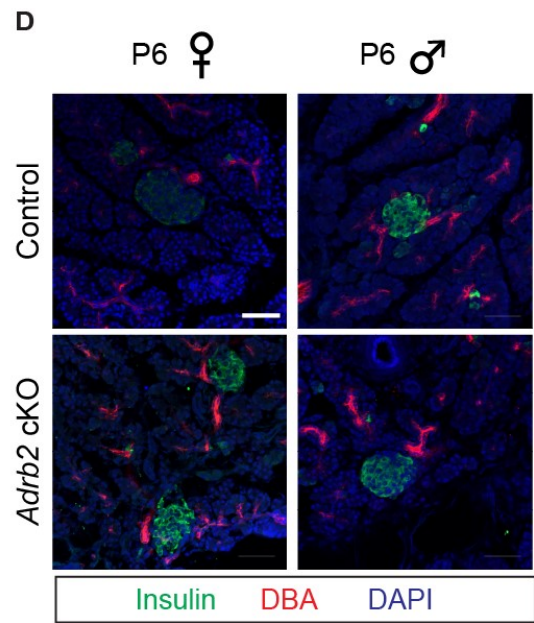
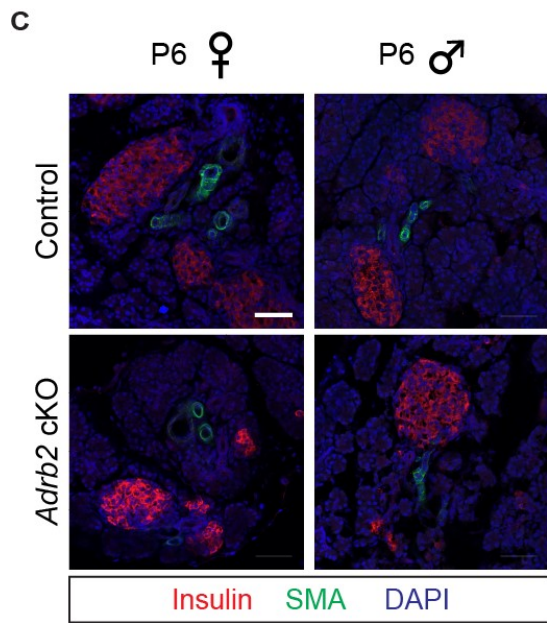
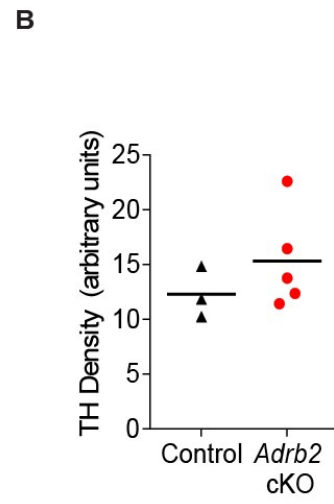
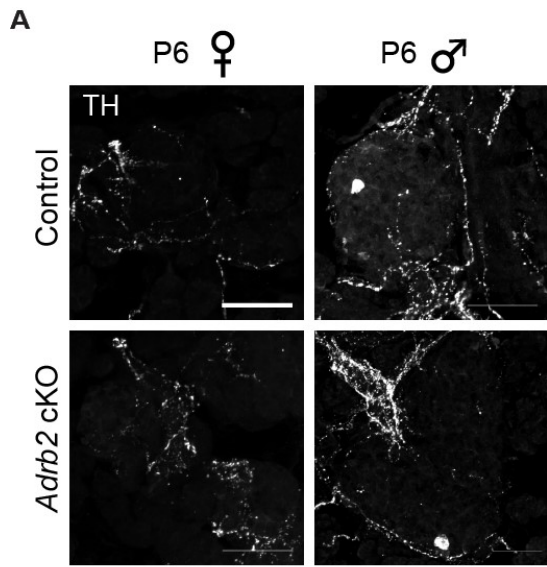


**Figure 2.5 Analysis of pancreatic structures in *Adrb2* cKO mice at P6.** (A) Tyrosine Hydroxylase (TH) immunoreactivity is unchanged surrounding both male and female *Adrb2* cKO islets. Scale bar 50 $\mu$ m. (B) Quantification of TH density surrounding control and *Adrb2* cKO islets (n=3-5 mice/genotype; *t*-test). (C) Large diameter blood vessels, marked by FITC-conjugated smooth muscle actin (SMA, green), are unchanged in both female and male *Adrb2* cKO pancreata. (D) Ducts, marked by rhodamine-conjugated dolichos biflorus agglutinin (DBA, red), are unchanged in both female and male *Adrb2* cKO pancreata. Scale bars 50 $\mu$ m.

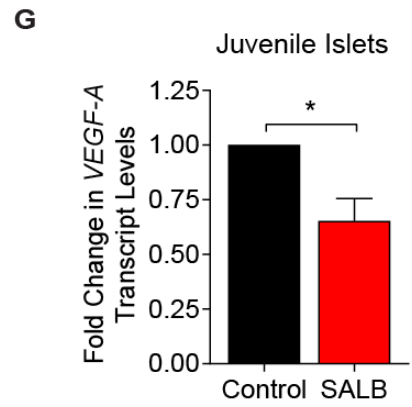
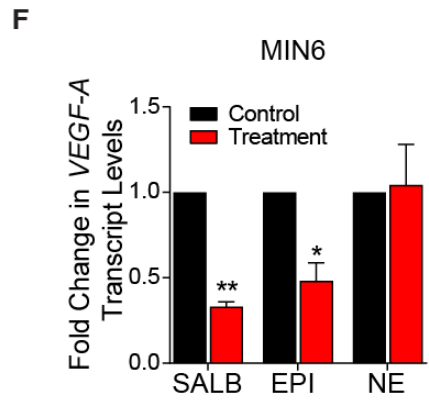
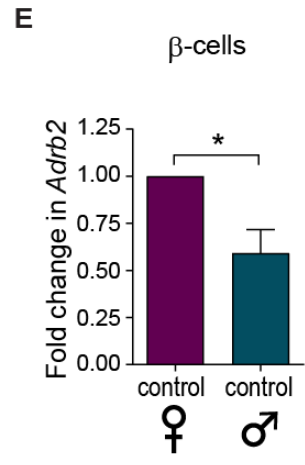
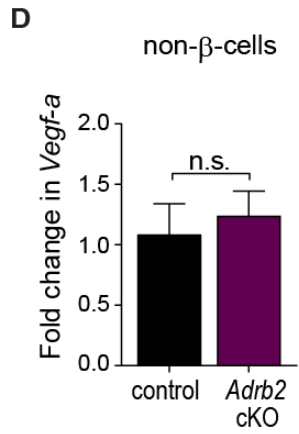
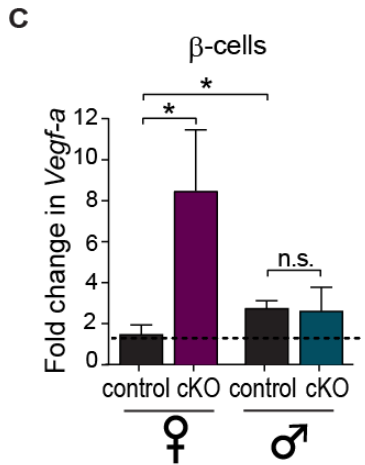
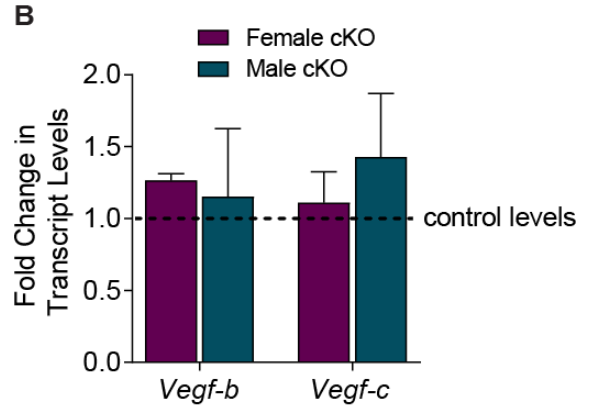
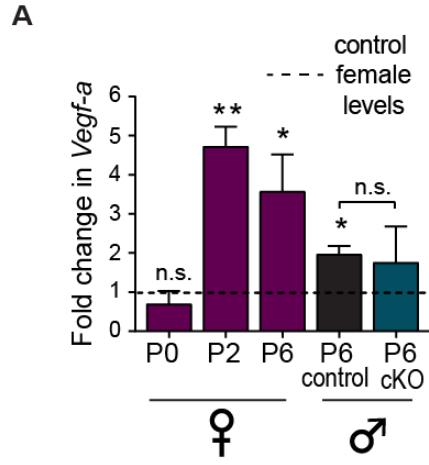


**Figure 2.6. Islet hyper-vascularization in female *Adrb2* cKO islets is likely due to excess Vegf-a signaling.** (A) *Vegf-a* transcript levels are unchanged at P0, peak at P2, and remain elevated at P6 in females. *Vegf-a* is higher in males than females, but unchanged in P6 male *Adrb2* cKO pancreata (compared to sex- and age-matched controls; n=3-10 mice/genotype/sex/age; one sample t-tests \*p<0.05, \*\*p<0.01, n.s. not significant). (B) No changes are seen in other Vegf isoforms (*Vegf-b* and *Vegf-c*) in either female or male P6 *Adrb2* cKO pancreata (n=3-5 mice/sex/genotype). (C) *Vegf-a* is significantly increased in  $\beta$ -cells from female *Adrb2* cKO mice. *Vegf-a* is higher in male  $\beta$ -cells than female  $\beta$ -cells (n=4-6 mice/sex/genotype; one sample t-test, t-test \*p<0.05). (D) *Vegf-a* levels are unchanged in non- $\beta$ -cells from female *Adrb2* cKO mice (n=5 female mice/genotype). (E) *Adrb2* levels are lower in male  $\beta$ -cells than female  $\beta$ -cells (n=4 mice/sex; one sample t-test \*p<0.05). (F) *Vegf-a* transcript levels are significantly decreased by Salbutamol (SALB), or epinephrine (EPI), but not norepinephrine (NE), in MIN6 cells. MIN6 cells were treated with each agonist (10 $\mu$ M) for 16 hr. Means  $\pm$  SEM and expressed as fold-change relative to control values. n=3 independent experiments for SALB and NE, 4 independent experiments for EPI. \*p<0.05, \*\*p<0.01, one-sample t-test. (G) *Vegf-a* transcript levels are significantly decreased by 16-hour Salbutamol (SALB) treatment (10 $\mu$ M) in isolated juvenile islets (n=8 mice/condition of mixed sex; one sample t-test \*p<0.05).

## DISCUSSION

During development, negative regulatory pathways are crucial to counter the unrestricted growth of tissues/organs. Here, we reveal a previously uncharacterized role for  $\beta$ 2-adrenergic receptors (Adrb2) in acting as an endogenous “brake” on excessive vascularization during islet development. Our findings support a scenario where Adrb2, acting in  $\beta$ -cells, suppresses Vegf-a production to limit excessive intra-islet vasculature during islet maturation. Islet endothelial cells are critical for regulation of insulin biosynthesis and exocytosis in neighboring  $\beta$ -cells. Loss of pancreatic Adrb2 disrupts the balance in bi-directional signaling between islet  $\beta$ -cells and endothelial cells, resulting in hyper-vascularized islets and enhanced insulin production. A variety of other factors previously shown to be differentially expressed in islets over-expressing Vegf-a were also affected, highlighting an instructive role for the vasculature in controlling  $\beta$ -cell gene transcription. Unexpectedly, we found that the phenotypes of islet vascularization and Ins2 and Vegf-a overproduction were specific to female mice, revealing an Adrb2-mediated sexually dimorphic pathway that underlies islet development.

In this study, we define a sexually dimorphic role for Adrb2 in controlling islet development. Loss of Adrb2 specifically impairs islet vasculature in female mice. The molecular underpinnings of sexually dimorphic Adrb2 functions in islets remain to be defined, however,  $\beta$ -adrenergic receptor expression and signaling is known to be influenced by steroid sex hormones (Marchetti et al., 1994; Yie and Brown, 1995), which are known to exert major organizational changes on organogenesis during the first postnatal week (McCarthy et al., 2012). Combined with our finding that females have

higher basal Adrb2 levels than males during this neonatal period, this suggests that testosterone may be inhibiting Adrb2 levels. It is important to consider the alternative that estrogen produced from testosterone during this perinatal may be capable of controlling Adrb2 expression. Testosterone is converted to estrogen by the cytochrome P450 complex called aromatase (Simpson et al, 2005). Although plasma estrogen levels are not significantly higher in males than females during the perinatal testosterone surge, estrogen levels in different tissues (such as the brain) have been shown to be higher in males during this time.

# METHODS

## Mice

All procedures relating to animal care and treatment conformed to The Johns Hopkins University Animal Care and Use Committee (ACUC) and NIH guidelines. Animals were group housed in a standard 12:12 light-dark cycle. Mice were maintained on a *C57BL/6* background, or mixed *C57BL/6* and *129P*, or *C57BL/6* and *FVB* backgrounds. Since phenotypes were specific to female mutant mice, animals of both sexes were used for initial analyses, and the sex of the animals used are clearly noted throughout the study. *Pdx-Cre* (*B6.FVB-Tg(Pdx1-cre)6Tuv/Nci*; RRID: IMSR\_NCIMR:01XL5) mice were obtained from NCI Frederick Mouse Repository. *MIP-GFP* (*B6.Cg-Tg(Ins1-EGFP)1Hara/J*; RRID: IMSR\_JAX:006864) mice were obtained from Jackson Laboratory. *Adrb2<sup>fl/fl</sup>* mice were a generous gift from Dr. Gerard Karsenty (Hinoi et al, 2008).

## qRT-PCR

RNA from either whole pancreata (P6) or isolated islets (adult) was isolated using TRIzol RNA extraction reagent phenol-chloroform extraction and ethanol precipitation. RNA from sorted cells was isolated using Direct-zol RNA Microprep (Zymo) kit. 1.5-2 $\mu$ g of total RNA was reverse-transcribed into cDNA with M-MLV Reverse Transcriptase (Promega). TaqMan assays (ThermoFisher) were used to quantitatively determine transcript levels of the adrenergic receptors, while Maxima SYBR Green/Rox Q-PCR Master Mix (ThermoFisher) reagents and primer sets (listed in Primer Table) were used to

determine transcript levels for other genes. Both assays were performed in a StepOnePlus Real-Time PCR System (ThermoFisher). Fold change in transcript levels was calculated using the  $2^{-\Delta\Delta Ct}$  method, and 18S was used as an endogenous control for normalization.

### **Morphometric Islet Analysis**

Cryosections were taken from P6 mouse pancreata at 10 $\mu$ m, every 200 $\mu$ m throughout the whole pancreas. Sections were washed with PBS, permeabilized in 1% Triton X-100 in PBS, and blocked for 1 hour at room temperature using 5% goat serum (GS) in PBS + 0.1% Triton X-100. Sections were then incubated overnight at 4°C with a guinea pig anti-insulin antibody (1:300) and a mouse IgG1 anti-glucagon antibody (1:500). Following PBS washes, sections were then incubated with anti-guinea pig Alexa-546 and anti-mouse IgG1 Alexa 488 secondary antibodies (1:200; ThermoFisher). Sections were then washed in PBS and mounted in Fluoromount Aqueous Mounting Medium containing 100 $\mu$ g/mL DAPI. Every islet in the collected sections was imaged on a Zeiss AxioImager. The number of  $\alpha$ - and  $\beta$ -cells was counted in each islet in each section, and the total  $\alpha$ - and  $\beta$ -cell number counted was divided by the number of sections imaged to determine average endocrine cell number. Islet area was determined using the Region Of Interest manager (ROI manager) and the FIJI (FIJI Is Just ImageJ) area measurement tool.

### **Other IHC**

50 $\mu$ m cryosections were taken from P6 mouse pancreata, then washed with PBS, permeabilized in 1% Triton X-100 in PBS, and blocked for 1 hour at room temperature



using 5% goat serum (GS) in PBS + 0.1% Triton X-100. Sections were then incubated for 2 nights at 4°C with either: rat anti-PECAM-1/CD-31 antibody (1:300), rabbit anti-TH antibody (1:500), rabbit anti-collagen IV (1:500), or chicken anti-laminin (1:200) in conjunction with guinea pig anti-insulin (1:300). Following PBS washes, sections were then incubated with anti-rat Alexa-546, anti-rabbit Alexa 488 or 647, anti-chicken 488 or 647, and anti-guinea pig 488, 546, or 647 secondary antibodies (1:200; ThermoFisher). Sections were then washed in PBS and mounted in Fluoromount Aqueous Mounting Medium containing 100µg/mL DAPI. Z-stacks of 1µm optical slices were taken using a Zeiss LSM 700 confocal microscope equipped with 405, 488, 555, and 633 lasers. Maximum intensity projections were generated with FIJI, and quantification of sympathetic innervation density was done by calculating integrated TH fluorescence density per unit area (FIJI) from multiple random images. Quantification of islet vasculature density was done by calculating integrated PECAM-1/CD-31 density per islet (ROI set by insulin immunoreactivity) area (FIJI) from multiple random images.

### **Transmission Electron Microscopy**

Pancreata were dissected and cut into ~1mm<sup>3</sup> pieces then fixed in 3% formaldehyde + 1.5% glutaraldehyde + 2.5% sucrose in 0.1M NaCacodylate + 5mM CaCl<sub>2</sub>, pH 7.4 at room temperature for 1 hour. Pieces were then washed in 2.5% sucrose in 0.1M NaCacodylate + 5mM CaCl<sub>2</sub> and post-fixed with 1% Palade's OsO<sub>4</sub> for 1 hour on ice, followed by incubation in Kellenberger's uranyl acetate overnight at room temperature. Samples were then dehydrated with a graded alcohol series (50%, 75%, 95%, and 100% ethanol, then propylene oxide), embedded in Epon, and sectioned (~90nm) and collected

onto EM grids. Grids were then imaged using an FEI Tecnai-12 TWIN transmission electron microscope operating at 100 kV and a SIS MegaView III wide-angle camera. A minimum of three endothelial cells adjacent to at least one  $\beta$ -cell were quantified per animal, and fenestrae and fused caveolae density was determined for the entirety of the endothelial cell.

### **Cell sorting**

Pancreata from control and *Adrb2* cKO animals in a MIP-GFP background were digested in 0.05% trypsin, 0.53M EDTA for 15 minutes at 37°C with intermittent trituration. Samples were then neutralized with Hank's Balanced Salt Solution (HBSS, Gibco) + 2% FBS, 5mM EDTA, and 10 $\mu$ g/mL DNase and filtered (70 $\mu$ m). Dissociated cells were then sorted using a Sony Biotechnology SH 800 cell sorter, and GFP-positive cells separated based on detection using the FL1 channel (absorption 530nm).

## **QUANTIFICATION AND STATISTICAL ANALYSIS**

Sample sizes were similar to those reported in previous publications (Borden et al., 2013; Houtz et al., 2016). For practical reasons, analyses of endocrine cell counts and quantifications from ultrastructural analyses (caveolae and fenestrae density, insulin granule density, insulin granule docking) were done in a semi-blinded manner, such that the investigator was aware of the genotypes prior to the experiment, but conducted the staining and data analyses without knowing the genotypes of each sample. All Student's *t*-tests were performed assuming Gaussian distribution, two-tailed, unpaired, and with a

confidence interval of 95%, with the exception of fold change analyses (such as for qPCR), which were done using a one sample *t*-test. One-way ANOVA analyses with post hoc Tukey test or two-way ANOVA analyses with post hoc Bonferroni test were performed when more than 2 or 3 groups were compared, respectively. Statistical analyses were based on at least 3 independent experiments, and are described in the figure legends. All error bars represent the standard error of the mean (S.E.M.).

**CHAPTER 3: NEONATAL  $\beta$ -  
ADRENERGIC SIGNALING IS  
REQUIRED FOR FEMALE ISLET  
FUNCTION**

# INTRODUCTION

## Physiology of blood glucose homeostasis

Glucose homeostasis is maintained by secretion of the hormone insulin from islets of Langerhans in the pancreas. Loss or dysfunction of insulin-producing  $\beta$ -cells in islets results in dysregulation of blood glucose levels and leads to diabetes.  $\beta$ -cells receive and integrate input from multiple extracellular cues throughout life to control insulin secretion. An important goal in diabetes prevention and treatment is a better understanding of the molecular and cellular processes governing  $\beta$ -cell development and function.

In response to nutrient intake, such as ingesting a meal or snack, our blood glucose levels rise rapidly due to sugar consumption. This rise is sensed by the  $\beta$ -cells of the pancreas, which respond by rapidly secreting insulin. Insulin then travels throughout the body to insulin responsive tissues, such as the liver, adipose, and skeletal muscle. Insulin signaling through the insulin receptor, a canonical receptor tyrosine kinase, in these tissues results in the recruitment of GLUT4 glucose transporters from intracellular endosomes to the cell membrane (Huang and Czech, 2007). Insertion of these receptors in the cell membrane allows for the rapid influx of glucose from the bloodstream, effectively lowering the concentration of glucose in the bloodstream. In contrast, when blood glucose levels fall too low, such as overnight when the body is in a fasted state, the secretion of insulin from  $\beta$ -cells is diminished, and glucagon secretion from  $\alpha$ -cells is enhanced (Hussain, 2014). Glucagon production is negatively regulated by insulin, so when blood glucose levels are low, less insulin is produced and secreted, and more glucagon is produced and secreted. Glucagon production has also been shown to be positively regulated through adrenergic

stimulation (Skoglund, Lundquist and Ahren 1987). Glucagon travels throughout the bloodstream and signals through its receptor, a GPCR, to promote gluconeogenesis and decrease the rate of glycolysis. This effectively raises the concentration of glucose in the bloodstream, bringing it back to a homeostatic state.

## **Regulation of insulin secretion**

### *Glucose stimulation*

The primary stimulator of insulin secretion from pancreatic  $\beta$ -cells is glucose. In response to elevated glucose levels in the blood, glucose is brought into  $\beta$ -cells via the glucose transporter Glut2 (Thorens et al, 1988; Johnson et al, 1990). Once in the cytoplasm, glucose is metabolized through glycolysis, effectively raising the intracellular ATP:ADP ratio (see introduction for details). ATP closes ATP-sensitive  $K^+$  channels (encoded by *Kcnj11* and *Abcc8*), resulting in decreased  $K^+$  efflux and rapid depolarization of the  $\beta$ -cell plasma membranes. This depolarization serves to open voltage-dependent  $Ca^{2+}$  channels (VDCCs), resulting in an influx of calcium ions (MacDonald et al, 2005). Increased cytosolic calcium then promotes insulin secretion through activation of synaptotagmins, calcium-dependent proteins that bind phospholipids and SNARE proteins to initiate vesicle fusion (Gustavsson et al. 2008).

Regulated insulin secretion from  $\beta$ -cells occurs in two phases, termed first and second phase insulin secretion. First phase insulin secretion is an immediate response (within five minutes of stimulus), while second phase insulin secretion can be sustained for hours after the initial stimulus (MacDonald et al, 2005). It is thought that the two phases

of insulin secretion emanate from two distinct pools of insulin in the cell, a readily releasable pool (RRP) located near the plasma membrane that consists of approximately 1% of the total insulin content of the cell, and a reserve pool located more internally that consists of the remaining 99% (Olofsson et al. 2002). These two different granule populations allow for both a blunt, rapid initial response as well as a longer, fine-tuned response.

First phase secretion is generated by fusion and release of insulin from docked insulin granules. In order to be docked, granules must be tethered to the membrane by a complex consisting of Syntaxin1A, Munc18 and granuphilin (Cheviet et al., 2004). It was previously believed that docked granules were primed and located at the membrane in order to be able to fuse rapidly. Recent studies, however, have shown that the docked granule complex, and specifically granuphilin, is inhibitory to secretion (Mizuno et al. 2016). Docked granules can be secreted, however, when granuphilin is released in order to allow for docked granule fusion. However, the exact mechanisms controlling the release of granuphilin in response to glucose are unknown. Granule secretion during the first phase of insulin secretion occurs at membrane niches containing already docked granules in close proximity with or in complex with L-type calcium channels, such as Cav1.2 (Schulla et al, 2003, Yang et al, 1999). Granules secreted during the first phase of insulin secretion have low calcium sensitivity, and thus need a high local concentration of calcium to be secreted (Yang et al, 1999).

Second phase insulin secretion involves trafficking of more centrally located granules to the plasma membrane; movement of granules through the cell requires remodeling of the cortical actin cytoskeleton (Nevins and Thurmond, 2003). Our lab has

previously shown that this process is, in part, regulated by nerve growth factor (NGF) signaling through tropomyosin receptor kinase A (TrkA) (Houtz et al. 2016). NGF-TrkA activation results in the internalization of TrkA, which recruits Rac1 to promote F-actin reorganization, thus allowing insulin granules to more easily reach the membrane. Calcium also contributes to this process by activating gelsolin, an actin-severing protein (Tomas et al. 2006). In this way, second phase insulin secretion is more sensitive to calcium, and occurs due to overall increased cytosolic calcium levels versus high local concentrations. Calcium influx in the second phase of insulin secretion has been shown to be regulated by the opening of R-type (and other non L-type) calcium channels, such as Cav2.3 (Jing et al. 2005). Calcium also plays an important role in insulin granule fusion. Activation of synaptotagmin by calcium is essential for forming a SNARE complex and promoting granule exocytosis (Gustavsson et al. 2008). Mobilization of intracellular calcium stores stimulates ATP synthesis in mitochondria, which further potentiates insulin secretion by closing more K<sup>+</sup> channels. Glucose-dependent generation of IP3 (Biden et al. 1987), as well as incretin actions (described below) are required to mobilize intracellular calcium stores. Intracellular calcium stores on their own are not sufficient to promote insulin granule exocytosis.

### **β-adrenergic signaling and acute insulin secretion**

Adrenergic signaling has long been associated with mediating hormone release from the endocrine pancreas. The exact outputs and mechanisms for this acute stimulation, however, are still debated. After perfusion of canine pancreata with both α- and β-adrenergic receptor agonists, glucagon secretion was stimulated while insulin secretion



was inhibited (Iversen, 1973). Pharmacological inhibition of  $\alpha$ - and  $\beta$ -adrenergic receptors in conjunction with catecholamine stimulation suggested that glucagon secretion was being stimulated through  $\beta$ -adrenergic signaling, while insulin secretion was being mediated through  $\alpha$ -adrenergic signaling. Studies in mouse and rat pancreata, however, revealed the opposite mechanism. In response to  $\beta$ -adrenergic receptor agonist stimulation with isopropylnoradrenaline, insulin secretion was stimulated in a dose-dependent manner (Ahren and Lundquist 1981). This secretion was attributed to  $\beta$ 2-adrenergic receptors specifically, as stimulation with terbutaline (a  $\beta$ 2-adrenergic receptor specific agonist) additionally stimulated insulin secretion in a dose-dependent manner (Ahren, Jarhult and Lundquist 1981, Ahren and Lundquist 1981). Stimulation of insulin secretion with a  $\beta$ 1-adrenergic receptor specific agonist (isopropylaminothiazoloxopropanol [ITP]) was only seen in response to high concentrations (Ahren and Lundquist 1981). While these results strongly support an acute role for  $\beta$ 2-adrenergic receptors in insulin secretion, further experiments with selective and non-selective  $\beta$ -adrenergic receptor antagonists raised more questions. Inhibition of  $\beta$ 2-adrenergic receptors with the selective antagonist ICI 118,551 diminished terbutaline stimulated insulin secretion, but inhibition with the selective antagonist butoxamine had no effect, raising the possibility that only a subset of  $\beta$ 2-adrenergic receptors play an acute role in insulin secretion (Ahren and Lundquist 1981). A caveat to these studies is that they relied on the measurement of plasma insulin *in vivo* after perfusion or infusion of pharmacological agonists or antagonists. These studies did not specifically address the role of insulin secretion versus insulin sensitivity and could not rule out off-target effects of stimulating adrenergic receptors signaling in other tissues. This

is especially relevant as central nervous system stimulation of adrenergic receptors has been implicated in insulin secretion as well (Ribes et al. 1989).

Studies from isolated islets have provided more insight into the specific actions of adrenergic activity in insulin secretion, though many questions remain. Stimulation of isolated male rat islets with the  $\beta$ 2-adrenergic receptor specific agonists clenbuterol or salbutamol had no effect on insulin secretion in either low or high glucose conditions (Lacey et al, 1990). In contrast, stimulation of human islets with these agonists resulted in an augmented insulin secretion response that was abrogated by the non-specific  $\beta$ -adrenergic receptor antagonist propranolol (Lacey et al, 1990). Finally, studies from isolated male rat islets showed that selective stimulation of  $\beta$ 2-adrenergic receptors with clenbuterol stimulated glucagon secretion, leading to the conclusion that while *in vivo* stimulation of  $\beta$ 2-adrenergic receptors acutely increased plasma insulin levels, the mechanism of  $\beta$ 2-adrenergic receptor activity in islets was to stimulate glucagon secretion in rats (Lacey et al. 1991). In humans, however,  $\beta$ 2-adrenergic receptor activity increases insulin secretion (Lacey et al, 1993). These results still leave many unanswered questions. While the differences between rat and human islets have been noted, mouse islets have been less explored. Furthermore, the studies in rat islets were only done from males, while many of the human studies were either biased towards one sex or failed to mention the sex of the donors altogether. Together, these studies highlight a potential role for  $\beta$ -adrenergic signaling in islet hormone secretion and therefore metabolic homeostasis. However, the pancreas specific role for *Adrb2* in insulin secretion is still unclear. We found that *Adrb2* controls islet vasculature by repressing *Vegf-a*. As previous studies have shown islet

vasculature to be important for islet function (Cai et al, 2012; Reinert et al 2014), we wished to assess glucose homeostasis and islet function in *Adrb2* cKO mice.

# RESULTS

## **Adrb2 contributes to glucose homeostasis**

Although the global knockout mouse for the  $\beta$ 2-adrenergic receptor has been previously characterized as having metabolic defects, the published studies only examined aged male mice (6-20 months; Santulli et al, 2012). Because we had seen developmental changes resulting from pancreas-specific loss of Adrb2, we wanted to know how early the metabolic defects arose in Adrb2<sup>-/-</sup> mice. To characterize the metabolic state of the Adrb2<sup>-/-</sup> mice, we examined male and female glucose tolerance. Fed and fasted blood glucose levels were unchanged between Adrb2<sup>-/-</sup> mice and wild types (Figure 3.1 A-B). We did observe, however, that male Adrb2<sup>+/+</sup> mice had higher fasting blood glucose levels than female Adrb2<sup>+/+</sup> mice (Figure 3.1 B). Interestingly, both male and female Adrb2<sup>-/-</sup> mice showed slightly enhanced glucose tolerance (Figure 3.1 C-E). Previous studies have shown that aged male (6 month and 20-month-old) Adrb2<sup>-/-</sup> mice have impaired glucose tolerance (Santulli et al. 2012), while our mice were only 2 months old. Therefore, it is probable that Adrb2<sup>-/-</sup> mice develop glucose intolerance with age. This interesting metabolic profile also suggests that multiple Adrb2-expressing tissues contribute to metabolic homeostasis, likely in different ways (i.e. inhibiting insulin uptake in peripheral tissues). While it is possible that compensation from Adrb1 (the only other  $\beta$ -adrenergic receptor expressed in islets) could confound these results, glucose tolerance tests of adult Adrb1<sup>-/-</sup> mice showed no defects in males or females (shown combined in Figure 3.2 A-B). This suggests that Adrb1 is dispensable for glucose homeostasis, and likely dispensable for insulin secretion.

Therefore, in order to characterize the pancreatic role for *Adrb2* in maintaining glucose homeostasis, we further characterized the metabolic profiles of the *Adrb2* cKO mice.

### **Developmental Vegf-a dependent vascular changes persist in *Adrb2* cKO adults.**

We first investigated whether the hyper-vascularization and increased *Vegf-a* expression was maintained in adult *Adrb2* cKO females. To do this, we perfused control and *Adrb2* cKO females with wheat germ agglutinin (WGA) conjugated to an Alexa-488 fluorophore to paint all the blood vessels within the animals. Indeed, we saw adult *Adrb2* cKO islets maintained excess vascular density (Figure 3.3 A). Additionally, qPCR showed a dramatic 11-fold increase in *Vegf-a* mRNA in female *Adrb2* cKO islets, while male islets showed control levels of *Vegf-a* (Figure 3.3 B).

### **Pancreatic *Adrb2* is required for glucose homeostasis**

In order to determine the metabolic consequences of pancreatic *Adrb2* loss, and because both excess islet vasculature and blockade of  $\beta$ -adrenergic signaling have been shown to result in disrupted metabolic homeostasis (Borden et al., 2013; Cai et al., 2012), we performed glucose tolerance tests on mature (2-month-old) *Adrb2* cKO animals. Interestingly, we saw no glucose tolerance defects in 2-month-old male or female *Adrb2* cKO animals (Figure 3.4A-E). However, we did note that female *Adrb2* cKO mice had higher fasting glucose levels (Figure 3.4A), an indicator of a pre-diabetic state. Therefore, in order to further challenge the *Adrb2* cKO mice, the glucose tolerance test was performed

with three consecutive glucose challenges. Excitingly, we saw a drastic impairment of glucose tolerance in female, but not male *Adrb2* cKO mice (Figure 3.4 G-J).

Because *Adrb2* loss has been associated with age-dependent metabolic phenotypes (Santulli et al. 2012), we additionally assessed glucose tolerance in aged (4-month-old) male and female *Adrb2* cKO mice. Interestingly, we saw glucose tolerance defects in aged male and female *Adrb2* cKO mice in response to a single glucose challenge (data not shown). However, the defects in the female *Adrb2* cKO mice were more robust, with the change in glucose levels being between 100 and 150mg/dL during the first 30 minutes after glucose challenge, while the males differed by only 70 to 90 mg/dL from controls. Additionally, aged female *Adrb2* cKO mice displayed increased fed blood glucose levels, while male *Adrb2* cKO fed blood glucose levels were unchanged (data not shown). Together, this suggests that the glucose tolerance defects worsen with age in female *Adrb2* cKO mice and, surprisingly, develop late in male *Adrb2* cKO mice. This also suggests that the mechanism by which *Adrb2* influences glucose homeostasis differs in males and females.

### **Pancreatic *Adrb2* is required for islet insulin secretion in female mice**

In order to determine why *Adrb2* cKO mice developed glucose intolerance, we assessed insulin sensitivity, plasma hormone levels, and insulin secretion. Insulin sensitivity was unaffected in male or female *Adrb2* cKO mice at both 2 months and 4 months of age, suggesting that defects in glucose tolerance do not stem from defects in insulin responsiveness in female *Adrb2* cKO mice, and that insulin hypersensitivity is not

masking glucose tolerance defects in male *Adrb2* cKO mice (Figure 3.5 A-D). We additionally saw no changes in fed or fasted serum glucagon levels in female or male *Adrb2* cKO mice (Figure 3.6 A-B), suggesting that glucose intolerance in *Adrb2* cKO mice may stem from dysregulation of insulin secretion. To assess this, we first looked at fed and fasted plasma insulin levels in male and female *Adrb2* cKO mice at 2 and 4 months of age. Excitingly, we observed significantly decreased fed plasma insulin levels in 2 and 4-month-old female, but not male *Adrb2* cKO mice (Figure 3.6 C-F). Fasted insulin levels trended toward a decrease in female *Adrb2* cKO mice, although the effects were statistically not significant. Male fasted insulin levels were unchanged. This suggests that although female *Adrb2* cKO mice produce excess insulin, they are unable to secrete it. Therefore, we hypothesized that regulated insulin secretion may also be deficient in female *Adrb2* cKO mice. To test this, we performed *in vivo* insulin secretion assays in male and female *Adrb2* cKO mice at 2 and 4 months old. We found significantly dampened glucose-stimulated insulin secretion (GSIS) in 2 and 4-month-old female *Adrb2* cKO mice compared to same-sex controls (*Adrb2<sup>fl/fl</sup>*; Figure 3.7 A-D). This suggests that the glucose intolerance seen in female *Adrb2* cKO mice is due to defective GSIS. While we did not extend our time-course to test this, it is possible that male *Adrb2* cKO mice would develop defects in GSIS later in life, as their glucose tolerance defects were also delayed. It is also possible that the male *Adrb2* cKO mice become glucose intolerant through a different mechanism, such as diminished insulin sensitivity. Further analyses would be needed to uncover the mechanism for the glucose intolerance in males.

Consistent with the *in vivo* observations, insulin secretion from isolated female *Adrb2* cKO islets was significantly dampened, both basally (2.8mM glucose) and in

response to high glucose (16.7mM; Figure 3.7E). Insulin content was significantly higher in female *Adrb2* cKO islets, consistent with the developmental findings, and suggesting that insulin secretion is not diminished due to a decrease in insulin biosynthesis (Figure 3.7F). Together, these results suggest that pancreatic *Adrb2* is required for glucose tolerance and islet insulin secretion in female mice.

### **Loss of *Adrb2* perturbs islet calcium responses and exocytosis**

Regulation of glucose-stimulated insulin secretion (GSIS) occurs at many levels in the  $\beta$ -cell, including glucose uptake and metabolism, membrane depolarization, calcium responsiveness, and insulin granule docking and fusion (MacDonald et al., 2005). To understand which step in GSIS requires *Adrb2*, we first assessed levels and localization of *Glut2*, the  $\beta$ -cell glucose transporter by IHC. We saw diminished overall expression of *Glut2*, suggesting that the GSIS defects in female *Adrb2* cKO islets may be due to an inability to sense high glucose levels (Figure 3.8 A). To assess if this was the primary cause of the diminished insulin secretion, we next exposed female islets to a high extracellular concentration of potassium (30mM KCl) to depolarize the  $\beta$ -cell plasma membranes and open voltage-dependent calcium channels (VDCCs), thus bypassing the need for glucose uptake and metabolism in insulin secretion (Hatlapatka et al., 2009). Islets from female *Adrb2* cKO mice had significantly diminished KCl-stimulated insulin secretion, suggesting *Adrb2* affects steps of GSIS after membrane depolarization in addition to affecting *Glut2* levels (Figure 3.8 B). To further assess the role for *Adrb2* in GSIS, we used TEM to examine insulin granule docking at the plasma membrane in response to glucose. Control animals showed significant recruitment of insulin granules to the plasma membrane (within



50nm of apical plasma membrane) following glucose injection compared to the fasted state (Figure 3.8 C-D). However, *Adrb2* cKO  $\beta$ -cells had significantly fewer docked insulin granules following glucose injection compared to glucose-injected controls, and showed no significant recruitment compared to the fasted state (Figure 3.8 C-D). These data suggest a requirement for *Adrb2* downstream of glucose sensing and membrane depolarization, likely in calcium signaling or insulin granule mobility.

To further assess potential mechanistic defects in female *Adrb2* cKO islets, we assessed overall cAMP levels, as *Adrb2* is thought to increase cAMP levels when signaling through a  $G_s$  protein, and thus promote insulin secretion in response to high glucose in this manner. Indeed, we saw significantly decreased levels of cAMP in female *Adrb2* cKO islets (Figure 3.9 A). This suggested that loss of *Adrb2*-cAMP signaling may contribute to the loss of GSIS. However, cAMP is not thought to play a primary role in basal insulin secretion, and as we saw defects in fed plasma insulin levels and islet insulin secretion in low glucose, we wanted to probe the insulin secretion defects further, as it was unlikely that decreased cAMP levels was the only cause of all the GSIS defects. To address whether *Adrb2* is required for glucose-dependent calcium response in  $\beta$ -cells, we loaded isolated islets with Fluo-4 AM, which fluoresces upon binding to calcium, and treated them with low glucose, high glucose, and KCl (Kenty and Melton, 2015). In response to high glucose (20mM) and subsequent KCl-stimulated membrane depolarization (30mM), control islets showed a significant increase in intracellular calcium (Figure 3.9 B-C). In contrast, islets from *Adrb2* cKO mice showed a significantly diminished calcium response in both conditions (Figure 3.9 B-C).

In order to assess the underlying cause of the diminished calcium response, we screened islets for transcripts encoding proteins involved in various GSIS events. We did not see changes in expression of glycolysis genes (*Aldob*, *Pfkl*, *Ldha*, *Tpi*, or *Pklr*) or potassium channel subunit genes (*Kcnj11* or *Abcc8*; Figure 3.9 D). Interestingly, we found down-regulation of genes involved in calcium-response during GSIS, including the L-type calcium channel (*Cacna1c* [Cav1.2]). We also saw significant down-regulation of *Snap25*, *Rph3al* (Noc2), and *Pclo* (Piccolo), which promote insulin granule exocytosis (Figure 3.9 D). Specifically, Noc2 interacts with components required for insulin granule exocytosis, such as those of the Rab and Munc family (Cheviet et al., 2004) and Piccolo is a scaffold protein that links ATP-gated potassium channels, L-type calcium channels (such as Cav1.2), and insulin granules to promote GSIS (Shibasaki et al., 2004). This was of particular interest to us because *Rph3al* and *Pclo* have been shown to be controlled in  $\beta$ -cells by the transcription factor Neurod1 (Gu et al., 2010), and we had previously noted significantly decreased levels of *Neurod1* in P6 *Adrb2* cKO pancreata (not shown). Therefore, we also assessed *Neurod1* levels in isolated adult islets and found a significant decrease in female *Adrb2* cKO islets. Neurod1 is thought to be a regulator of  $\beta$ -cell maturation (Gu et al., 2010), so we assessed levels of other maturity markers in *Adrb2* cKO islets. While we saw no changes in some markers (the transcription factors Nkx5.1 and Pdx1, or Urocortin 3 [Ucn3]), we did note a significant increase in Neuropeptide Y (NPY; Figure 3.9D). NPY is of interest as it is a marker of immature  $\beta$ -cells that is thought to play a role in inhibiting insulin secretion via inhibition of adenylyl cyclase activity (Motulsky and Michel, 1988). While loss of *Adrb2*-G<sub>s</sub> signaling could be the cause of the decreased cAMP levels we saw in *Adrb2* cKO islets, increased NPY may also contribute to decreased cAMP

levels. We additionally noted diminished *Slc2a2* (Glut2) levels, as seen with IHC previously (Figure 3.9 D). This transcriptional profile suggests that female *Adrb2* cKO  $\beta$ -cells may be functionally immature and may have diminished insulin secretion due to not only dampened cAMP response, but also decreased expression of calcium-response GSIS genes, and failure to form the insulin secretion complex.

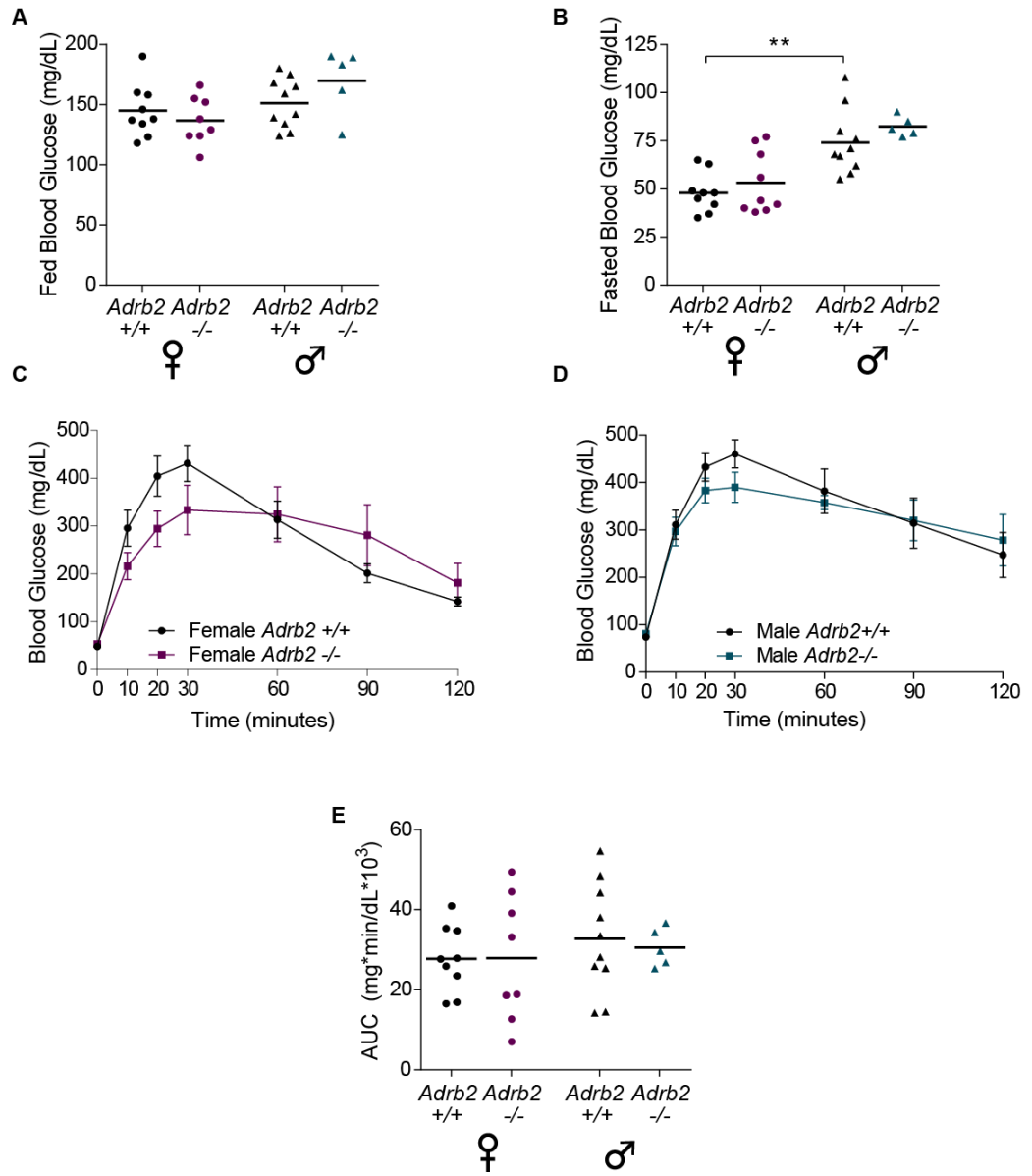
### ***Adrb2* is not required for GSIS in adult islets**

We next asked whether *Adrb2* is required in  $\beta$ -cells to regulate insulin secretion and glucose homeostasis. Therefore, we crossed floxed *Adrb2* (*Adrb2<sup>f/f</sup>*) mice with transgenic mice expressing tamoxifen-inducible Cre-ER fusion protein driven by the *Pdx1* promoter (*Tg(Pdx1-cre/Esr1\*)<sup>Dam</sup>*) (Gu, 2002). *Pdx1* expression is restricted to  $\beta$ -cells and somatostatin-expressing  $\delta$ -cells after birth (Guz, 1995; DiGruccio, 2016). Thus, tamoxifen-induced Cre activity at postnatal stages should allow for inducible ablation of *Adrb2* in  $\beta$ -cells, as well as  $\delta$ -cells, in *Pdx1-cre/Esr1\*<sup>Dam</sup>;Adrb2<sup>f/f</sup>* mice (henceforth referred to as *Adrb2* i-cKO mice). Tamoxifen was administered subcutaneously to adult (5-6 week old) female mice, and glucose tolerance and islet insulin secretion was tested 4 weeks after the final injection (Figure 3.10 A). Tamoxifen significantly induced deletion of *Adrb2* from *Adrb2* i-cKO islets (Figure 3.10 B). No changes were seen in glucose tolerance, *in vivo* insulin secretion, or islet GSIS in female tamoxifen-treated *Adrb2* i-cKO mice (Figure 3.10 C-F), suggesting that *Adrb2* is dispensable for the control of GSIS in adulthood. Because we had seen more pronounced glucose tolerance defects in aged mice, and in both males and females, we also used the *Adrb2* i-cKO mice to assess the requirement for *Adrb2* in aged islets (Figure 3.11 A). Again, we saw significant deletion of *Adrb2* from *Adrb2* i-

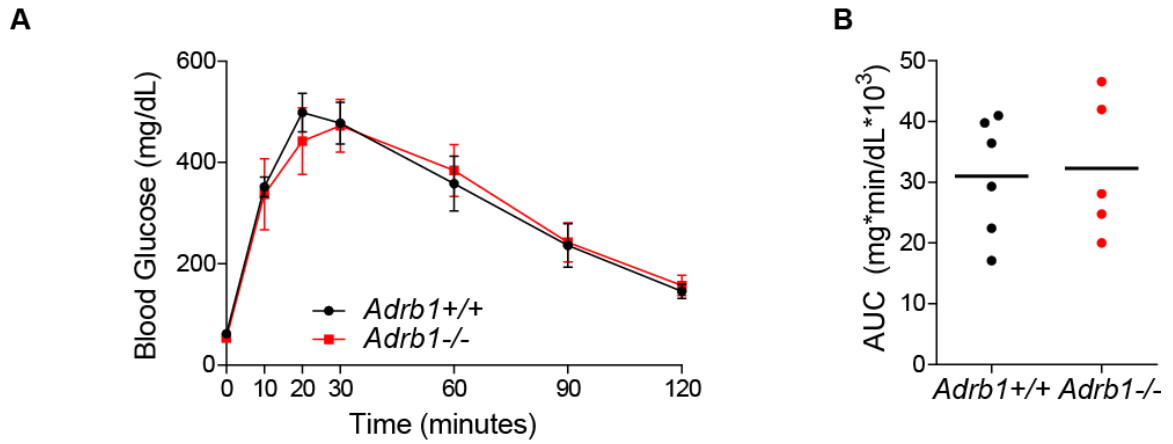
cKO islets (both male and female had similar deletion; Figure 3.11 B). We saw no defects in glucose tolerance in either female or male *Adrb2* i-cKO mice, further suggesting that *Adrb2* is dispensable for control of glucose homeostasis in adult mice (Figure 3.11 C-F).

### ***Adrb2* is required in $\beta$ -cells for metabolic homeostasis**

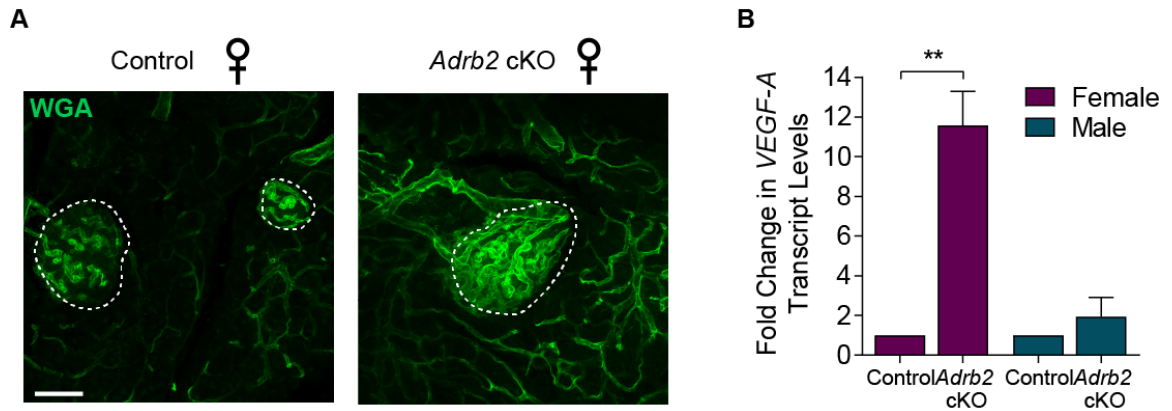
Because the *Adrb2* cKO mice are a pan-pancreatic deletion, and the *Adrb2* i-cKO mice are a  $\beta$ -cell specific deletion, there is also a possibility that *Adrb2* is required (for islet GSIS) in non- $\beta$ -cells. To address this, we administered tamoxifen to neonatal (P0-P1) female *Adrb2* i-cKO mice to delete *Adrb2* from  $\beta$ -cells before we saw it to be required in the pancreas (Figure 3.12 A). We then let the mice grow to 2 months of age. We saw efficient deletion of *Adrb2* in islets isolated from neonatally injected *Adrb2* i-cKO mice (Figure 3.12 B). Excitingly, we also saw defects in glucose tolerance and *in vivo* insulin secretion similar to those seen in *Adrb2* cKO mice, suggesting that the defects seen in *Adrb2* cKO mice were indeed due to loss of *Adrb2* from  $\beta$ -cells (Figure 3.12 C-F). This also further suggests that *Adrb2* is developmentally required, but not required in the adult for GSIS.



**Figure 3.1. Global Adrb2 knockout mice have slightly dampened glucose response at 2 months of age.** (A-B) Fed and fasted blood glucose levels are unchanged in male and female mice lacking the  $\beta$ 2-adrenergic receptor. Male mice have significantly higher fasted blood glucose levels than female mice. Means for n= 5-10 mice/sex/genotype; one-way ANOVA with Tukey's post-test  $**p<0.01$ ). (C-D) Glucose tolerance is enhanced in (C) female and (D) male Adrb2<sup>-/-</sup> mice. Mean  $\pm$  SEM for n= 8 female mice/genotype, 10 male control and 5 male Adrb2<sup>-/-</sup> mice. (E) Area under the curve (AUC) for female and male glucose tolerance.

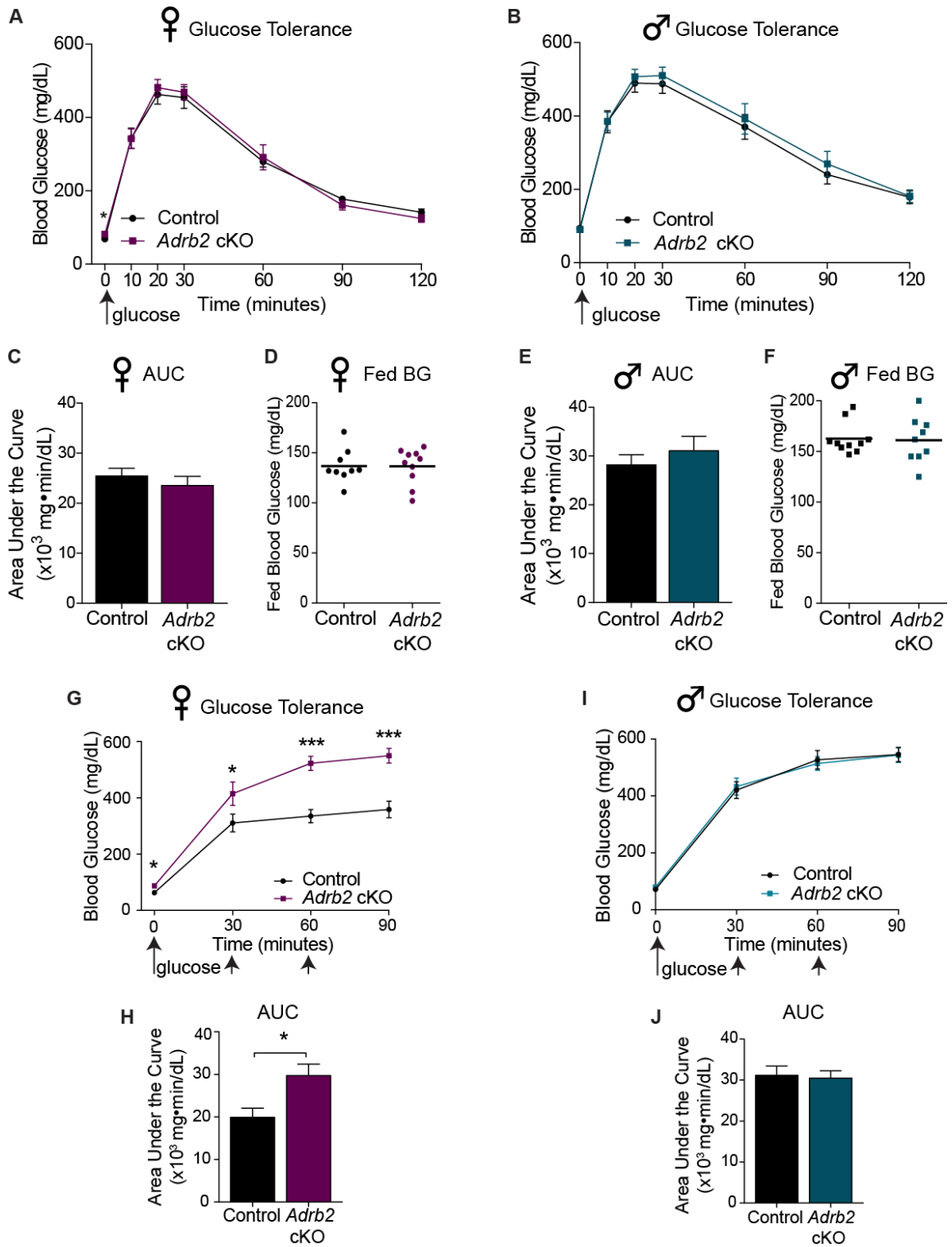


**Figure 3.2. Global loss of *Adrb1* does not affect glucose tolerance.** (A) Glucose tolerance test shows no changes in glucose levels following glucose challenge in mice lacking *Adrb1*. Means  $\pm$  SEM for n= 5-6 mixed sex mice/genotype. (B) Area Under the Curve (AUC) for glucose tolerance.

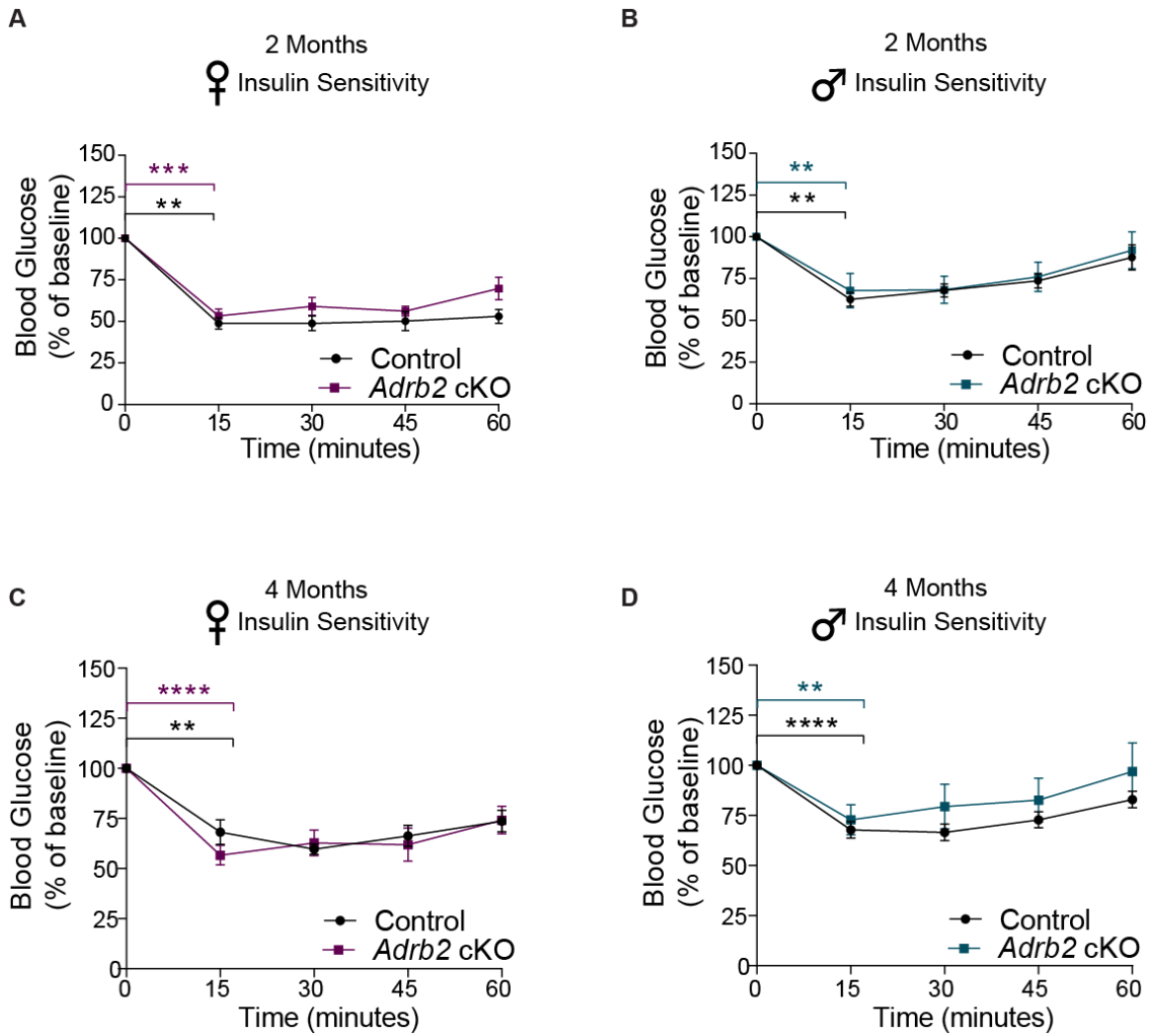


**Figure 3.3 Developmental Vegf-a dependent vascular changes persist in *Adrb2* cKO adults.** (A) Wheat Germ Agglutinin (WGA) vessel painting shows hyper-vascularization persists in adult female *Adrb2* cKO islets (outlined in white). Scale bar 50 $\mu$ m. (B) *Vegf-a* mRNA levels are significantly increased in islets isolated from adult female *Adrb2* cKO mice, and unchanged in male *Adrb2* cKO islets (n=3-5 mice/sex/genotype; one sample *t*-tests \*\*p<0.01).

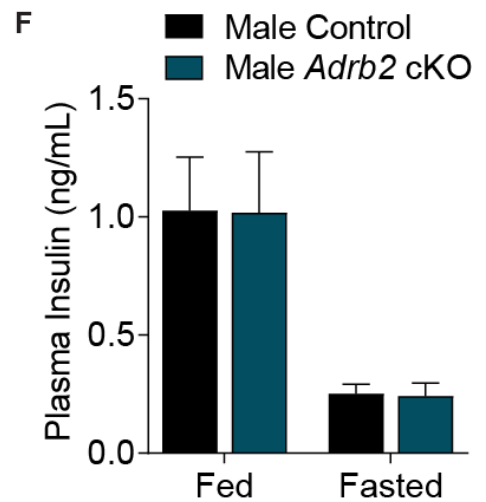
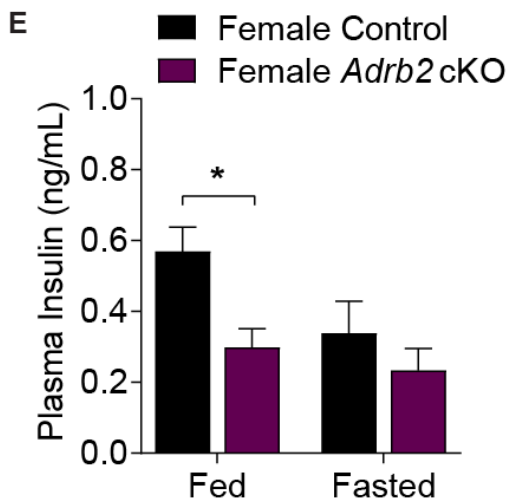
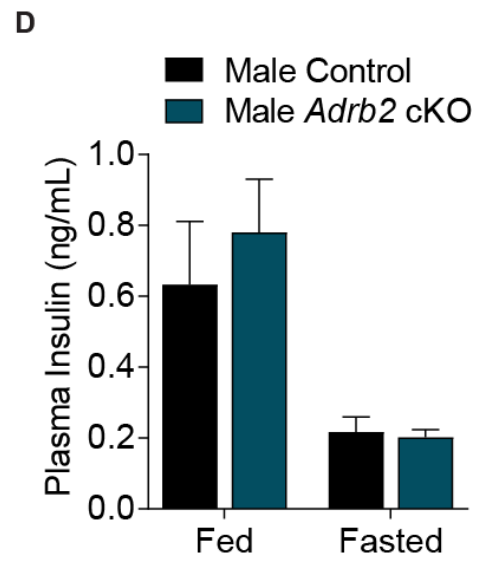
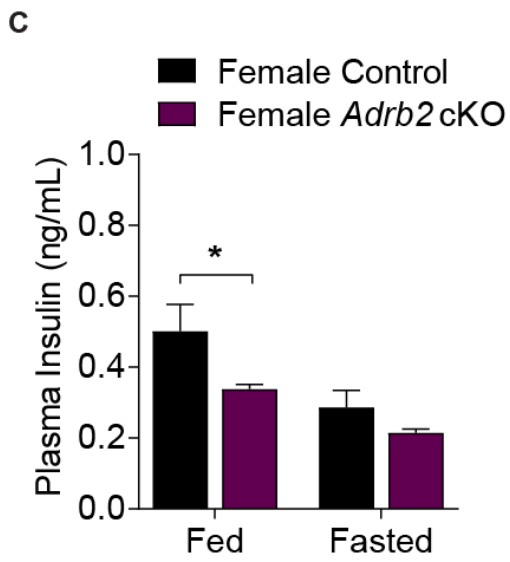
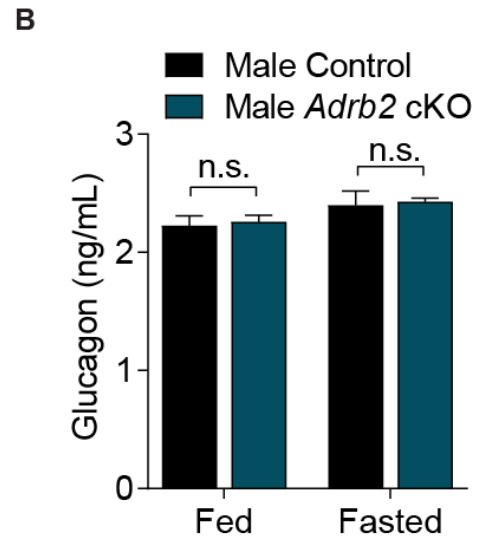
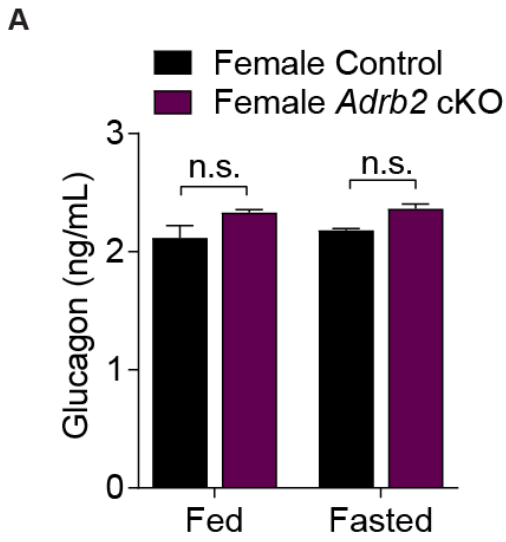




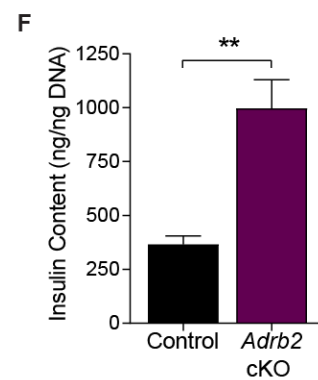
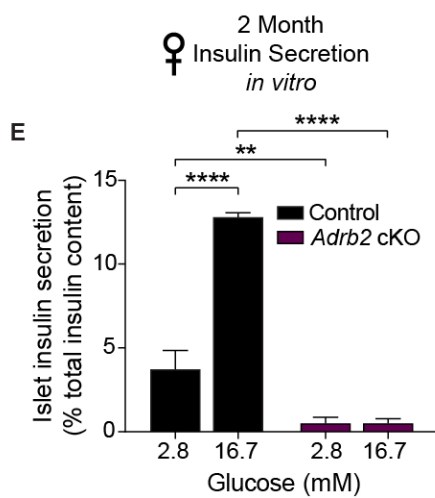
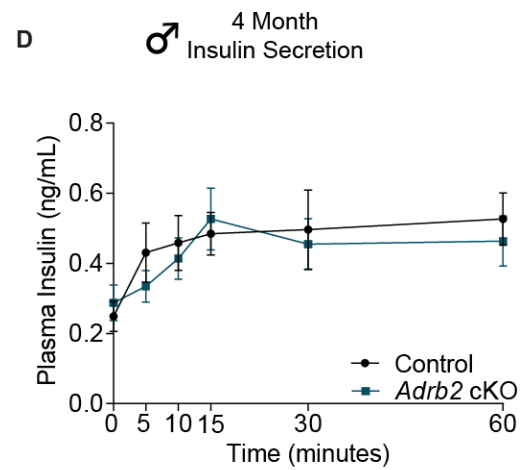
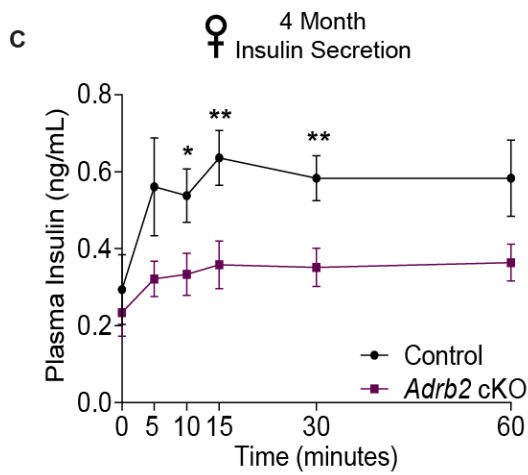
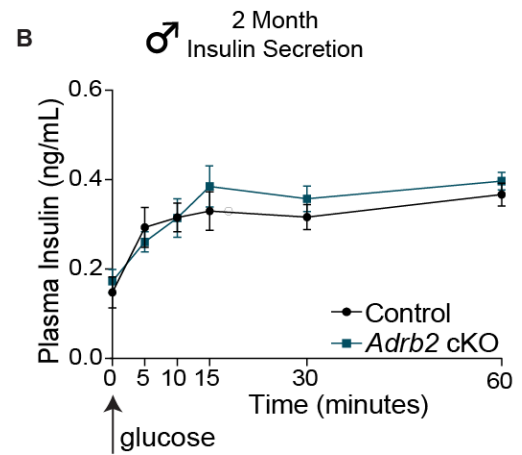
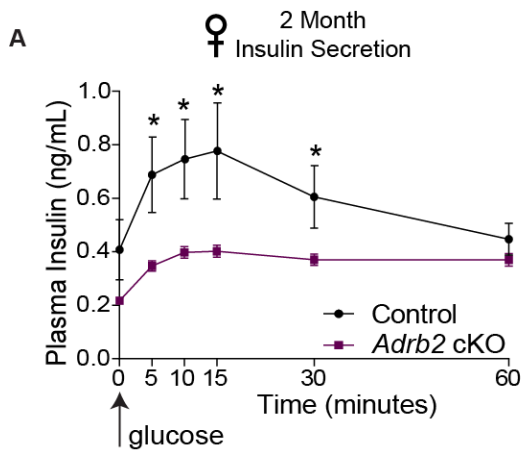
**Figure 3.4. Glucose tolerance of 2-month-old *Adrb2* cKO mice.** (A) Neither female nor (B) male *Adrb2* cKO mice show glucose tolerance defects in response to a single glucose challenge. Female *Adrb2* cKO mice have significantly higher fasted blood glucose levels compared to same-sex controls. Means  $\pm$  SEM for n= 9-10 mice/sex/genotype; *t*-tests \**p*<0.05. (C) AUC for female glucose tolerance. (D) Fed blood glucose levels are unchanged between female control and *Adrb2* cKO mice. (E) AUC for male glucose tolerance. (F) Fed blood glucose levels are unchanged between male control and *Adrb2* cKO mice. (G) In response to three consecutive glucose challenges, female *Adrb2* cKO mice display significant defects in glucose tolerance. Means  $\pm$  SEM for n= 6-7 mice/genotype; *t*-tests \**p*<0.05, \*\*\**p*<0.001. (H) AUC for female three injection glucose tolerance (\**p*<0.05, *t*-test). (I) Male *Adrb2* cKO mice display normal glucose tolerance in response to three consecutive glucose challenges. Means  $\pm$  SEM for n= 6-9 mice/genotype. (J) AUC for male three injection glucose tolerance.



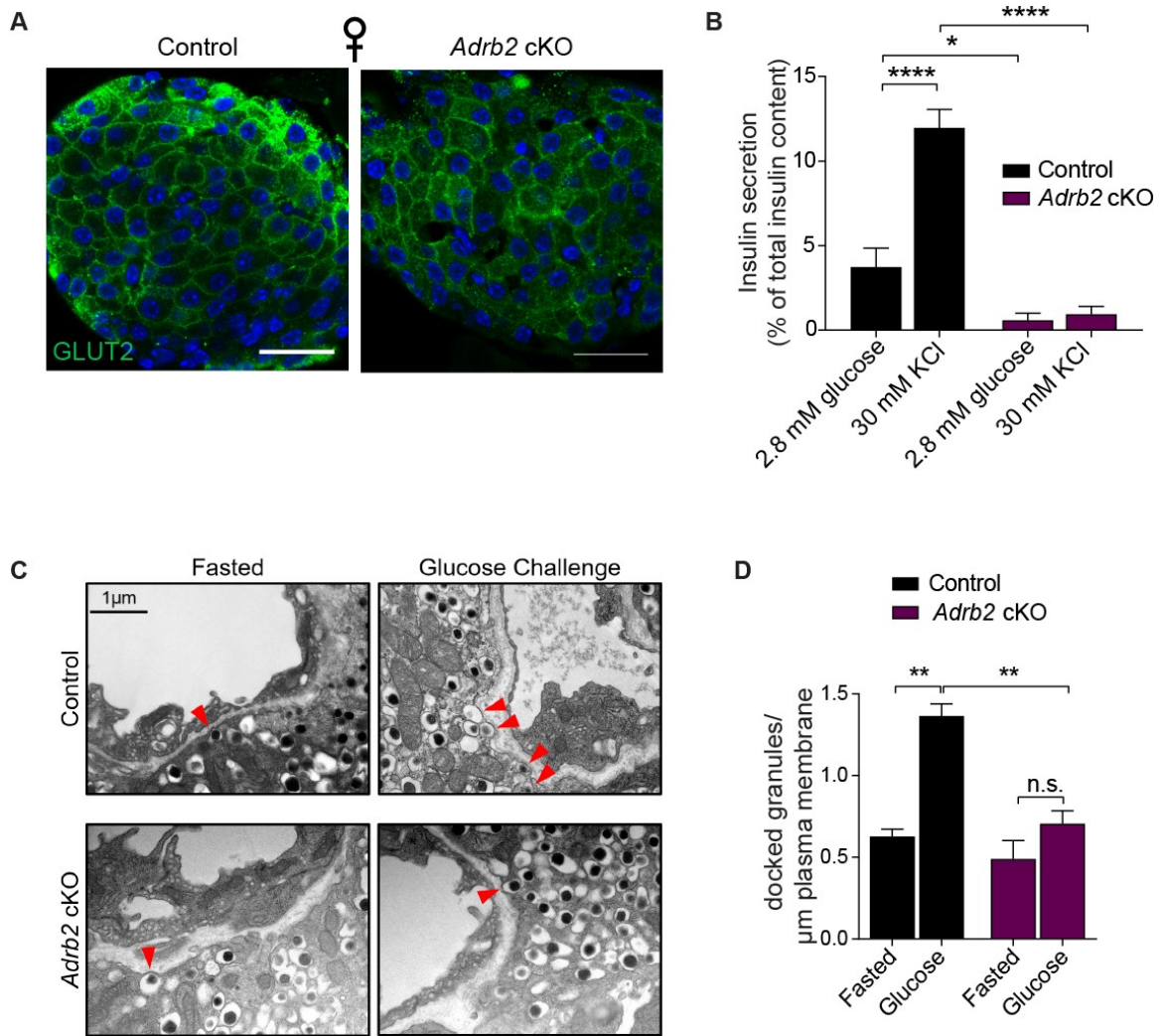
**Figure 3.5. Insulin sensitivity is unaffected by pancreatic *Adrb2* loss.** (A) 2-month-old female and (B) male *Adrb2* cKO mice are insulin sensitive. Means  $\pm$  SEM for  $n=3-6$  mice/genotype/sex; one sample *t*-tests \*\* $p<0.01$ , \*\*\* $p<0.001$ ). (C) Insulin sensitivity is maintained in 4-month-old female and (D) male *Adrb2* cKO mice. Means  $\pm$  SEM for  $n=6-12$  mice/genotype/sex; one sample *t*-tests \*\* $p<0.01$ , \*\*\*\* $p<0.0001$ ).



**Figure 3.6 Insulin and glucagon levels in female and male *Adrb2* cKO mice.** (A) Fed and fasted serum glucagon levels are unchanged in female and (B) male *Adrb2* cKO mice. Means  $\pm$  SEM for n= 3-6 mice/genotype/sex; two-way ANOVA with Bonferroni's post-test, n.s. not significant. (C) Fed plasma insulin levels are significantly reduced in female *Adrb2* cKO mice at 2 months of age. Means  $\pm$  SEM for n= 10-11 mice/genotype; two-way ANOVA with Sidak's post-test, \*p<0.05. (D) Neither fed nor fasted plasma insulin levels are changed in 2-month-old male *Adrb2* cKO mice. Means  $\pm$  SEM for n =8-10 mice/genotype; two-way ANOVA with Sidak's post-test. (E) Fed plasma insulin levels remain significantly reduced in female *Adrb2* cKO mice at 4 months of age. Means  $\pm$  SEM for n= 7-9 mice/genotype; two-way ANOVA with Sidak's post-test, \*p<0.05. (F) Fed and fasted plasma insulin levels are unchanged in 4-month-old male *Adrb2* cKO mice. Means  $\pm$  SEM for n= 8-11 mice/genotype; two-way ANOVA with Sidak's post-test.

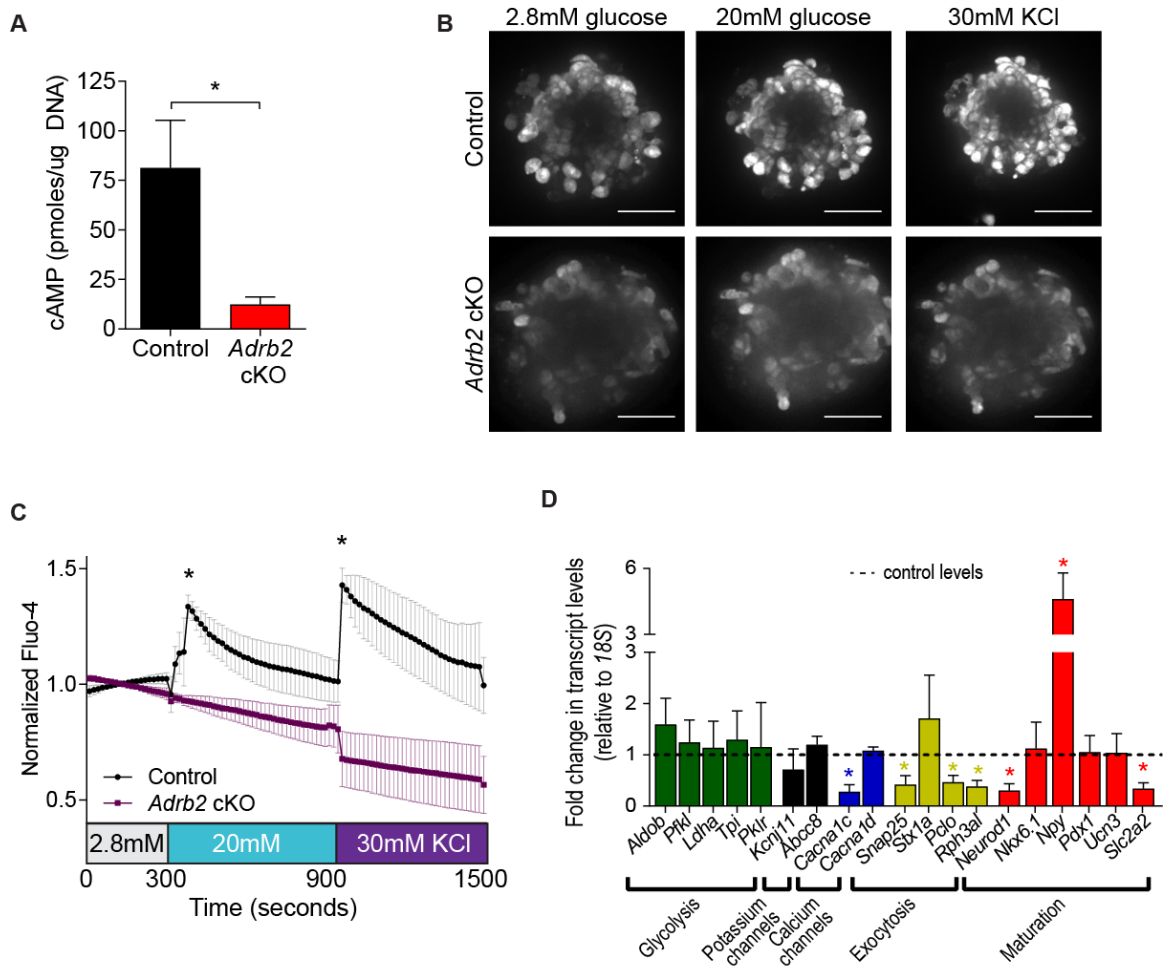


**Figure 3.7 Insulin secretion is impaired in female *Adrb2* cKO mice.** (A) Insulin secretion in response to a glucose challenge is significantly impaired in 2-month-old female, but not (B) male *Adrb2* cKO mice. Means  $\pm$  SEM for n= 5-8 mice/genotype/sex; *t*-tests, \**p*<0.05. (C) Insulin secretion remains impaired in 4-month-old *Adrb2* cKO female and unchanged in (D) 4 month old male *Adrb2* cKO mice. Means  $\pm$  SEM for n= 8-11 mice/sex/genotype; *t*-tests, \**p*<0.05, \*\**p*<0.01. (E) Insulin secretion from isolated female *Adrb2* cKO islets is significantly dampened both basally and in response to glucose challenge. Means  $\pm$  SEM for n= 4-6 mice/genotype; two-way ANOVA with Bonferroni's post-test, \*\**p*<0.01, \*\*\*\**p*<0.0001). (F) Insulin content is significantly increased in female *Adrb2* cKO islets. Means  $\pm$  SEM for n= 5-7 mice/genotype; *t*-test \*\**p*<0.01.

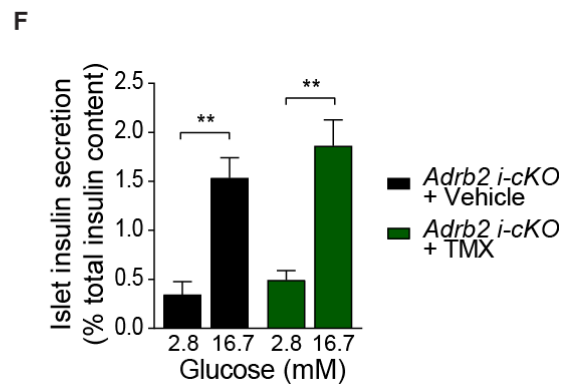
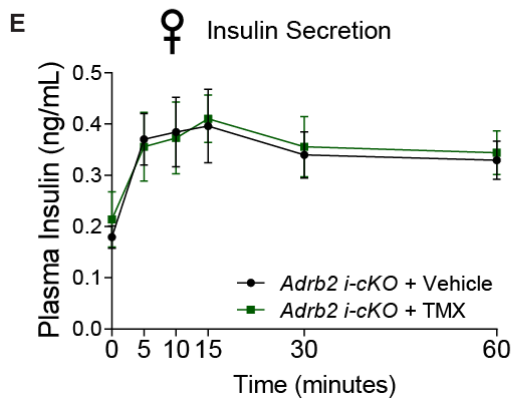
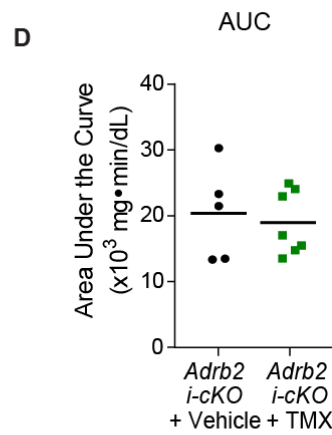
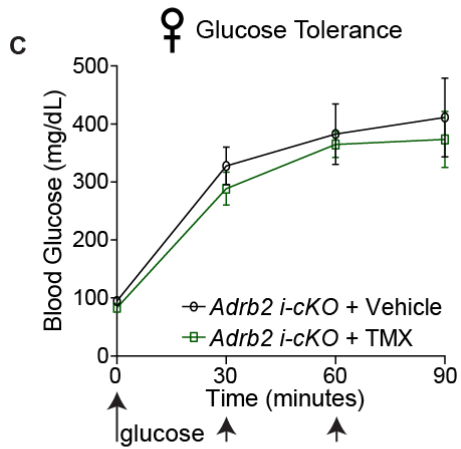
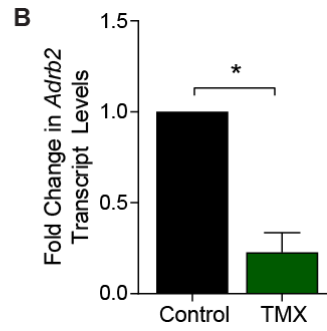
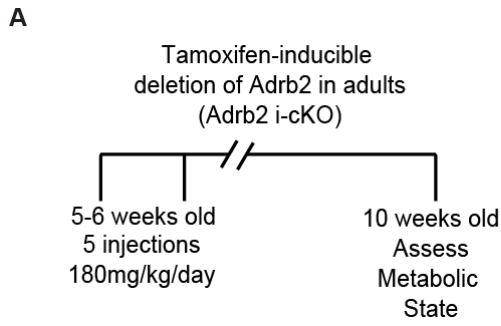


**Figure 3.8. Loss of *Adrb2* diminishes *Glut2* levels and insulin exocytosis.** (A) *Glut2* levels are decreased in female *Adrb2* cKO islets. Scale bar 25  $\mu$ m. (B) Potassium-stimulated insulin secretion is significantly diminished in isolated islets from female *Adrb2* cKO mice. means  $\pm$  SEM for n= 4-5 mice/genotype; two-way ANOVA with Bonferroni's post-test, \* $p$ <0.05, \*\*\*\* $p$ <0.0001. (C) Ultrastructural analysis of insulin granule docking reveals *Adrb2* is necessary for glucose-stimulated surface localization of insulin granules in female  $\beta$ -cells. Docked insulin granules (within 50nm of apical plasma membrane) are indicated by red arrowheads. Scale bar 1  $\mu$ m. (D) Quantification of granule docking per micrometer of plasma membrane. Means  $\pm$  SEM for n= 3 mice/genotype/condition; two-way ANOVA with Bonferroni's post-test, \*\* $p$ <0.01, n.s. not significant.

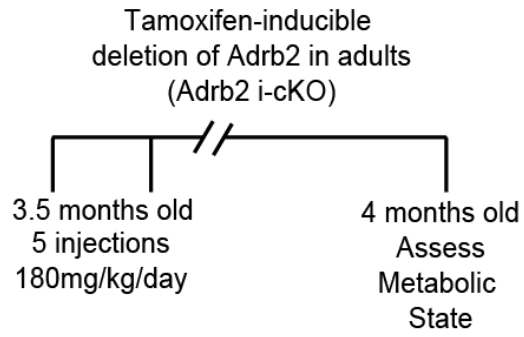
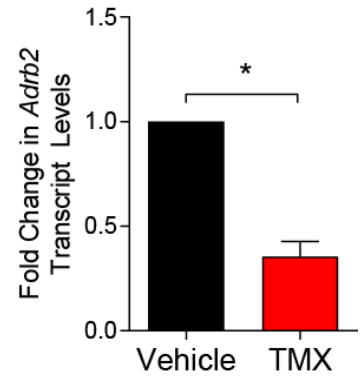
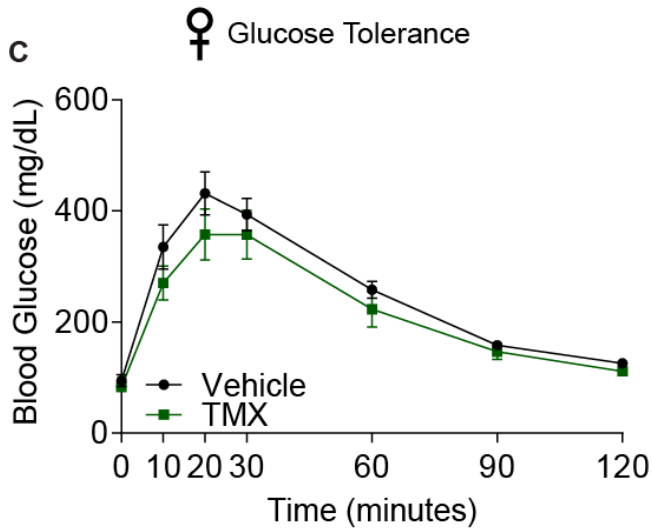
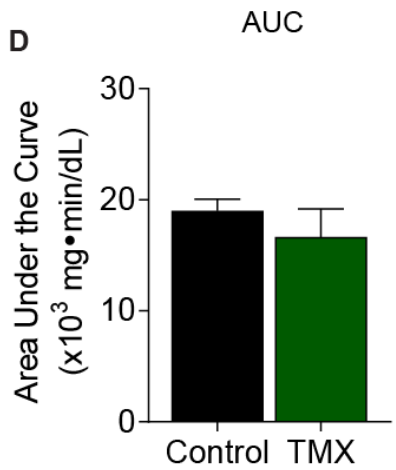
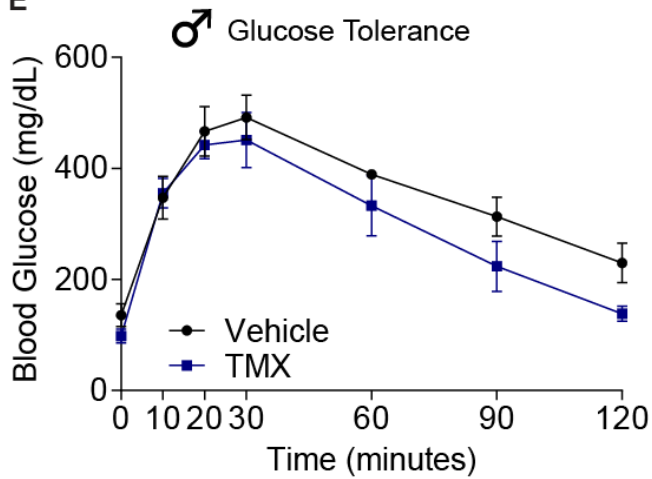
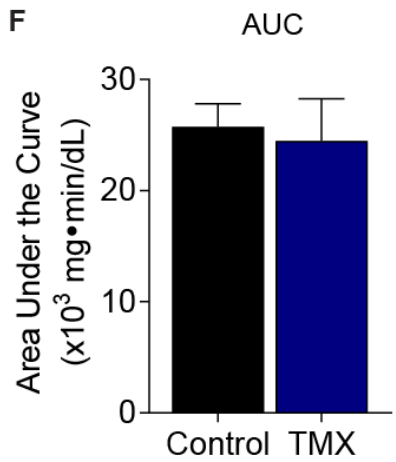




**Figure 3.9. Defects in calcium signaling in *Adrb2* cKO islets.** (A) cAMP levels are significantly decreased in female *Adrb2* cKO islets. Means  $\pm$  SEM for n= 3-4 mice/genotype; *t*-test \**p*<0.05. (B) Representative images from movies of control and *Adrb2* cKO islets loaded with Fluo-4 in response to low glucose, high glucose, and potassium chloride shows diminished calcium response in female *Adrb2* cKO islets. Scale bar 50 $\mu$ m. (C) Quantification of intracellular calcium (normalized Fluo-4 intensity) area under the curve in response to high glucose and potassium chloride. Means  $\pm$  SEM for n= 3 mice/genotype, 10 cells per mouse; *t*-tests of AUC, \**p*<0.05). (D) Female *Adrb2* cKO islets have decreased expression of genes involved in GSIS. Means  $\pm$  SEM for n= 3-5 mice/genotype; one sample *t*-tests, \**p*<0.05.



**Figure 3.10. Deletion of *Adrb2* from 2-month-old adult  $\beta$ -cells does not affect glucose homeostasis or insulin secretion.** (A) Schematic for tamoxifen-inducible deletion of *Adrb2* from adult  $\beta$ -cells. (B) *Adrb2* mRNA levels are significantly diminished in *Adrb2* i-cKO islets following tamoxifen administration. n=3 mice/condition; one sample *t*-test, \**p*<0.05. (C) Glucose tolerance is unaffected in females following adult-deletion of  $\beta$ -cell *Adrb2*. Means  $\pm$  SEM for n= 5-7 mice/condition. (D) Area under the curve (AUC) for glucose tolerance. (E) *In vivo* insulin secretion is unchanged in *Adrb2* i-cKO mice. Means  $\pm$  SEM for n= 5-6 mice/condition. (F) Islet insulin secretion is normal in female *Adrb2* i-cKO islets. Means  $\pm$  SEM for n= 3 mice/condition; two-way ANOVA with Bonferroni's post-test, \*\**p*<0.01).

**A****B****C****D****E****F**

**Figure 3.11. Deletion of *Adrb2* from 4-month-old adult  $\beta$ -cells does not affect glucose homeostasis or insulin secretion.** (A) Schematic for tamoxifen-inducible deletion of *Adrb2* from adult  $\beta$ -cells. (B) *Adrb2* mRNA levels are significantly diminished in *Adrb2* i-cKO islets following tamoxifen administration. Deletion was 60-80% independent of sex. n=3 mice/condition of mixed sex; one sample *t*-test, \*p<0.05). (C) Glucose tolerance is unaffected in females following 4-month-old adult-deletion of  $\beta$ -cell *Adrb2*. Means  $\pm$  SEM for n= 7 mice/condition. (D) Area under the curve (AUC) for female glucose tolerance. (E) Glucose tolerance is unaffected in males following 4-month-old adult-deletion of  $\beta$ -cell *Adrb2*. Means  $\pm$  SEM for n= 4-5 mice/condition. (F) Area under the curve (AUC) for male glucose tolerance.

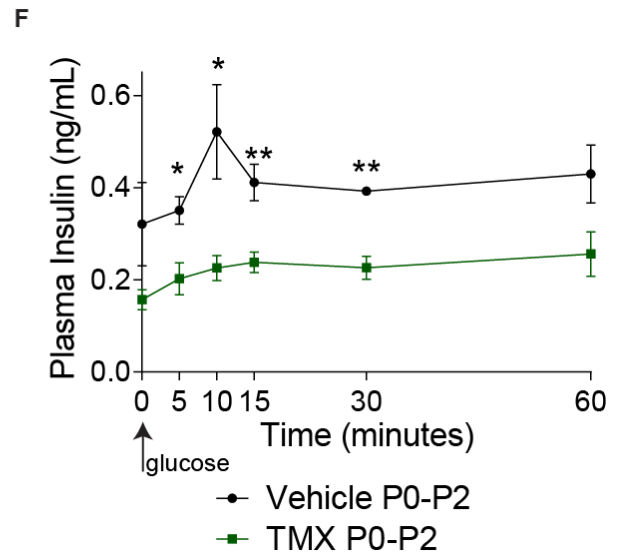
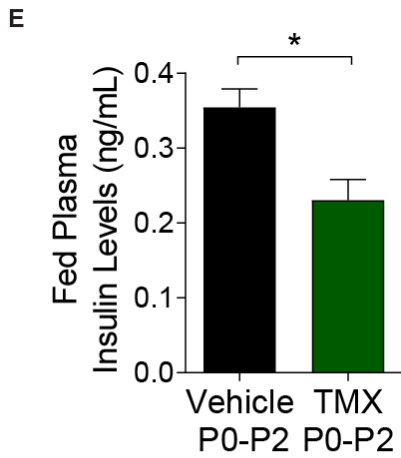
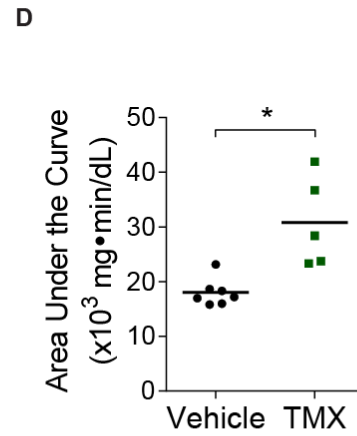
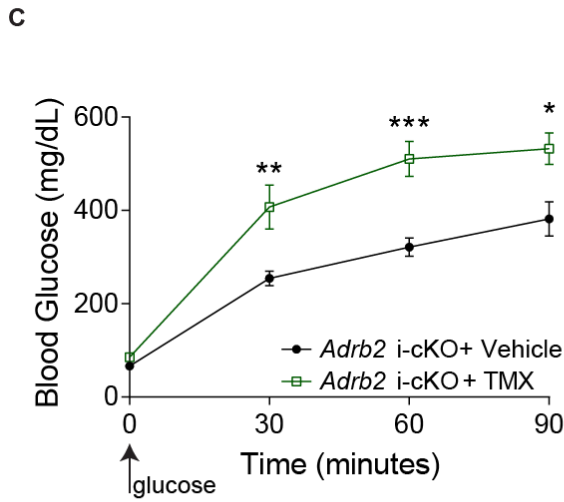
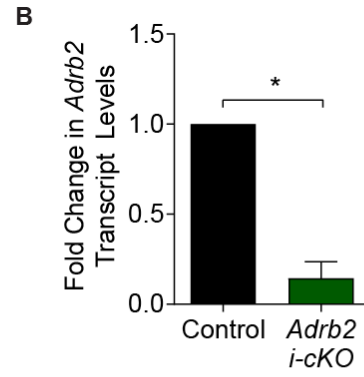
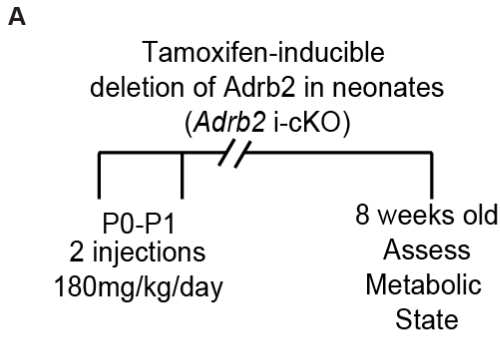


**Figure 3.12. Deletion of *Adrb2* from neonatal female  $\beta$ -cells impacts glucose homeostasis and insulin secretion.** (A) Schematic for tamoxifen-inducible deletion of *Adrb2* from neonatal  $\beta$ -cells. (B) *Adrb2* mRNA levels are significantly diminished in female *Adrb2* i-cKO islets following tamoxifen administration. n=3 female mice/condition; one-sample *t*-test, \**p*<0.05. (C) Neonatal deletion of *Adrb2* from female  $\beta$ -cells results in glucose intolerance. Means  $\pm$  SEM for n= 5-7 mice/condition. (D) Area under the curve (AUC) for female glucose tolerance. *t*-test, \**p*<0.05. (E) Fed plasma insulin levels are lower in female *Adrb2* i-cKO mice. Means  $\pm$  SEM from n= 3-4 female mice/condition; *t*-test, \**p*<0.05). (F) *In vivo* glucose-stimulated insulin secretion is diminished in *Adrb2* i-cKO female mice. Means  $\pm$  SEM for n= 4 mice/condition; *t*-tests \**p*<0.05, \*\**p*<0.01.

**Table 2.** Primer sets used in Chapter 3.

Oligonucleotides		
Sequence	Source	Identifier
Ins2-F: 5'-TGCAAGCAGCACCTTTGTG-3'	This paper	
Ins2-R: 5'-ACATGGGTGTGTAGAAGAAGCC-3'	This paper	
Adrb2-F: 5'-GGGAACGACAGCGACTTCTT-3'	This paper	
Adrb2-R: 5'-GCCAGGACGATAACCGACAT-3'	This paper	
Vegf-a-F: 5'-GCACATAGAGAGAATGAGCTTCC-3'	Ford et al, 2011	
Vegf-a-R: 5'-CTCCGCTCTGAACAAGGCT-3'	Ford et al, 2011	
Aldob-F: 5'-AGAAGGACAGCCAGGGAAAT-3'	Gu et al, 2010	
Aldob-R: 5'-GTTCAGAGAGGCCATCAAGC-3'	Gu et al, 2010	
PFKL-F: 5'-GCTGCAATGGAGAGTTGTGA-3'	Gu et al, 2010	
PFKL-R: 5'-GGATGTTGAAAGGGTCCTCA-3'	Gu et al, 2010	
LDHA-F: 5'-TGTCTCCAGCAAAGACTACTGT-3'	Gu et al, 2010	
LDHA-R: 5'-GACTGTACTTGACAATGTTGGGA-3'	Gu et al, 2010	
TPI-F: 5'-CCAGGAAGTTCTTCGTTGGGG-3'	Gu et al, 2010	
TPI-R: 5'-CAAAGTCGATGTAAGCGGTGG-3'	Gu et al, 2010	
PKLR-F: 5'-TCAAGGCAGGGATGAACATTG-3'	Gu et al, 2010	
PKLR-R: 5'-CACGGGTCTGTAGCTGAGTG-3'	Gu et al, 2010	
Kcnj11-F: 5'-AGGGCATTATCCCTGAGGAA-3'	Harvard Primer Bank	ID 6754426a1
Kcnj11-R: 5'-TTGCCTTTCTTGACACGAAG-3'	Harvard Primer Bank	ID 6754426a1
Abcc8-F: 5'-TCAACTTGTCTGGTGGTCAGC-3'	Gu et al, 2010	
Abcc8-R: 5'-GAGCTGAGAAAGGGTCATCCA-3'	Gu et al, 2010	
Cacna1c-F: 5'-ATGAAAACACGAGGATGTACGTT-3'	Harvard Primer Bank	ID 6753228a1
Cacna1c-R: 5'-ACTGACGGTAGAGATGGTTGC-3'	Harvard Primer Bank	ID 6753228a1
Cacna1d-F: 5'-AGAGGACCATGCGAACGAG-3'	Harvard Primer Bank	ID 20338999a1
Cacna1d-R: 5'-CCTTCACCAGAAATAGGGAGTCT-3'	Harvard Primer Bank	ID 20338999a1
Snap25-F: 5'-CAACTGGAACGCATTGAGGAA-3'	Harvard Primer Bank	ID 6755588a1
Snap25-R: 5'-GGCCACTACTCCATCCTGATTAT-3'	Harvard Primer Bank	ID 6755588a1
Stx1A-F: 5'-AGAGATCCGGGGCTTTATTGA-3'	Harvard Primer Bank	ID 15011853a1
Stx1A-R: 5'-AATGCTCTTTAGCTTGGAGCG-3'	Harvard Primer Bank	ID 15011853a1
Pelo-F: 5'-TACTCGGACCCATTTGTGAA-3'	Gu et al, 2010	



Pclo-R: 5'-TACTGTTTGATTCCACTCGGGATT-3'	Gu et al, 2010	
Rph3al-F: 5'-GCAGTGGAAATGATCAGTGG-3'	Gu et al, 2010	
Rph3al-R: 5'-TCAGGCACTGGCTCCTCCTC-3'	Gu et al, 2010	
Neurod1-F: 5'- ATGACCAAATCATACAGCGAGAG-3'	Harvard Primer Bank	ID 33563268a1
Neurod1-R: 5'- TCTGCCTCGTGTTCCCTCGT-3'	Harvard Primer Bank	ID 33563268a1
Nkx5.1-F: 5'-CTGCACAGTATGGCCGAGATG-3'	Harvard Primer Bank	ID 21450629a1
Nkx5.1-R: 5'CCGGTTATGTGAGCCCAA-3'	Harvard Primer Bank	ID 21450629a1
Npy-F: 5'-AGAGATCCAGCCCTGAGACA-3'	Gu et al, 2010	
Npy-R: 5'-GATGAGGGTGGAAACTTGGA-3'	Gu et al, 2010	
Pdx1-F: 5'-CCCCAGTTTACAAGCTCGCT-3'	Harvard Primer Bank	ID 22122647a1
Pdx1-R: 5'-CTCGGTTCCATTCGGGAAAGG-3'	Harvard Primer Bank	ID 22122647a1
Ucn3-F: 5'-AAGCCTCTCCACAAGTTCTA-3'	Harvard Primer Bank	ID 21492632a1
Ucn3-R: 5'-GAGGTGCGTTTGGTTGTCATC-3'	Harvard Primer Bank	ID 21492632a1
Slc2a2-F: 5'-TCAGAAGACAAGATCACCGGA-3'	Harvard Primer Bank	ID 13654262a1
Slc2a2-R: 5'-GCTGGTGTGACTGTAAGTGGG-3'	Harvard Primer Bank	ID 13654262a1
18SrRNA-F: 5'-CGCCGCTAGAGGTGAAATTC-3'	Park et al, 2016	
18SrRNA-R: 5'-TTGGCAAATGCTTTCGCTC-3'	Park et al, 2016	

## DISCUSSION

Here we demonstrate that pancreatic *Adrb2* is essential for insulin secretion and long-term glycemic control, and our results support a causal relationship between the early developmental perturbations in islet vasculature and the later functional deficits in *Adrb2* cKO mice. However, the precise molecular mechanisms by which *Adrb2* regulates *Vegf-a* production in  $\beta$ -cells remain to be determined. *Adrb2* is activated both by circulating epinephrine, derived from adrenal glands, and norepinephrine, secreted locally by sympathetic nerves, although *Adrb2* has 100-fold higher affinity for epinephrine (Molinoff, 1984). Our findings that epinephrine, but not norepinephrine, suppressed *Vegf-a* expression in MIN6 cells, together with observations of differences in phenotypes between *Adrb2* cKO and sympathectomized mice (Borden et al., 2013), suggest that epinephrine is the likely ligand responsible for *Adrb2*-mediated effects on *Vegf-a* levels and islet vasculature. *Adrb2* is a prototypical GPCR that is classically thought to couple with  $G\alpha_s$  proteins and activate transcriptional events via a cAMP-PKA-CREB pathway, which stimulates *Vegf-a* expression in several cell types (Claffey et al., 1992; Lee et al., 2009; Wu et al., 2007). However, association of GPCRs with specific  $G\alpha$  proteins is dependent upon the cellular context. Our findings suggest that in pancreatic  $\beta$ -cells, *Adrb2* might act via  $G\alpha_i$  to negatively regulate cAMP-mediated transcriptional signaling and thus repress *Vegf-a* levels. In support of this idea, loss of *Adrb2* enhanced CREB phosphorylation in bone osteoblasts (Kajimura et al., 2011). However, we did note decreased cAMP levels in adult *Adrb2* cKO islets, which may suggest that *Adrb2* acts through a  $G\alpha_s$  to positively mediate cAMP levels. However, due to the significant transcriptional changes, specifically the robust increase in NPY, which is known to inhibit cAMP signaling (Motulsky and

Michel, 1988), we believe that the decreased cAMP levels are a secondary consequence of increased NPY, and not a direct result of *Adrb2* loss. More studies would be necessary to further elucidate this signaling pathway.

Vascular endothelial cells instruct  $\beta$ -cell gene expression and maturation, by supplying extracellular matrix molecules and soluble factors including hepatocyte growth factor and thrombospondin-1 (Eberhard et al., 2010; Hogan and Hull, 2017; Johansson et al., 2009; Johansson et al., 2006b; Olerud et al., 2011). In neonatal *Adrb2* cKO islets, we observed an upregulation of insulin expression, in agreement with previous reports of endothelial cells regulating insulin gene transcription via producing vascular basement membrane proteins (Kaido et al., 2004; Nikolova et al., 2006; Nikolova et al., 2007). Given the enhanced insulin biosynthesis in *Adrb2* cKO islets, the decrease we observed in mature  $\beta$ -cell secretory function is even more striking. We reason that this is due, in part, to reduced expression of genes associated with calcium responsiveness and exocytosis. It is unclear if these changes reflect compensatory efforts to counter excessive insulin production and protect against hypoglycemia, or a *bonafide* effect of endothelial cells in instructing mature  $\beta$ -cell phenotype. It is also plausible that enhanced insulin content in *Adrb2* cKO islets is a result of a build-up of insulin granules that are unable to be secreted.

Of note, in contrast to previous studies where Vegf-a over-expression and islet vascular hypertrophy is accompanied by  $\beta$ -cell loss, we did not observe major disruptions in  $\beta$ -cell mass or islet architecture in *Adrb2* cKO animals (Agudo et al., 2012; Brissova et al., 2014; Cai et al., 2012). This could reflect differences in the timing and levels of Vegf-a over-expression elicited by *Adrb2* loss versus transgenic over-expression of Vegf-a. Early increases in Vegf-a expression and islet vascular density preceding the onset of

hyperglycemia have been observed in animal models of type 2 diabetes (Li et al., 2006). An expanded islet capillary network has also been noted in human islets from individuals with type 2 diabetes (Brissova et al., 2015), although the patterning and density of the human islet micro-vasculature differs significantly from that in rodents (Brissova et al., 2015). Together, these studies underscore the need to fully delineate the pathways underlying the tight control of  $\beta$ -cell-endothelial cell communication and their long-term impact on islet function.

Our results support a causal relationship between the early developmental perturbations in islet vasculature and the later functional deficits in *Adrb2* cKO mice. That *Adrb2* loss from mature  $\beta$ -cells did not impair insulin secretion was surprising in the context of previously reported effects of  $\beta$ 2-adrenergic agonists on acutely stimulating insulin release from adult islets (Ahren and Schersten, 1986; Lacey et al., 1993). Thus, in adult islets, the effects of *Adrb2* agonists on insulin release are likely indirect, perhaps via regulating glucagon release from  $\alpha$ -cells (Ahren and Schersten, 1986), or suggest species-specific differences in adult *Adrb2* functions in  $\beta$ -cells. The effects of *Adrb2* on neonatal islet vascularization overlap with the current model of  $\beta$ -cell maturation (Qiu et al, 2017). This suggests that intra-islet vasculature may play an instructive role in promoting  $\beta$ -cell maturation, and that *Adrb2* may be a major regulator of this process. Previous studies have shown that islet *Adrb2* levels decline over time, and it was hypothesized that the age-related loss contributes to adult phenotypes (Berger et al, 2015; Santulli et al, 2012). While we additionally note *Adrb2* levels diminishing in adult islets, we hypothesize that this is because *Adrb2* is no longer required in adult islets. Our study reveals that  $\beta$ -cell *Adrb2* is required in neonates for long-term glycemic control. In contrast, *Adrb2* in adult  $\beta$ -cells is

dispensable for glucose tolerance and insulin secretion. Together with the declining expression data, this suggests that the primary role for  $\beta$ -cell *Adrb2* is in programming neonatal islet vasculature, and that *Adrb2* levels decline with age because *Adrb2* is no longer required.

$\beta$ -adrenergic receptors have been best characterized for mediating diverse physiological responses to stress in adult mammals and are one of the most common targets of therapeutic drugs.  $\beta$ -adrenergic receptor antagonists ( $\beta$ -blockers) are commonly used to treat cardiovascular disease and hypertension, including in pregnant women (Easterling, 2014; Parati and Esler, 2012; Sharma et al., 2001), and administered to infants for treating hemangiomas (Chinnadurai et al., 2016). Our findings in mice suggest that inhibition of pancreatic *Adrb2* activity during development could have a lasting impact on glycemic control.

# METHODS

## Mice

All procedures relating to animal care and treatment conformed to The Johns Hopkins University Animal Care and Use Committee (ACUC) and NIH guidelines. Animals were group housed in a standard 12:12 light-dark cycle. Mice were maintained on a *C57BL/6* background, or mixed *C57BL/6* and *129P*, or *C57BL/6* and *FVB* backgrounds. Since phenotypes were specific to female mutant mice, animals of both sexes were used for initial analyses, and the sex of the animals used are clearly noted throughout the study. *Pdx-Cre* (*B6.FVB-Tg(Pdx1-cre)6Tuv/Nci*; RRID: IMSR\_NCIMR:01XL5) mice were obtained from NCI Frederick Mouse Repository. *MIP-GFP* (*B6.Cg-Tg(Ins1-EGFP)1Hara/J*; RRID: IMSR\_JAX:006864) mice were obtained from Jackson Laboratory. *Adrb2<sup>fl</sup>* mice were a generous gift from Dr. Gerard Karsenty (Hinoi et al, 2008).

## Vessel Painting

2-5 month old mice were anesthetized with 200 mg/kg avertin (intra-peritoneal injection) and perfused with 6µg/mL Alexa-488 conjugated wheat germ agglutinin (WGA; Life Technologies W11261). Pancreata were then dissected, incubated in 30% sucrose overnight, equilibrated in 1:1 Sucrose:OCT, then embedded in OCT and stored at -80°C. Floating 400µm cryo-sections were collected into 1X PBS. Sections were treated with 1% TritonX-100 for 1 hour at room temperature, blocked in 2% TritonX-100; 10% goat serum; 0.02% sodium azide for 1 hour at room temperature, then incubated in primary antibody

(1:50 guinea pig anti-insulin) in antibody buffer (0.25% TritonX-100; 1% goat serum; 0.02% sodium azide in 1X PBS) at room temperature for 24 hours. Sections were then washed and incubated in secondary antibody (anti-guinea pig Alexa-546 at 1:200; DAPI at 1:1000) in antibody buffer at room temperature for 2 hours. Sections were cleared with 2:1 benzyl benzoate:benzyl alcohol overnight at room temperature, mounted, and Z-stacks of 1 $\mu$ m optical slices were taken using a Zeiss LSM 700 confocal microscope equipped with 405, 488, 555, and 633 lasers. Maximum intensity projections through equal tissue depths were generated with FIJI.

### **Other IHC**

50 $\mu$ m cryosections were taken from P6 mouse pancreata, then washed with PBS, permeabilized in 1% Triton X-100 in PBS, and blocked for 1 hour at room temperature using 5% goat serum (GS) in PBS + 0.1% Triton X-100. Sections were then incubated for 2 nights at 4°C with either: rat anti-PECAM-1/CD-31 antibody (1:300), rabbit anti-TH antibody (1:500), rabbit anti-collagen IV (1:500), or chicken anti-laminin (1:200) in conjunction with guinea pig anti-insulin (1:300). Following PBS washes, sections were then incubated with anti-rat Alexa-546, anti-rabbit Alexa 488 or 647, anti-chicken 488 or 647, and anti-guinea pig 488, 546, or 647 secondary antibodies (1:200; ThermoFisher). Sections were then washed in PBS and mounted in Fluoromount Aqueous Mounting Medium containing 100 $\mu$ g/mL DAPI. Z-stacks of 1 $\mu$ m optical slices were taken using a Zeiss LSM 700 confocal microscope equipped with 405, 488, 555, and 633 lasers. Maximum intensity projections were generated with FIJI, and quantification of sympathetic innervation density was done by calculating integrated TH fluorescence

density per unit area (FIJI) from multiple random images. Quantification of islet vasculature density was done by calculating integrated PECAM-1/CD-31 density per islet (ROI set by insulin immunoreactivity) area (FIJI) from multiple random images.

## **Metabolic Assays**

### *Glucose Tolerance*

Young adult (2-4-month-old) mice were individually housed and fasted overnight (16 hours) before being given a 2g/kg intraperitoneal (IP) glucose injection. Blood glucose levels were measured with a OneTouch Ultra 2 glucometer before glucose injection, and 2 additional 2g/kg glucose injections were given at 30 minutes and 60 minutes after the first injection. Glucose levels were monitored over a 1.5-hour period.

### *In vivo insulin tolerance*

Mice were individually housed overnight with *ad libitum* food and water before being given a 0.75U/kg IP insulin injection (Novolin-R). Blood glucose levels were measured with a OneTouch Ultra 2 glucometer before insulin injection, and every 15 minutes post-injection over a 1-hour period.

### *In vivo insulin secretion*

Mice were individually housed and fasted overnight (16 hours) before being given a 3g/kg IP glucose injection. Plasma insulin levels were measured with an Ultrasensitive Insulin



ELISA kit (Crystal Chem) before fasting (fed), the next morning before injection, and over a 1-hour period following injection.

### ***Mouse islet isolations***

Islets were isolated as previously described (Wollheim et al, 1990). Islets were isolated by collagenase distension through the bile duct (Collagenase P [Roche], 0.375-0.4mg/mL in HBSS) and digestion at 37°C. Digested pancreata were washed with HBSS + 0.1% BSA and subjected to discontinuous density gradient using histopaque (6:5 Histopaque 1119:1077; Sigma-Aldrich). The islet layer (found at the interface) was collected and islets were handpicked under an inverted microscope for subsequent analysis.

### ***In vitro insulin secretion***

Isolated islets were cultured overnight in RPMI-1640 (5% FBS, 5U/L penicillin-streptomycin). Islets were then handpicked to be size and quantity matched, and 5-10 islets/mouse were washed and pre-incubated for 1 hour in Krebs-Ringer HEPES buffer (KRHB) containing 2.8mM glucose. Islets were then incubated in 2.8mM or 16.7mM glucose, or 30mM KCl in KRHB for another 30 minutes. Supernatant fractions were removed, and islets lysed in acid-ethanol overnight and subsequently neutralized in Tris buffer (0.885M). Both cellular and supernatant fractions were subjected to insulin ELISA (Crystal Chem). Total insulin was normalized to DNA by Quant-it PicoGreen dsDNA kit (Invitrogen).

## **Transmission Electron Microscopy**

Pancreata were dissected from control and *Adrb2* cKO mice that had either been fasted or given a 3mg/kg glucose challenge (15 minutes) and cut into ~1mm<sup>3</sup> pieces then fixed in 3% formaldehyde + 1.5% glutaraldehyde +2.5% sucrose in 0.1M NaCacodylate + 5mM CaCl<sub>2</sub>, pH 7.4 at room temperature for 1 hour. Pieces were then washed in 2.5% sucrose in 0.1M NaCacodylate + 5mM CaCl<sub>2</sub> and post-fixed with 1% Palade's OsO<sub>4</sub> for 1 hour on ice, followed by incubation in Kellenberger's uranyl acetate overnight at room temperature. Samples were then dehydrated with a graded alcohol series (50%, 75%, 95%, and 100% ethanol, then propylene oxide), embedded in Epon, and sectioned (~90nm) and collected onto EM grids. Grids were then imaged using an FEI Tecnai-12 TWIN transmission electron microscope operating at 100 kV and a SIS MegaView III wide-angle camera. A minimum of three  $\beta$ -cells adjacent to a vessel per animal were quantified, and granules were considered docked if they were within 50nm of the apical plasma membrane.

## **Calcium imaging**

Isolated islets were cultured overnight on laminin-coated (0.05-0.1mg/mL in HBSS + Ca<sup>2+</sup> + Mg<sup>2+</sup>) MatTek 35mm, No. 1.5 coverslip, 20mm glass diameter dishes in high glucose DMEM + L-glutamine supplemented with 10% fetal bovine serum (FBS), 5mL sodium pyruvate, 5U/L penicillin-streptomycin, and 2 $\mu$ l  $\beta$ -mercaptoethanol. Adhered islets were loaded with 4 $\mu$ M Fluo-4 AM (ThermoFisher) for 45 minutes in KRHB with 2.8mM glucose, then washed and incubated for 30 additional minutes in KRHB with 2.8mM glucose on a stage incubator (37°C and 5% CO<sub>2</sub>) for equilibration prior to imaging. Z-

stacks representing 1µm optical slices of individual islets were collected every 15 seconds on a Zeiss AxioObserver Yokogawa CSU-X1 spinning disk confocal equipped with dual Evolve EMCCDs and 405, 488, 555, and 633 nm lasers. Zen Blue (2012) image collection software was used to maintain experimental parameters between individual experiments. Concentrated glucose was added by hand after 5 minutes and of background fluorescence collection (final concentration 20mM) and imaging continued for 10 minutes, before addition of concentrated KCl by hand (final concentration 30mM) to depolarize membranes. Imaging continued for 10 additional minutes, for a total of 25 minutes. No more than 30 seconds elapsed between imaging conditions.

### **qRT-PCR**

RNA from either whole pancreata (P6) or isolated islets (adult) was isolated using TRIzol RNA extraction reagent phenol-chloroform extraction and ethanol precipitation. RNA from sorted cells was isolated using Direct-zol RNA Microprep (Zymo) kit. 1.5-2µg of total RNA was reverse-transcribed into cDNA with M-MLV Reverse Transcriptase (Promega). TaqMan assays (ThermoFisher) were used to quantitatively determine transcript levels of the adrenergic receptors, while Maxima SYBR Green/Rox Q-PCR Master Mix (ThermoFisher) reagents and primer sets (listed in Key Resources Table) were used to determine transcript levels for other genes. Both assays were performed in a StepOnePlus Real-Time PCR System (ThermoFisher). Fold change in transcript levels was calculated using the  $2^{(-\Delta\Delta C_t)}$  method, and 18S was used as an endogenous control for normalization.

## **Tamoxifen injections**

### *Neonatal deletion*

*Adrb2* i-cKO mice were injected subcutaneously with 180mg/kg tamoxifen (Sigma) in corn oil or corn oil alone at P0 and P1. Mice were subjected to metabolic assays at eight weeks of age.

### *Adult deletion*

Beginning at five-six weeks of age, *Adrb2* i-cKO mice were injected subcutaneously with 180mg/kg tamoxifen (Sigma) in corn oil or corn oil alone, every day for five days. Four weeks after the last injection, vehicle- and tamoxifen-injected mice were subjected to metabolic assays.

## **QUANTIFICATION AND STATISTICAL ANALYSIS**

Sample sizes were similar to those reported in previous publications (Borden et al., 2013; Houtz et al., 2016). For practical reasons, analyses of endocrine cell counts and quantifications from ultrastructural analyses (caveolae and fenestrae density, insulin granule density, insulin granule docking) were done in a semi-blinded manner, such that the investigator was aware of the genotypes prior to the experiment, but conducted the staining and data analyses without knowing the genotypes of each sample. All Student's *t*-tests were performed assuming Gaussian distribution, two-tailed, unpaired, and with a confidence interval of 95%, with the exception of fold change analyses (such as for qPCR),

which were done using a one sample t test. One-way ANOVA analyses with post hoc Tukey test or two-way ANOVA analyses with post hoc Bonferroni test were performed when more than 2 or 3 groups were compared, respectively. Statistical analyses were based on at least 3 independent experiments and described in the figure legends. All error bars represent the standard error of the mean (S.E.M.).

**CHAPTER 4: DEVELOPMENTAL  
ADRB2-MEDIATED VASCULAR  
REPRESSION IS REQUIRED FOR  
MATURE ISLET FUNCTION**

# INTRODUCTION

Developmental loss of  $\beta$ -cell Vegf-a and subsequent islet vasculature loss results in metabolic defects, in part due to insufficient exchange of hormones between  $\beta$ -cells and the bloodstream (Brissova et al., 2006; Lammert et al., 2003). In contrast, hyper-vascularization of islets during development by overexpression of  $\beta$ -cell Vegf-a also results in glucose intolerance (Cai et al., 2012). However, loss of Vegf-a, and subsequent decrease in islet vasculature in adult islets has little effect on islet function (Reinert et al., 2013), suggesting a larger role for developmental Vegf-a signaling and islet vascular patterning in programming adult islet function. Islet endothelial cells also produce the vascular basement membrane, a specialized extracellular matrix consisting of collagen and laminin proteins that offer structural support, influence  $\beta$ -cell proliferation, and insulin gene transcription (Kaido et al., 2004; Nikolova et al., 2006; Nikolova et al., 2007). The signaling mechanisms controlling developmental vasculature patterning are not well understood, and there remains a need to fully delineate how islet vasculature is established, and how neonatal vascular patterning affects adult islet function. Here, we have shown that loss of *Adrb2* in the pancreas results in increased intra-islet vasculature and functional defects in islet insulin secretion, in part due to an immature transcriptional profile. The question still remains, however, whether the developmental changes in islet vasculature are causal to the adult metabolic phenotypes. Previous studies have suggested that islet vascularization via Vegf-a is essential during development, but dispensable during adulthood (Reinert et al, 2013) to maintain glucose homeostasis. This is likely due to signaling through VEGFR-2 (KDR or Flk1), the primary Vegf-a receptor expressed in intra-islet endothelial cells (Brissova et al., 2006; Kim et al., 2011). Therefore, to assess if

the metabolic phenotypes seen in *Adrb2* cKO mice were due to the increased islet vasculature, we used a blocking antibody against VEGFR-2 (Kim et al, 2011) to normalize the islet vasculature in *Adrb2* cKO neonates.



## RESULTS

### **Blocking Vegf-a signaling ameliorates *Adrb2* cKO morphological defects**

To investigate the underlying cause of the metabolic defects observed in *Adrb2* cKO mice, we hypothesized that the excess vasculature caused by *Adrb2* deletion was the primary contributor to the metabolic defects. This hypothesis is built in part due to the published reports that vascular imbalance in islets results in glucose intolerance (Cai et al., 2012; Reinert et al., 2013). To test this hypothesis, we used a vascular endothelial growth factor receptor 2 (VegfR-2/Flk1) blocking antibody to prevent the excess islet vasculature from occurring in *Adrb2* cKO mice (Kim et al., 2011). Because we did not see increased Vegf-a transcription and islet hyper-vascularization in *Adrb2* cKO mice before P2 (see Figures 2.4 and 2.6), we began injections with the blocking antibody at P0 so we could block the hyper-vascularization from occurring. We injected mice at P0 and P3 and then either collected them at P6 or gave them a final injection and allowed them to grow to adulthood (Figure 4.1 A). Injections were stopped at P6 as islet vascularization is thought to be complete by that stage (Johansson et al., 2006a). Antibody-injected *Adrb2* cKO mice survived to adulthood, had normal body weight, and did not exhibit any gross morphological abnormalities. Injection of the blocking antibody restored islet vasculature to control levels, as seen by IHC for PECAM1 (Figure 4.1 B-C). We additionally saw normalization of the basement membrane markers laminin and collagen IV (Figure 4.1 D). Because excess insulin production is a consequence of increased islet vasculature (Nikolova et al., 2006), and we demonstrated insulin production is increased in *Adrb2* cKO hyper-vascularized islets, we assessed *Ins2* transcript levels in antibody injected *Adrb2*

cKO pancreata. We found *Ins2* transcription to be indistinguishable from control animals, and significantly reduced from control-injected *Adrb2* cKO animals (Figure 4.1 E). This suggests the increased insulin in *Adrb2* cKO islets is a consequence of increased vasculature.

### **Blocking Vegf-a signaling ameliorates *Adrb2* cKO functional defects**

In order to determine the contribution of the developmental morphological defects to the glucose intolerance observed in *Adrb2* cKO animals, we assessed the metabolic profile in antibody injected *Adrb2* cKO animals. Developmental blockade of islet hypervascularization in *Adrb2* cKO mice ameliorated the glucose intolerance seen in untreated *Adrb2* cKO females to control levels (Figure 4.2 A-B). We additionally saw significant rescue of *in vivo* insulin secretion defects in antibody-injected *Adrb2* cKO mice (Figure 4.2 C). To be sure that restored glucose tolerance was due to restored islet insulin secretion, we assessed GSIS *in vitro* and saw full rescue of glucose-stimulated insulin secretion from antibody-injected *Adrb2* cKO islets (Figure 4.2 D). Finally, we screened islets from *Adrb2* cKO females that had been treated with the VegfR2/Flk1 blocking antibody. Excitingly, we saw normalization of transcript levels of all GSIS genes as well as *Neurod1* (Figure 4.3 A). Together, these results suggest that *Adrb2*-dependent developmental vascular patterning through Vegf-a is required for acquisition of genes involved in GSIS, and whole animal metabolic homeostasis.

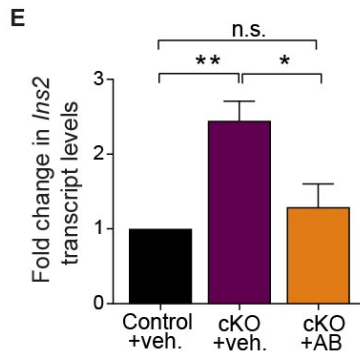
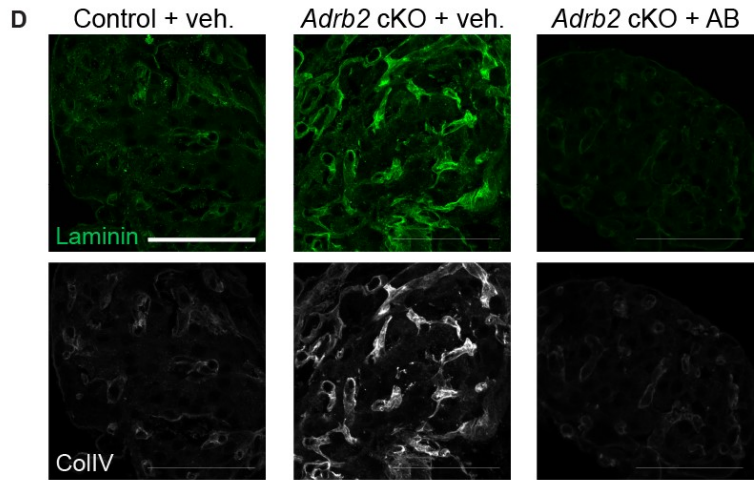
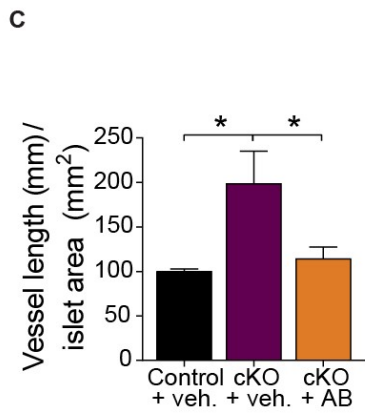
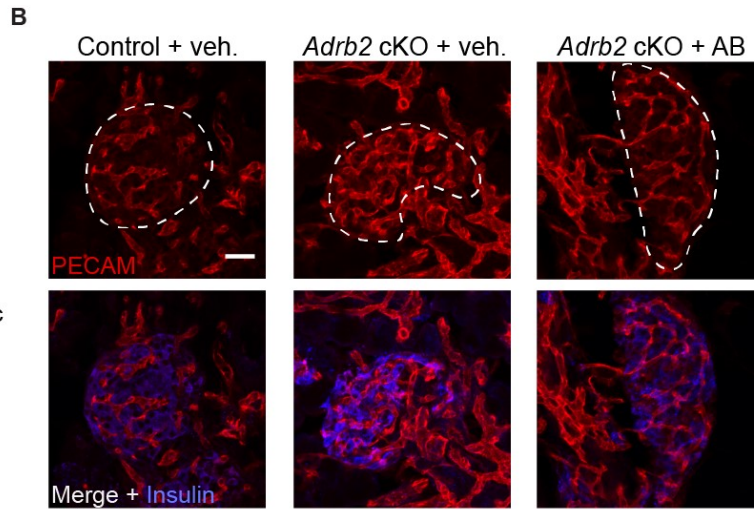
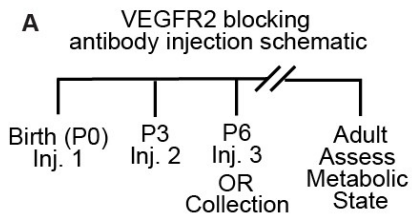


**Figure 4.1. Vegf pathway inactivation ameliorates developmental defects in *Adrb2* cKO mice.** (A) Schematic for blocking activity of the Vegf-a receptor, Vegfr2, during development in *Adrb2* cKO mice. (B) Neonatal hyper-vascularization and insulin immunoreactivity are rescued by blocking antibody injection. Scale bar, 25 $\mu$ m. (C) Quantification of vessel length (mm/mm<sup>2</sup>) shows significant rescue of hyper-vascularization in Vegfr2 injected *Adrb2* cKO mice. Means  $\pm$  SEM from 3-4 female mice/condition, multiple islets per animal; one-way ANOVA, \*p<0.05. (D) Laminin and Collagen IV immunoreactivity are normalized in *Adrb2* cKO animals following blocking antibody injection. Scale bar 50 $\mu$ m. (E) Insulin transcript levels are normalized in female antibody injected *Adrb2* cKO neonates (n=5-17 mice/condition; one-way ANOVA with Tukey's post-test \*p<0.05, \*\*p<0.01, n.s. not significant).

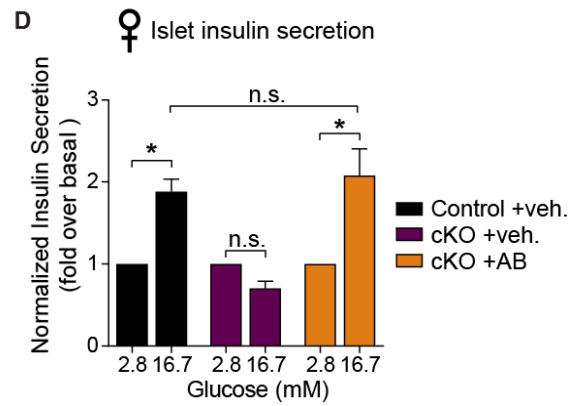
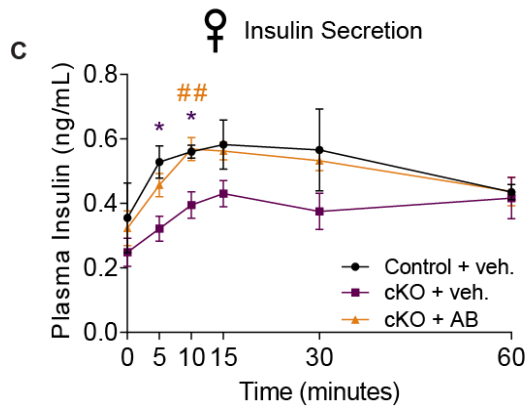
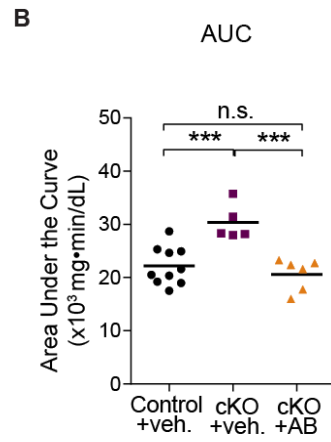
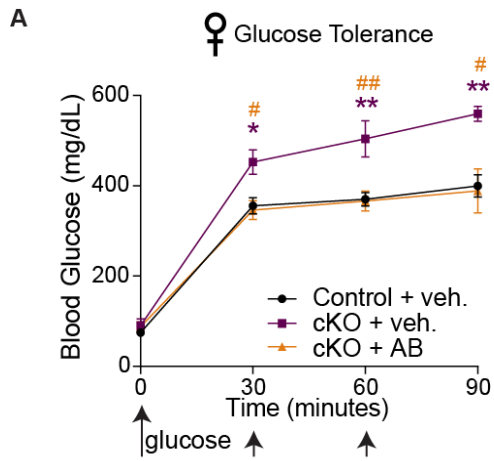


**Figure 4.2. Developmental Vegf pathway inactivation ameliorates adult functional defects in *Adrb2* cKO mice.** (A) Glucose tolerance defects in *Adrb2* cKO mice are significantly improved by blocking antibody injection during development. Means  $\pm$  SEM from n= 5-10 mice/condition; one-way ANOVA with Tukey's post-test \*p<0.05, \*\*p<0.01 *Adrb2* cKO + veh. compared to control, #p<0.05, ##p<0.01 *Adrb2* cKO + veh. compared to *Adrb2* cKO + AB. (B) Area under the curve (AUC) for glucose tolerance (one-way ANOVA with Tukey's post-test \*\*\*p<0.001, n.s. not significant). (C) *In vivo* insulin secretion is significantly improved by blocking antibody injection. Means  $\pm$  SEM for n= 4-6 mice/condition; one-way ANOVAs with Tukey's post-test \*p<0.05 *Adrb2* cKO + veh. compared to control, ##p<0.01 *Adrb2* cKO + veh. compared to *Adrb2* cKO + AB. (D) Islet insulin secretion is improved in *Adrb2* cKO mice after developmental blockade of Vegf-a signaling. Means  $\pm$  SEM from n= 3-5 mice/condition; one-sample *t*-tests and *t*-tests \*p<0.05, n.s. not significant.

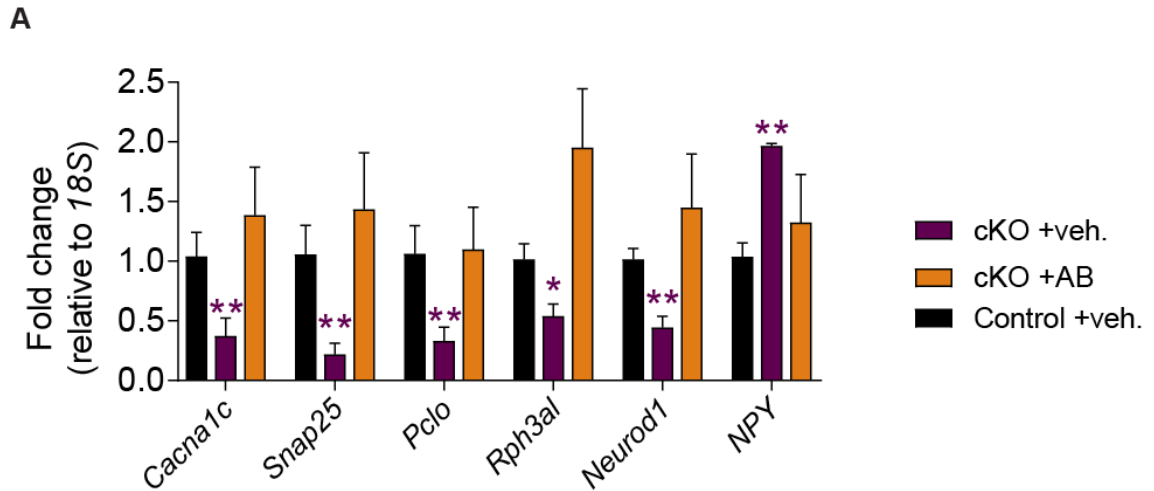


**Figure 4.3. Developmental Vegf pathway inactivation ameliorates adult transcriptional defects in *Adrb2* cKO islets.** (A) Developmental blockage of Vegf signaling in *Adrb2* cKO mice returns expression of islet GSIS genes to control levels. Means – SEM from n= 3-6 mice/condition; one-sample *t*-tests and *t*-test, \* $p < 0.05$ , \*\* $p < 0.01$ .

## DISCUSSION

Pancreatic islets constitute less than 2% of the total pancreatic volume but receive disproportionality greater blood supply (Jansson and Hellerstrom, 1983), in part, because of the exquisite dependence of islet  $\beta$ -cells on a high and sustained oxygen supply for aerobic glycolysis. An intimate relationship between  $\beta$ -cells and intra-islet microvasculature is critical for multiple aspects of islet biology including  $\beta$ -cell mass, islet innervation, insulin secretion, and regenerative capacity of islets (Brissova et al., 2014; Brissova et al., 2006; Cai et al., 2012; Eberhard et al., 2010; Hogan and Hull, 2017; Reinert et al., 2014). This cross-talk between islet endothelial cells and  $\beta$ -cells is under precise regulation (Brissova et al., 2006; Cai et al., 2012), and a set-point of endothelial to  $\beta$ -cell ratios is critical for mature islet function (Hogan and Hull, 2017). In mice, hypo- or hyper-vascularization of newly formed islets by  $\beta$ -cell-specific deletion (Brissova et al., 2006) or over-expression of Vegf-a (Cai et al., 2012), respectively, both elicit detrimental effects on  $\beta$ -cell mass and function, suggesting that Vegf-a levels in  $\beta$ -cells must be maintained within a narrow range. Surprisingly, inactivation of Vegf-a and subsequent islet hypo-vascularization in adulthood did not perturb islet mass and insulin secretion and elicited only modest elevations in blood glucose (D'Hoker et al., 2013; Reinert et al., 2013). Together, these studies imply that the influence of the intra-islet vasculature and Vegf-a levels on islet morphology and function is predominately exerted during development. However, the factors modulating the precise control of  $\beta$ -cell Vegf-a expression, and the link between early islet vascular patterning and later metabolic functions, have remained poorly defined. Here, we reveal that *Adrb2* in  $\beta$ -cells constitutes an endogenous brake to suppress Vegf-a production and curtail excessive endothelial cell expansion during the first



week of birth in mice, a period that is characterized by pronounced growth of intra-islet capillary network and endothelial cell proliferation (Johansson et al., 2006a). Our findings that normalization of islet vasculature in *Adrb2* cKO mice additionally normalizes the transcriptional profile of these mice suggests that endothelial cells play a significant role in instructing mature  $\beta$ -cell phenotype.

# METHODS

## Mice

All procedures relating to animal care and treatment conformed to The Johns Hopkins University Animal Care and Use Committee (ACUC) and NIH guidelines. Animals were group housed in a standard 12:12 light-dark cycle. Mice were maintained on a *C57BL/6* background, or mixed *C57BL/6* and *129P*, or *C57BL/6* and *FVB* backgrounds. Since phenotypes were specific to female mutant mice, animals of both sexes were used for initial analyses, and the sex of the animals used are clearly noted throughout the study. *Adrb2<sup>ff</sup>* mice were a generous gift from Dr. Gerard Karsenty (Hinoi et al, 2008). *Pdx-Cre (B6.FVB-Tg(Pdx1-cre)6Tuv/Nci*; RRID: IMSR\_NCIMR:01XL5) mice were obtained from NCI Frederick Mouse Repository.

## VegfR2/Flk1 antibody injections

*Adrb2* cKO pups were injected with either 1 $\mu$ g of VegfR2/Flk1 blocking antibody (R&D AF644) or vehicle at P0 and P3, then either collected at P6 for RNA or immunohistochemistry, or given a third injection and allowed to mature. Pups given 3 injections were subjected to glucose tolerance tests at 2 months of age, then collected for *in vitro* islet insulin secretion assays.

## Metabolic Assays

### *Glucose Tolerance*

Young adult (2-4-month-old) mice were individually housed and fasted overnight (16 hours) before being given a 2g/kg intraperitoneal (IP) glucose injection. Blood glucose levels were measured with a OneTouch Ultra 2 glucometer before glucose injection, and 2 additional 2g/kg glucose injections were given at 30 minutes and 60 minutes after the first injection. Glucose levels were monitored over a 1.5-hour period.

#### *In vivo insulin tolerance*

Mice were individually housed overnight with *ad libitum* food and water before being given a 0.75U/kg IP insulin injection (Novolin-R). Blood glucose levels were measured with a OneTouch Ultra 2 glucometer before insulin injection, and every 15 minutes post-injection over a 1-hour period.

#### *In vivo insulin secretion*

Mice were individually housed and fasted overnight (16 hours) before being given a 3g/kg IP glucose injection. Plasma insulin levels were measured with an Ultrasensitive Insulin ELISA kit (Crystal Chem) before fasting (fed), the next morning before injection, and over a 1-hour period following injection.

#### **Mouse islet isolations**

Islets were isolated as previously described (Wollheim et al, 1990). Islets were isolated by collagenase distension through the bile duct (Collagenase P [Roche], 0.375-0.4mg/mL in

HBSS) and digestion at 37°C. Digested pancreata were washed with HBSS + 0.1% BSA and subjected to discontinuous density gradient using histopaque (6:5 Histopaque 1119:1077; Sigma-Aldrich). The islet layer (found at the interface) was collected and islets were handpicked under an inverted microscope for subsequent analysis.

### **In vitro insulin secretion**

Isolated islets were cultured overnight in RPMI-1640 (5% FBS, 5U/L penicillin-streptomycin). Islets were then handpicked to be size and quantity matched, and 5-10 islets/mouse were washed and pre-incubated for 1 hour in Krebs-Ringer HEPES buffer (KRHB) containing 2.8mM glucose. Islets were then incubated in 2.8mM or 16.7mM glucose, or 30mM KCl in KRHB for another 30 minutes. Supernatant fractions were removed, and islets lysed in acid-ethanol overnight and subsequently neutralized in Tris buffer (0.885M). Both cellular and supernatant fractions were subjected to insulin ELISA (Crystal Chem). Total insulin was normalized to DNA by Quant-it PicoGreen dsDNA kit (Invitrogen).

### **Other IHC**

50µm cryosections were taken from P6 mouse pancreata, then washed with PBS, permeabilized in 1% Triton X-100 in PBS, and blocked for 1 hour at room temperature using 5% goat serum (GS) in PBS + 0.1% Triton X-100. Sections were then incubated for 2 nights at 4°C with either: rat anti-PECAM-1/CD-31 antibody (1:300), rabbit anti-collagen IV (1:500), or chicken anti-laminin (1:200) in conjunction with guinea pig anti-

insulin (1:300). Following PBS washes, sections were then incubated with anti-rat Alexa-546, anti-rabbit Alexa 488 or 647, anti-chicken 488 or 647, and anti-guinea pig 488, 546, or 647 secondary antibodies (1:200; ThermoFisher). Sections were then washed in PBS and mounted in Fluoromount Aqueous Mounting Medium containing 100 $\mu$ g/mL DAPI. Z-stacks of 1 $\mu$ m optical slices were taken using a Zeiss LSM 700 confocal microscope equipped with 405, 488, 555, and 633 lasers. Maximum intensity projections were generated with FIJI, and quantification of sympathetic innervation density was done by calculating integrated TH fluorescence density per unit area (FIJI) from multiple random images. Quantification of islet vasculature density was done by calculating integrated PECAM-1/CD-31 density per islet (ROI set by insulin immunoreactivity) area (FIJI) from multiple random images.

### **qRT-PCR**

RNA from either whole pancreata (P6) or isolated islets (adult) was isolated using TRIzol RNA extraction reagent phenol-chloroform extraction and ethanol precipitation. RNA from sorted cells was isolated using Direct-zol RNA Microprep (Zymo) kit. 1.5-2 $\mu$ g of total RNA was reverse-transcribed into cDNA with M-MLV Reverse Transcriptase (Promega). TaqMan assays (ThermoFisher) were used to quantitatively determine transcript levels of the adrenergic receptors, while Maxima SYBR Green/Rox Q-PCR Master Mix (ThermoFisher) reagents and primer sets (listed in Key Resources Table) were used to determine transcript levels for other genes. Both assays were performed in a StepOnePlus Real-Time PCR System (ThermoFisher). Fold change in transcript levels was

calculated using the  $2^{(-\Delta\Delta C_t)}$  method, and 18S was used as an endogenous control for normalization.

## QUANTIFICATION AND STATISTICAL ANALYSIS

Sample sizes were similar to those reported in previous publications (Borden et al., 2013; Houtz et al., 2016). For practical reasons, analyses of vessel length were done in a semi-blinded manner, such that the investigator was aware of the genotypes prior to the experiment, but conducted the staining and data analyses without knowing the genotypes of each sample. All Student's *t*-tests were performed assuming Gaussian distribution, two-tailed, unpaired, and with a confidence interval of 95%, with the exception of fold change analyses (such as for qPCR), which were done using a one sample *t* test. One-way ANOVA analyses with post hoc Tukey test or two-way ANOVA analyses with post hoc Bonferroni test were performed when more than 2 or 3 groups were compared, respectively. Statistical analyses were based on at least 3 independent experiments and described in the figure legends. All error bars represent the standard error of the mean (S.E.M.).

**CHAPTER 5: TAMOXIFEN AFFECTS  
GLUCOSE TOLERANCE IN A SEX,  
STRAIN, AND DELIVERY  
DEPENDENT MANNER**

# INTRODUCTION

The development of many cancer treatments stems from the clinical hypothesis that chemical compounds could be generated in such a way that they would be toxic only to the tumor without affecting the patient. This hypothesis depends on the identification and specific targeting of a factor present only on the tumorous tissue, and not present in any healthy host tissue. These ideas spurred a logical approach for chemotherapy design. As early as 1896, estrogen and estrogen receptor signaling was implicated in breast cancer development and progression after the discovery that surgical removal of the ovaries resulted in longer life expectancies for women with breast cancer (Jordan, 2001; Jordan, 2006). From that point, estrogen-like chemicals (now called Selective Estrogen Receptor Modulators, or SERMs) became a widely researched drug category in an attempt to combat breast cancer. Unfortunately, the majority of drugs developed from this discovery had wide-spread and severe side-effects, and as such no SERMs were deemed acceptable for breast cancer treatment through the 1960s. During that same period of time, estrogen receptor modulators were also being developed in an attempt to generate emergency contraceptives. From this study, the drug Tamoxifen (TMX) was discovered. TMX itself is not highly effective at activating estrogen receptors, though it is metabolized by cytochrome P450 enzymes to 4-hydroxytamoxifen (4-HT), which binds both ER $\alpha$  and ER $\beta$  with higher affinities than estrogen itself (Sasson and Notides, 1988). While TMX had absolutely no useful properties as a contraceptive (in humans) and was almost discarded, the connection was made that it may be useful as a breast cancer therapeutic. Many clinical trials began in the 1970's and 80's, and shortly thereafter TMX was declared effective at preventing breast cancer return. Since then, research on how and why TMX works has been



slow but steady. Currently, TMX is effective in both pre- and post- menopausal women with estrogen receptor (ER) positive breast cancer. Additionally, clinical trials are in process to determine the effectiveness of TMX at preventing breast cancer development in high-risk patients (such as those with ductal abnormalities).

The term SERM was used to describe these compounds signaling properties as they act to both activate and repress estrogen receptor signaling depending on the species, tissue type, receptor specificity, and co-activators or co-repressors available (Jordan, 2001). This signaling complexity can be broken down into four core signaling decisions. The first decision TMX (or any SERM) must make is which estrogen receptor (ER $\alpha$  or ER $\beta$ ) to bind to. This results in a conformational change in the receptor, which can influence the second decision: whether or not the receptor binds to a coactivator or corepressor. Depending on coactivator/repressor binding, the estrogen receptors can either homodimerize or heterodimerize, the third decision. The final decision point is whether the homo- or heterodimerized receptors activate or repress transcription. Transcriptional activation is either direct, via interaction with the DNA, or indirect, through interactions between the dimerized receptors and FOS and JUN. Repression is thought to be through direct contact with the DNA. Direct contact of dimerized receptors, both activating and repressing, occurs at estrogen response elements (EREs). While the exact mechanisms of TMX action are not well understood, these core 'decisions' are thought to underlie the species and tissue specific actions of TMX. For example, TMX was highly effective as a contraceptive in rodent models, but promoted ovulation (and increased pregnancy chances) in humans (Jordan, 2006). Furthermore, TMX is effective at preventing cancer recurrence in breast

tissue because it acts to repress growth, while it activates signaling in other tumor tissues, such as endometrial tumors.

Considering the millions of individuals (mainly women) that have been treated with TMX, there is a very little clinical data available regarding the effects of tamoxifen treatment on body composition or energy homeostasis. In rodent models, TMX has been implicated in protecting against weight gain and adipose tissue accumulation (Wade and Heller 1993, Hesselbarth et al. 2015). TMX has also been found to prevent obesity, steatosis, and insulin resistance in high-fat diet (HFD) fed OVX mice (Guillaume et al. 2017). Despite these findings, the full effects of TMX on metabolic homeostasis in wild-type male and female mouse lines is unknown. A few studies investigating the effects of TMX have been done in only one sex (females, with the exception of one study on males in subcutaneous adipose tissue), and in different strains (CD1 and different C57BL6 variants). However, it is likely that these effects of TMX are not only seen in one sex or in one genetic strain. These effects are likely dependent on a variety of factors, including TMX dose, and time allowed between TMX administration and phenotype testing (chase time). However, there are also potentially effects of background strain and delivery system (injection/injection type versus oral). To date, none of these effects of TMX have been characterized.

Understanding the effects of TMX on metabolism is especially pertinent, as TMX is widely used to promote temporal genetic recombination in rodent systems using a modified Cre-Lox system. The Cre-Lox system involves Cre-recombinase and loxP sites, which were found in bacteriophage P1. Cre-recombinase, driven by a tissue-specific promoter, specifically ‘cuts’ DNA at specific sites, loxP sites, similar to restriction

enzymes. Depending on the orientation of these loxP sites, Cre-recombinase either excises the DNA between the sites or inverts it. By placing two loxP sites in an essential region of a gene of interest (generating a floxed allele) and combining this with a transgenic tissue-specific promoter-driven Cre-recombinase, the gene of interest can be silenced in a tissue-specific manner. This system is extremely powerful, but lacks temporal regulation, which is essential to differentiate adult versus developmental roles for genes, as well as avoiding embryonic lethality in certain systems. To avoid these confounds, the inducible Cre-lox system (Cre<sup>ER</sup>) was developed. This was done by fusing a modified estrogen receptor to Cre-recombinase. As previously mentioned, estrogen receptors are nuclear hormone receptors, which reside inactive in the cytosol, and only become active and transport to the nucleus upon ligand binding. The modified Cre-recombinase used in the Cre<sup>ER</sup> system is highly sensitive to the TMX metabolite 4-hydroxytamoxifen (4-OHT), and as such, delivery of TMX to a genetically modified organism results in spatiotemporally regulated gene inactivation.

## RESULTS

Tamoxifen has long been used as a potent inducer of Cre activity in transgenic mice carrying Cre fused to a modified estrogen receptor (Cre<sup>ER</sup>). However, recent evidence suggests that tamoxifen causes significant physiological side effects, such as increased triglyceride and free fatty acid levels in male mice (Hesselbarth et al, 2015). Tamoxifen has also been shown to prevent weight gain and insulin resistance in ovariectomized female mice during high fat diet (Guillaume et al, 2017). Together, this suggests that in both male and female mice, tamoxifen alters whole body metabolism. To determine if tamoxifen affects glucose metabolism in mice, we performed a commonly used and recommended paradigm for tamoxifen-inducible deletion in three inbred strains: *129S1/SvImJ*, *BALB/cJ*, and *C57BL/6J*. Following intraperitoneal (I.P.) injection of tamoxifen (100mg/kg/day for 5 consecutive days), neither male nor female mice from any of the three strains showed significant changes in body weight (Figure 5.1 A-C).

### **Glucose tolerance is improved by I.P. tamoxifen administration**

To determine the effects of tamoxifen on glucose metabolism, we performed glucose tolerance tests on males and females from all three strains following I.P. tamoxifen administration. While male *129S1/SvImJ* mice did not display robust changes in glucose tolerance, we observed significantly improved glucose tolerance in tamoxifen treated *129S1/SvImJ* females, as well as *BALB/cJ* and *C57BL/6J* males and females (Figure 5.2 A-D). These results highlight an important consequence of tamoxifen administration in improving glucose tolerance. Indeed, if a tamoxifen-induced knock-out showed no glucose

tolerance defects, then the effects of tamoxifen may have masked phenotypes if relevant tamoxifen-treated controls were not included. These results also highlight the importance of considering strain and sex while performing metabolic analyses. In agreement with this, we noted no changes in fed (*ad libitum*) blood glucose levels in response to tamoxifen in either *129S1/SvImJ* or *BALB/cJ* male or female mice (Figure 5.3 A-B). However, both male and female *C57BL/6J* mice showed a significant but short-lived decrease in fed blood glucose levels in response to tamoxifen administration (Figure 5.3 C). Together, these results suggest that tamoxifen affects mouse strains with different propensities.

### **Improved glucose tolerance persists following I.P. tamoxifen administration**

In order to determine the persistence of these effects, we extended the recovery period following tamoxifen administration to 21 days (3 weeks) after the final injection. Male *129S1/SvImJ* mice did not develop improved glucose tolerance at 21 days post-injection (Figure 5.4 A). Female *129S1/SvImJ* and *C57BL/6J* mice displayed normal glucose tolerance by 21 days post-injection, while female *BALB/cJ*, male *BALB/cJ*, and male *C57BL/6J* mice retained their improved glucose tolerance (Figure 5.4 B-I). This suggests the glucose lowering effect that tamoxifen is having persists differently in a strain-dependent manner, and weeks beyond the usually accepted ‘chase’ periods following tamoxifen administration in inducible Cre lines.

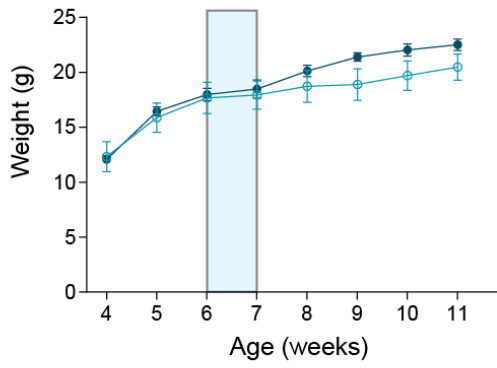
### **Insulin sensitivity is unaffected by I.P. tamoxifen administration**

Enhanced glucose tolerance can be caused by a variety of factors, including enhanced insulin secretion or sensitivity. To examine these possibilities, we tested whether I.P. tamoxifen administration increased insulin sensitivity in male *C57BL/6J* mice. We found no change in insulin tolerance two weeks following I.P. administration (Figure 5.5 A). In contrast, we found a significant increase in glucose-stimulated insulin secretion (Figure 5.5 B). This suggests that increased insulin secretion is likely the cause of enhanced glucose tolerance following tamoxifen administration. Additionally, tamoxifen activity has been shown to be prolonged in pancreatic islets following tamoxifen treatment (Reinert et al, 2012), in agreement with the lasting nature of the effects we see. Furthermore, Estrogen Receptor signaling has been shown to promote glucose-stimulated insulin secretion, and tamoxifen is capable of binding to and activating endogenous estrogen receptors (Liu et al, 2009; Wong et al, 2010).

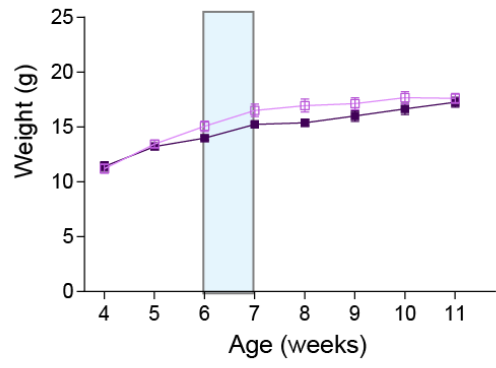
### **Oral tamoxifen delivery does not affect glucose tolerance**

Because tamoxifen metabolites have been shown to remain in circulation longer when delivered through I.P. injection versus oral administration (Wilson et al, 2014), we wanted to address whether the mechanism of tamoxifen delivery affected the glucose tolerance phenotypes. To test this, we placed mice on a tamoxifen or control diet for 10 days (with a two-day break half-way through), allowed a 6-day recovery, and then examined glucose tolerance. Interestingly, we saw no changes in glucose tolerance following oral tamoxifen administration in male or female mice in any strain tested (Figure 5.6 A-I). To ensure this was not due to a difference in dose, we calculated the amount of tamoxifen consumed based on food intake and found no significant difference in the total

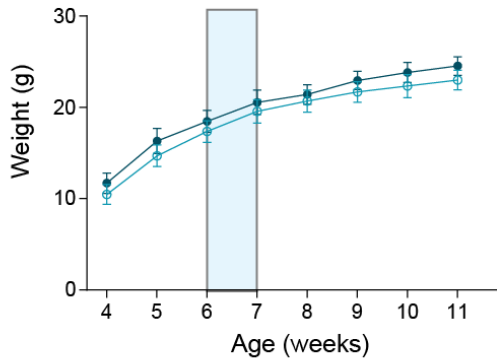
amount of tamoxifen the animals received (approximately 500 mg/kg from injection compared to  $440 \pm 77$  mg/kg for males and  $432 \pm 73$  mg/kg for females (values are mean  $\pm$  SD for n=10 males and 11 females from all three strains)). This suggests that the method of tamoxifen administration significantly impacts the effects of tamoxifen on glycemic control.

**A**

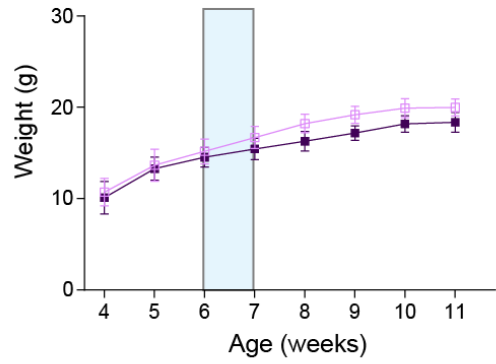
● Male 129S1/SVLMJ + Vehicle I.P.  
○ Male 129S1/SVLMJ + TMX I.P.



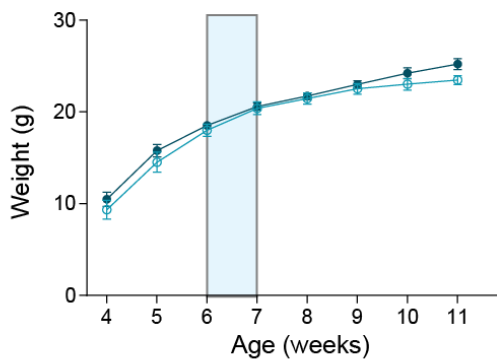
■ Female 129S1/SVLMJ + Vehicle I.P.  
□ Female 129S1/SVLMJ + TMX I.P.

**B**

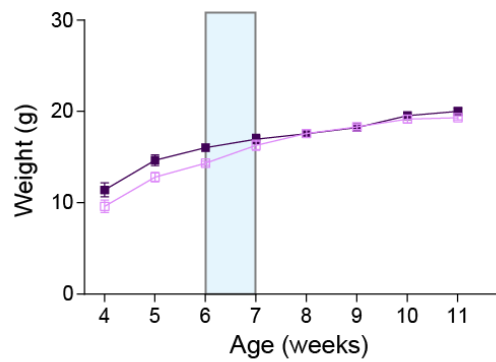
● Male BALB/CJ + Vehicle I.P.  
○ Male BALB/CJ + TMX I.P.



■ Female BALB/CJ + Vehicle I.P.  
□ Female BALB/CJ + TMX I.P.

**C**

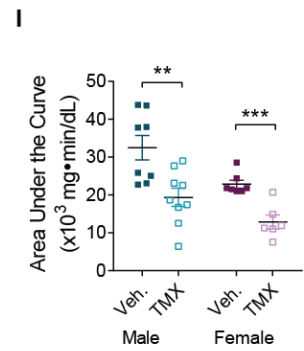
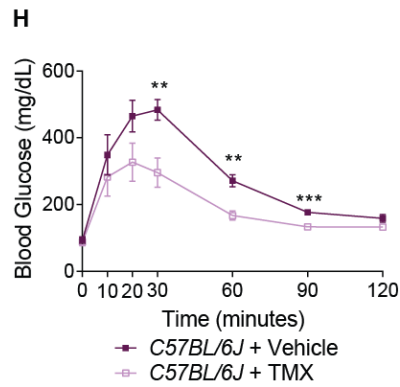
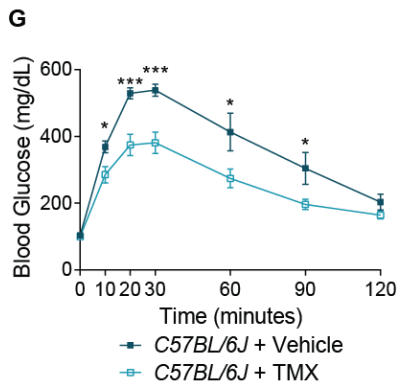
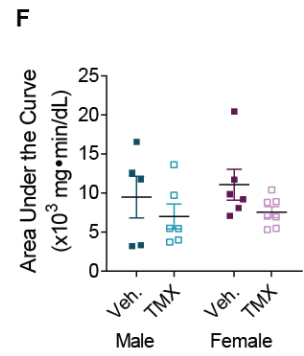
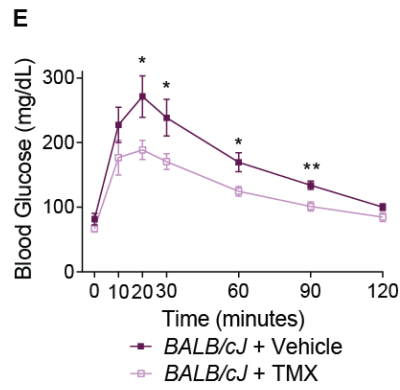
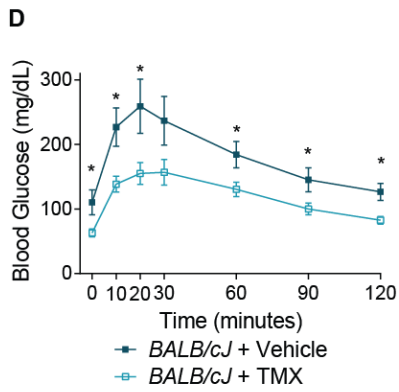
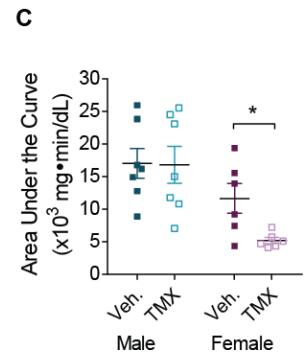
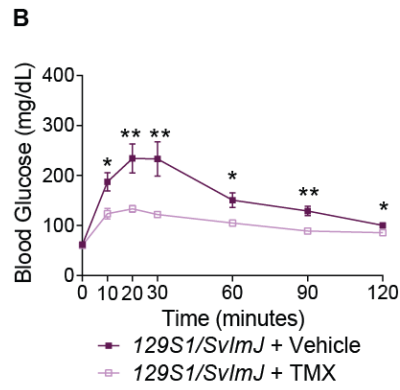
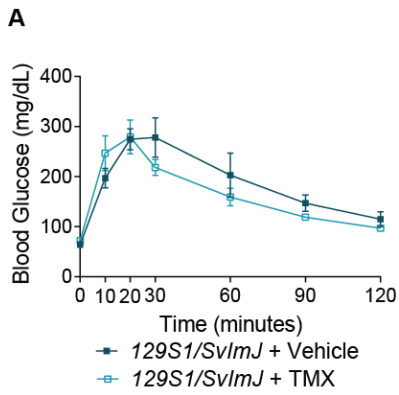
● Male C57BL/6J + Vehicle I.P.  
○ Male C57BL/6J + TMX I.P.



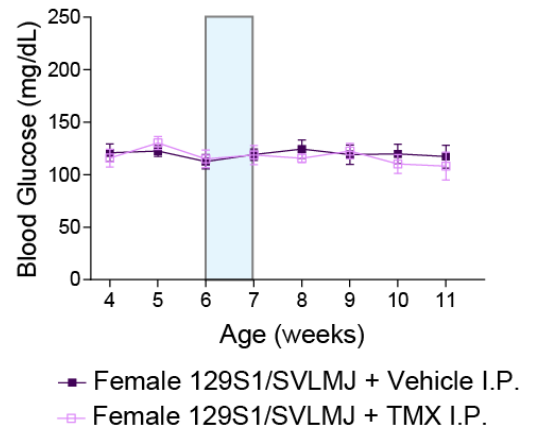
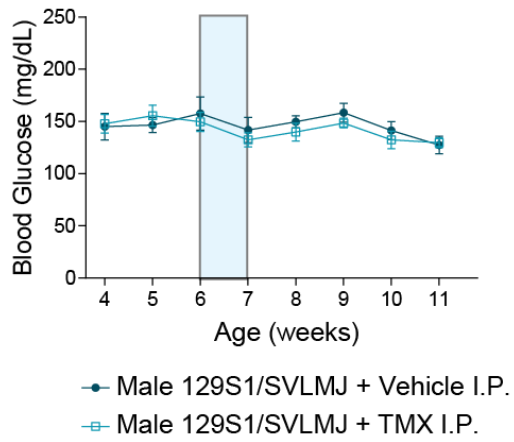
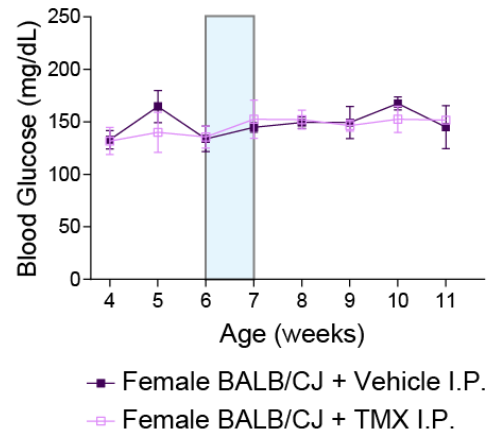
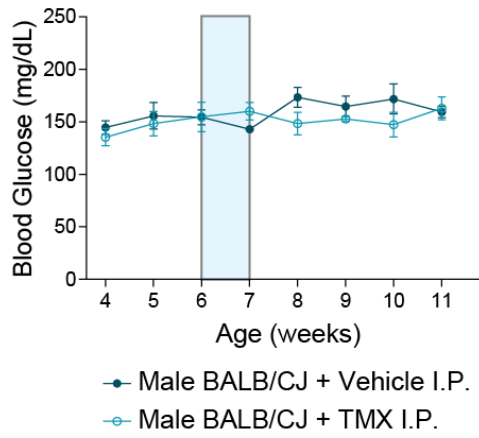
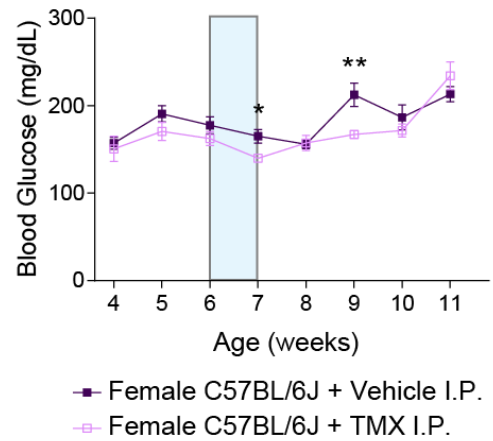
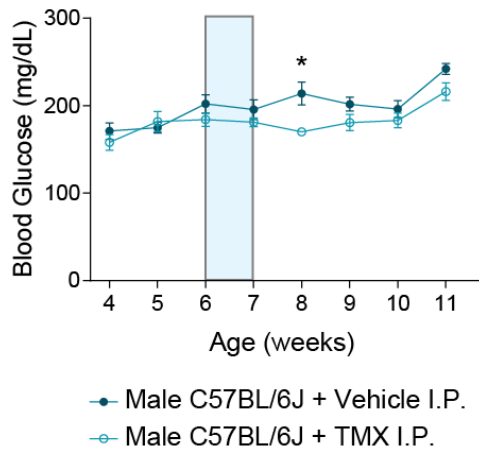
■ Female C57BL/6J + Vehicle I.P.  
□ Female C57BL/6J + TMX I.P.



**Figure 5.1. I.P. Tamoxifen administration does not affect weight in mice.** (A) Male and female *129S1/SvImJ* (B) *BALB/cJ*, or (C) *C57BL/6J* mice did not experience changes in weight gain in response to tamoxifen administration (blue bar). Means  $\pm$  SEM from n= 6 male vehicle *129S1/SvImJ* mice, 5 male TMX *129S1/SvImJ* mice, 6 female vehicle *129S1/SvImJ* mice, 8 female TMX *129S1/SvImJ* mice, 5 male *BALB/cJ* mice per condition, 5 female vehicle *BALB/cJ* mice, 6 female TMX *BALB/cJ* mice, 6 male and female *C57BL/6J* mice per condition.



**Figure 5.2. I.P. Tamoxifen administration improves glucose tolerance in mice one week after administration.** (A) Male *129S1/SvImJ* mice do not show changes in glucose tolerance in response to I.P. tamoxifen administration. Means  $\pm$  SEM for n= 7 male 129S mice per condition. (B) TMX-injected female *129S1/SvImJ* mice show significantly improved glucose tolerance. Means  $\pm$  SEM for n=6 female *129S1/SvImJ* mice per condition. (C) Area Under the Curve (AUC) for *129S1/SvImJ* glucose tolerance. (D) Both male and (E) female *BALB/cJ* mice show significantly improved glucose tolerance following I.P. tamoxifen administration. Means  $\pm$  SEM for n=5-7 *BALB/cJ* mice per sex per condition. (F) Area Under the Curve (AUC) for *BALB/cJ* glucose tolerance. (G) Both male and (H) female *C57BL/6J* mice show significantly improved glucose tolerance following I.P. tamoxifen administration. Means  $\pm$  SEM for n= 6-9 *C57BL/6J* mice per sex per condition. (I) Area Under the Curve (AUC) for *C57BL/6J* glucose tolerance. \*p<0.05, \*\*p<0.01, \*\*\*p<0.001; t-tests.

**A****B****C**

**Figure 5.3. I.P. Tamoxifen administration affects blood glucose levels in a strain-dependent manner.** (A) Male and female *129S1/SvImJ* and (B) *BALB/cJ* mice did not experience changes in fed blood glucose levels in response to tamoxifen administration (blue bar). n= 6 male vehicle *129S1/SvImJ* mice, 5 male TMX *129S1/SvImJ* mice, 6 female vehicle *129S1/SvImJ* mice, 8 female TMX *129S1/SvImJ* mice, 5 male *BALB/cJ* mice per condition, 5 female vehicle *BALB/cJ* mice and 6 female TMX *BALB/cJ* mice. (C) Male and female *C57BL/6J* mice showed acutely lower fed blood glucose levels following tamoxifen injection. Levels normalized three weeks after the final injection in both sexes. n= 6 male and female *C57BL/6J* mice per condition. All data shown are means  $\pm$  SEM. \* $p < 0.05$ , \*\* $p < 0.01$ , *t*-tests.

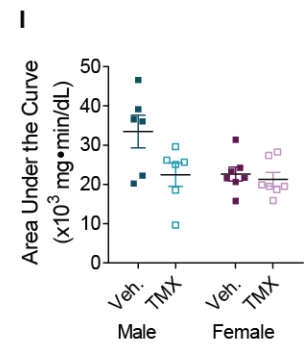
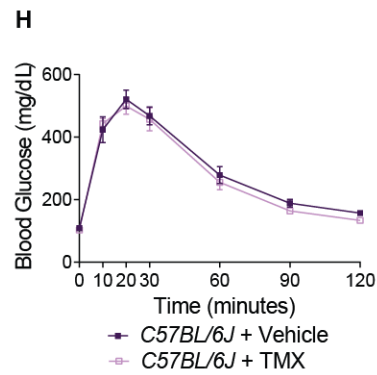
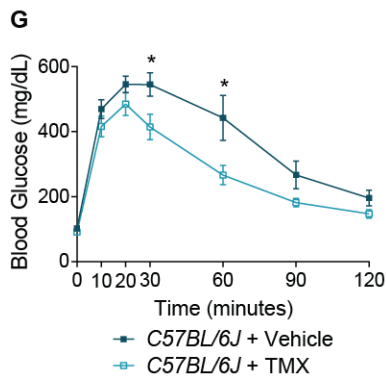
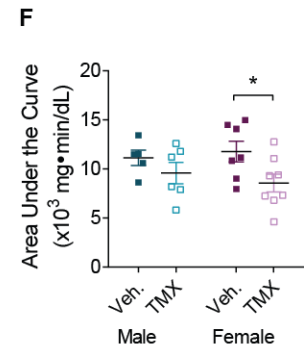
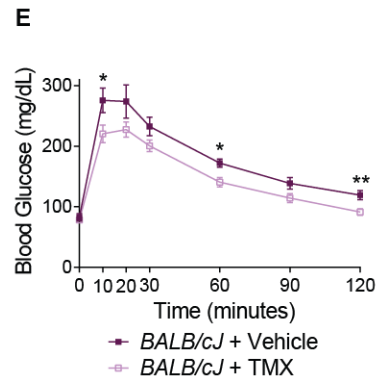
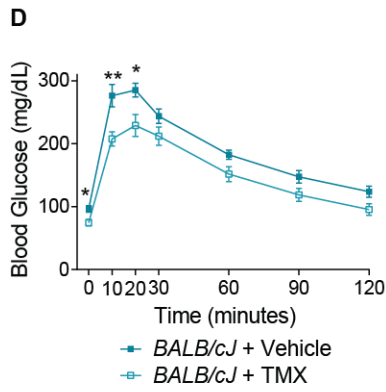
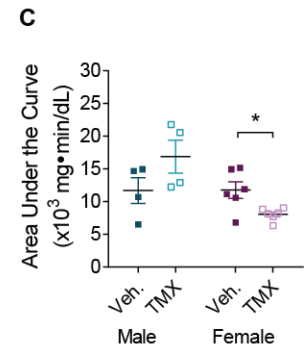
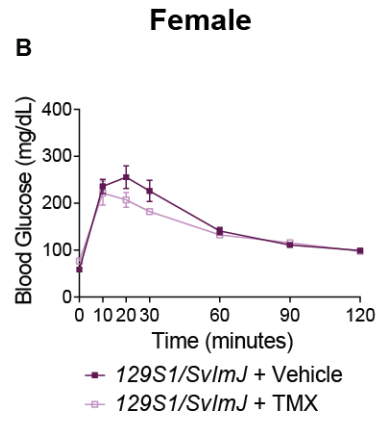
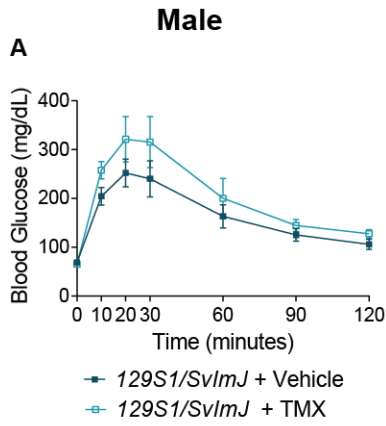


**Figure 5.4. Improved glucose tolerance in I.P. tamoxifen injected mice persists three weeks after administration.** (A) Male *129S1/SvImJ* mice do not show changes in glucose tolerance in response to I.P. tamoxifen administration. Means  $\pm$  SEM for n= 4 male *129S1/SvImJ* mice per condition. (B) Glucose tolerance in TMX-injected female *129S1/SvImJ* mice is normalized three weeks after tamoxifen injection. Means  $\pm$  SEM for n=6 female *129S1/SvImJ* mice per condition. (C) Area Under the Curve (AUC) for *129S1/SvImJ* glucose tolerance. (D) Both male and (E) female *BALB/cJ* mice retain significantly improved glucose tolerance three weeks post-I.P. tamoxifen administration. Means  $\pm$  SEM for n=5-8 *BALB/cJ* mice per sex per condition. (F) Area Under the Curve (AUC) for *BALB/cJ* glucose tolerance. (G) Male, but not (H) female, *C57BL/6J* mice retain significantly improved glucose tolerance three weeks following I.P. tamoxifen administration. Means  $\pm$  SEM for n=6-7 *C57BL/6J* mice per sex per condition. (I) Area Under the Curve (AUC) for *C57BL/6J* glucose tolerance. \*p<0.05, \*\*p<0.01, \*\*\*p<0.001; *t*-tests.

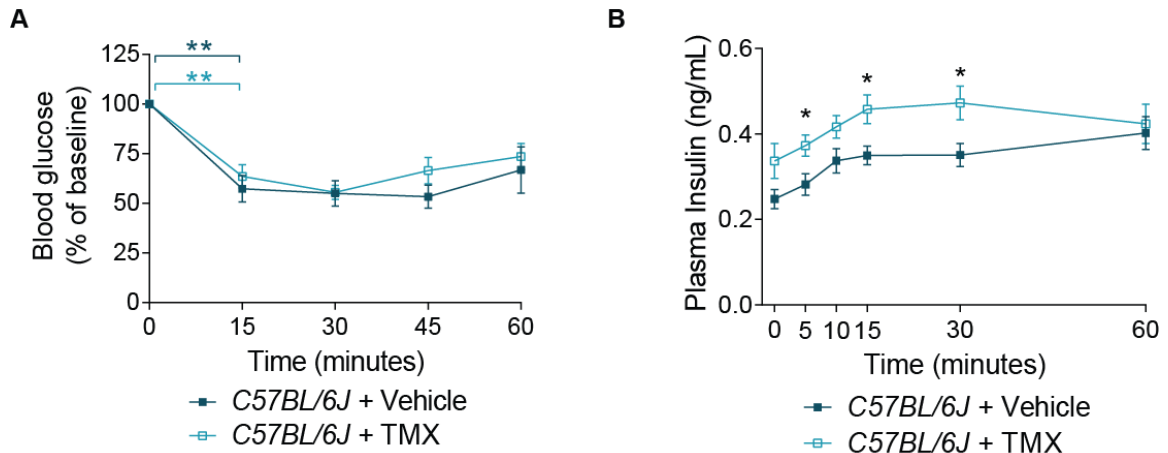


**Figure 5.5. Insulin sensitivity is unaffected by I.P. tamoxifen administration, but glucose-stimulated insulin secretion is increased.** (A) Male *C57BL/6J* mice do not show changes in insulin sensitivity in response to I.P. tamoxifen administration.  $n=6$  male mice per condition.  $**p<0.01$ ; one-sample *t*-tests. (B) Glucose-stimulated insulin secretion (GSIS) is improved following intraperitoneal tamoxifen administration in male *C57BL/6J* mice. Means  $\pm$  SEM for  $n=5-11$  male mice per condition.  $*p<0.05$ ; *t*-tests.



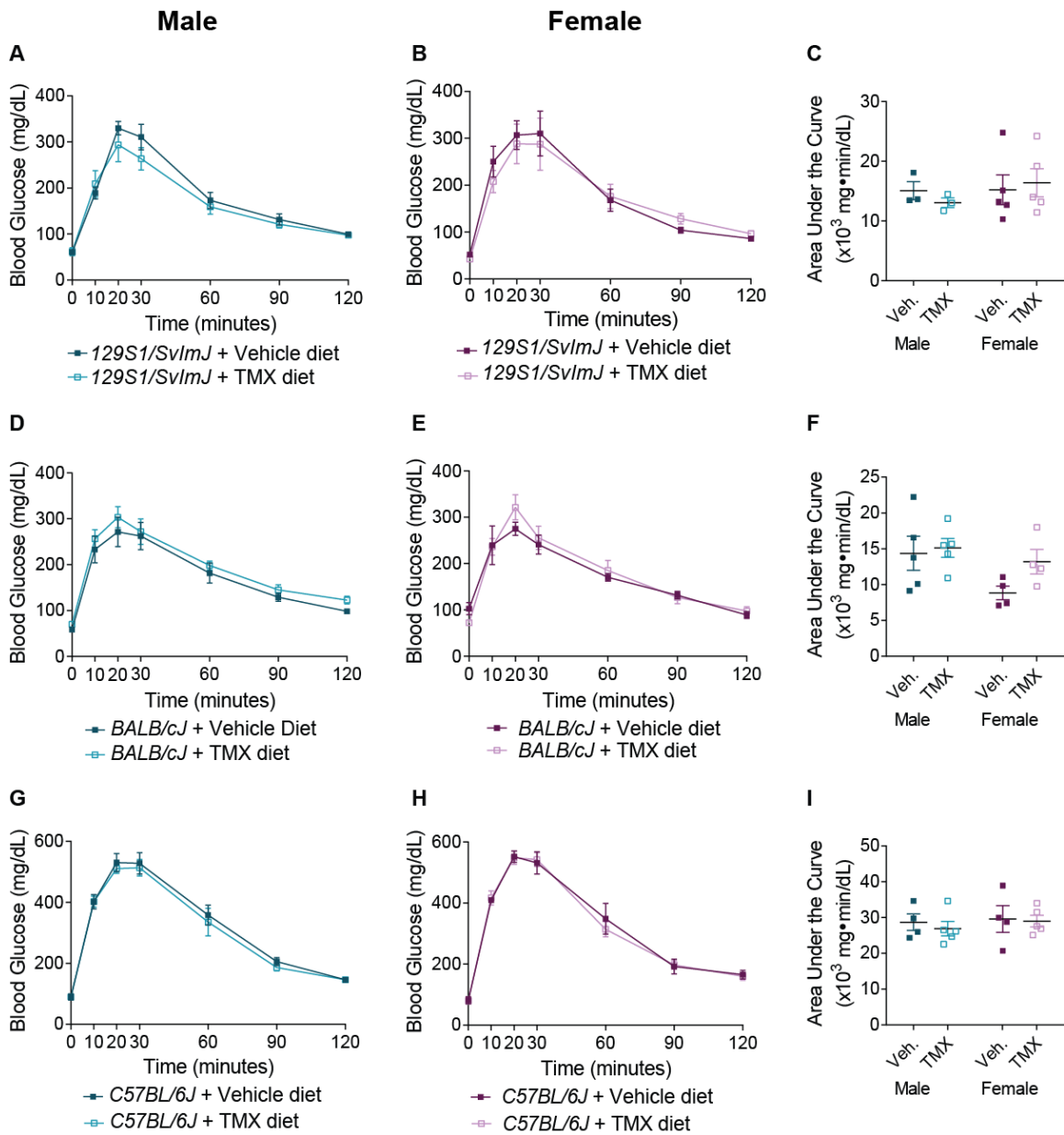


**Figure 5.6. Oral tamoxifen administration does not affect glucose tolerance.** (A) Male and (B) female *129S1/SvImJ* mice do not show changes in glucose tolerance in response to tamoxifen diet. Means  $\pm$  SEM for n=3-5 *129S1/SvImJ* mice per sex per condition. (C) Area Under the Curve (AUC) for *129S1/SvImJ* glucose tolerance. (D) Male and (E) female *BALB/cJ* mice do not show changes in glucose tolerance in response to tamoxifen diet. Means  $\pm$  SEM for n=4-5 *BALB/cJ* mice per sex per condition. (F) Area Under the Curve (AUC) for *BALB/cJ* glucose tolerance. (G) Male and (H) female *C57BL/6J* mice do not show changes in glucose tolerance in response to tamoxifen diet. Means  $\pm$  SEM for n=4-5 *C57BL/6J* per sex per condition. (I) Area Under the Curve (AUC) for *C57BL/6J* glucose tolerance.

## DISCUSSION

Here, we report that intraperitoneal (I.P.) tamoxifen administration to inbred strains has differential effects on glucose metabolism and insulin secretion. In three common strains, *129S1/SvImJ*, *BALB/cJ*, and *C57BL/6J*, I.P. tamoxifen administration induced a significant and sustained improvement of glucose tolerance without affecting insulin sensitivity. The amplitude of the effects and the persistence of the effects were sex and strain dependent. Intriguingly, oral administration of tamoxifen did not cause these effects. These results highlight the need to adjust widely accepted tamoxifen administration protocols, such as by providing an extensive chase period following tamoxifen administration, testing different methods of administration, as well as including relevant tamoxifen-treated wild-type controls.

The persistence of tamoxifen in the body appears to be highly age- and tissue-dependent. These parameters are important to define in order to accurately utilize inducible Cre-loxP systems, especially in the context of temporally restricted results, such as lineage tracing. In young adult mice (2-3 months), tamoxifen and its metabolites are no longer detectable in brain tissue within 6-8 days of injection in a dose-dependent manner. Aged mice (older than 15 months), however, are unable to effectively clear tamoxifen from the same tissue (Valny et al, 2016). In pancreatic islets, however, the action of tamoxifen persists for much longer, on the order of weeks rather than days following administration in a dose-dependent manner (Reinert et al, 2012). Our findings that glucose tolerance is enhanced following tamoxifen administration by I.P. injection highlights the importance of considering maximum induction efficiency as well of timing between injections and testing of metabolic parameters in mice. While the metabolic fates of tamoxifen following

I.P. injection versus oral administration is not known, it has been shown that 4-OHT, the tamoxifen metabolite most potent in terms of Cre<sup>ER</sup> activation, remains in plasma longer following I.P. injection compared to oral administration (Wilson et al, 2014). Together with our results showing that oral administration of tamoxifen does not impact glucose tolerance, this highlights the importance of considering and controlling for all aspects of tamoxifen administration in inducible systems.

Although tamoxifen administration has been shown to protect against insulin resistance in ovariectomized females under high fat diet conditions (Guillaume et al, 2017), we found that under normal chow conditions, tamoxifen does not affect insulin sensitivity. We also found that this effect is, for the most part, not specific to female mice, with the exception of male *129S1/SvImJ* mice. This is not all together surprising as it has been shown that estrogen directly affects insulin secretion from pancreatic islets (Lui et al, 2009). Estrogen receptors in islets signal primarily through cytosolic pathways, in contrast to the canonical nuclear hormone receptor signaling pathways. Although tamoxifen is used because of its enhanced sensitivity for modified estrogen receptors, it is still capable of interacting with endogenous estrogen receptors. Combined, these results suggest that tamoxifen affects estrogen receptor signaling in multiple tissues, and that its effects may vary based on the parameters being studied (i.e. high fat diet, etc.).

# METHODS

## **Animals**

All procedures relating to animal care and treatment conformed to The Johns Hopkins University Animal Care and Use Committee (ACUC) and NIH guidelines. Animals were group housed in a standard 12:12 light-dark cycle. Animals of both sexes were used for all analyses and the sex of the animals used is clearly noted throughout. *129S1/SvImJ*, *BALB/CJ*, and *C57BL/6J* mice were obtained from Jackson Laboratories.

## **Metabolic Assays**

### *Glucose Tolerance*

Mice were individually housed and fasted overnight (16 hours) before being given a 2g/kg intraperitoneal (IP) glucose injection. Blood glucose levels were measured with a OneTouch Ultra 2 glucometer before glucose injection, and over a 2-hour period following injection.

### *In vivo insulin secretion*

Mice were individually housed and fasted overnight (16 hours). Plasma insulin levels were measured with an Ultrasensitive Insulin ELISA kit (Crystal Chem) before injection and over a 1-hour period following injection.

### **Tamoxifen injections**

Beginning at 6 weeks of age, mice were injected intraperitoneally with 100 mg/kg tamoxifen (Sigma) in corn oil or corn oil alone, every day for 5 days. 1, 3, and 4 weeks after the last injection, vehicle- and tamoxifen-injected mice were subjected to metabolic assays.

### **Tamoxifen diet**

At 5 weeks of age, mice were switched to either control diet or tamoxifen diet (Envigo TD.07570 and TD.130856) for five days. All mice were transferred to control diet for 2 days, and then returned to either control or tamoxifen diet for another five days (total of ten days on diet over a twelve-day period). Because oral tamoxifen administration reduces food intake and body weight, mice were then given six days to recover (on standard chow) before glucose tolerance testing.

## **QUANTIFICATION AND STATISTICAL ANALYSIS**

Sample sizes were similar to those reported in previous publications (Borden et al., 2013; Houtz et al., 2016). All Student's *t*-tests were performed assuming Gaussian distribution, two-tailed, unpaired, and with a confidence interval of 95%, with the exception of insulin tolerance assays which were analyzed with one-sample *t*-tests. Statistical analyses were based on at least 3 independent experiments and described in the figure legends. All error bars represent the standard error of the mean (S.E.M.).

# **CLOSING REMARKS**

### **Developmental roles for adrenergic signaling**

Adrenergic signaling has been well-studied in the context of the fight-or-flight response, a series of acute, physiological responses to stress. However, the receptors and ligands that make up this complex signaling network are present throughout development in a variety of tissues, but their potential developmental roles have largely been ignored. This study uncovers a developmental role for  $\beta$ 2-adrenergic signaling in organizing tissue-tissue interactions during organogenesis (Figure 6). In the future it would be of interest to dissect the molecular pathway(s) through which this occurs, as well as to address whether other tissues similarly use adrenergic pathways during development.

### **Sexual dimorphisms in islet biology**

Although it is well-established that males and females differ in many metabolic processes from food intake to fat storage, many studies in mice only address phenotypes in males. While the underlying reasons for this were not malicious (more females than males are needed as breeders to maintain mouse colonies, and hormone cycling can impact a variety of outputs), it has resulted in studies that are only relevant for half the population. The drastic female-specific phenotypes that we have described here highlight the need for including both sexes in mouse studies.

How pancreatic islets, whose primary role is to control blood glucose homeostasis, develop and function differently in males versus females is unfortunately not often studied, even though islets are highly sexually dimorphic (recently reviewed Gannon et al, 2018). Furthermore, islets undergo massive changes in response to pregnancy, a female-specific requirement. This alone suggests that islet maintenance and function is, at least in part,



controlled by sex hormones. In agreement with this, intra-islet vasculature expands concurrently with  $\beta$ -cell expansion during pregnancy (Johansson et al, 2006b), supporting the thought that the vasculature of the pancreas should be more adaptable in females than in males. Our research suggests that this difference may be set up early in neonatal development. Additionally, islets from female donors have been suggested to be more amenable to transplantation than islets from male donors (Marchese et al, 2015). As failure to re-vascularize is one of the leading causes of islet graft failure, this again supports the hypothesis that female islets are more amenable to changes in vasculature status.

### **Vasculature- $\beta$ -cell interactions in diabetes**

Instructive roles of the vasculature in  $\beta$ -cell development have been previously described, though the mechanisms that control islet vascularization are largely unknown. Of the few studies available, even less has been elucidated regarding negative regulators, or pathways that put on the ‘brakes’ to restrict vasculature development. However, discovering these pathways is highly relevant considering excess intra-islet vasculature is known to cause metabolic defects. As mentioned previously, failure of islets to revascularize following transplantation is one of the leading causes of islet graft failure, our finding that  $\beta$ 2-adrenergic signaling is a negative regulator of islet vasculature suggests that inhibition of  $\beta$ 2-adrenergic signaling may improve islet transplant outcomes. Considering there are well established inhibitors of  $\beta$ -adrenergic signaling already approved for use in humans (commonly known as  $\beta$ -blockers), an exciting next step would be to see if our findings hold true in humans, and if the use of  $\beta$ -blockers could improve islet transplant outcomes.

## **Tamoxifen administration and use in mice**

Tamoxifen has been widely used to induce Cre activity in transgenic mice carrying a modified estrogen receptor (Cre<sup>ER</sup>). Tamoxifen is also widely known to act as an agonist and antagonist of estrogen receptor signaling, depending on a variety of factors, including tissue type and developmental stage. Yet despite this knowledge, tamoxifen-treated controls are rarely included in studies utilizing these Cre<sup>ER</sup> lines. This may be due to an effort to conserve the drug, or simply a consequence of available genotypes – because Cre<sup>ER</sup>; floxed animals should have no Cre activity, and therefore should be phenotypically wild-type, Cre<sup>ER</sup>; floxed animals are often mated to each other to increase the availability of Cre<sup>ER</sup>; floxed offspring for studies. This mating, however, results in very few, if any, Cre-negative animals to allow for littermate drug controls. However, our finding that tamoxifen lowers glucose during a glucose tolerance test across strains emphasizes the need to ensure relevant controls are performed.

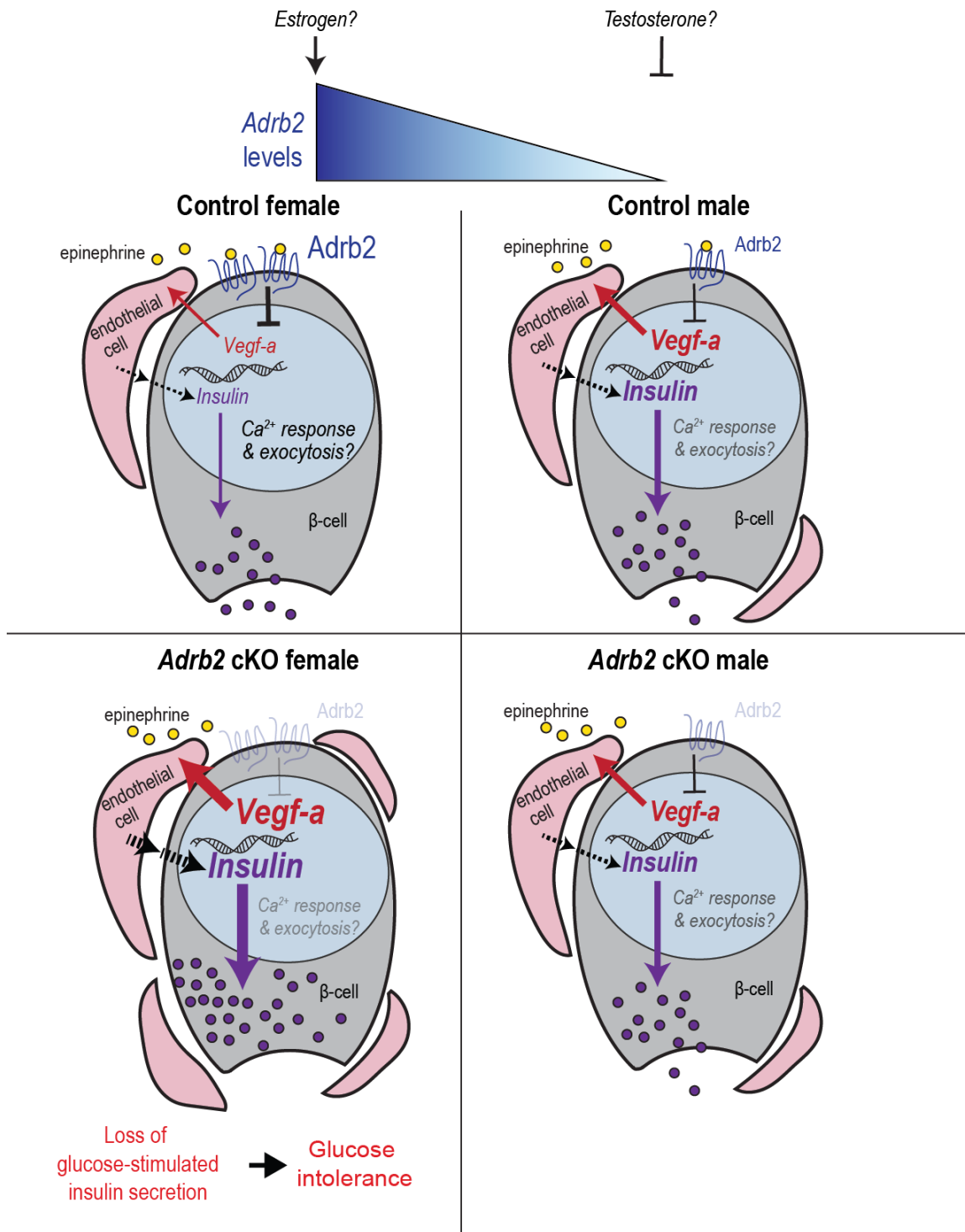


**Figure 6. Adrb2 limits vascular growth in pancreatic islets during development to control islet function**

During islet development,  $\beta$ -cell-Adrb2 receptors suppress VEGF-A expression to limit excessive growth of intra-islet endothelial cells. Endothelial cells, in turn, are critical for precise regulation of insulin gene expression in neighboring  $\beta$ -cells, via producing vascular basement membrane proteins, and likely for transcriptional regulation of key components of insulin exocytosis. Loss of Adrb2 disrupts bi-directional signaling between islet  $\beta$ -cells and endothelial cells during development, resulting in islet hyper-vascularization, aberrant insulin expression, and impaired glucose-stimulated insulin secretion in adult islets.

## REFERENCES

2017. IDF diabetes atlas - Home.

Agudo, J., Ayuso, E., Jimenez, V., Casellas, A., Mallol, C., Salavert, A., Tafuro, S., Obach, M., Ruzo, A., Moya, M., *et al.* (2012). Vascular endothelial growth factor-mediated islet hypervascularization and inflammation contribute to progressive reduction of beta-cell mass. *Diabetes* 61, 2851-2861.

Ahren, B., J. Jarhult & I. Lundquist (1981) Insulin secretion induced by glucose and by stimulation of beta 2 -adrenoceptors in the rat. Different sensitivity to somatostatin. *Acta Physiol Scand*, 112, 421-6.

Ahren, B. & I. Lundquist (1981) Effects of selective and non-selective beta-adrenergic agents on insulin secretion in vivo. *Eur J Pharmacol*, 71, 93-104.

Ahren, B., and Schersten, B. (1986). Beta 2-adrenoceptor induced increase of plasma insulin levels in man: evidence of direct and indirect B-cell stimulation and liver effects. *Diabetes research* 3, 443-445.

Apelqvist, A., H. Li, L. Sommer, P. Beatus, D. J. Anderson, T. Honjo, M. Hrabe de Angelis, U. Lendahl & H. Edlund (1999) Notch signalling controls pancreatic cell differentiation. *Nature*, 400, 877-81.

Bearer, E.L., and Orci, L. (1985). Endothelial fenestral diaphragms: a quick-freeze, deep-etch study. *The Journal of cell biology* 100, 418-428.

Beery, A. K. & I. Zucker (2011) Sex Bias in Neuroscience and Biomedical Research. *Neurosci Biobehav Rev*, 35, 565-72.

- Benninger, R. K., W. S. Head, M. Zhang, L. S. Satin & D. W. Piston (2011) Gap junctions and other mechanisms of cell-cell communication regulate basal insulin secretion in the pancreatic islet. *J Physiol*, 589, 5453-66.
- Benninger, R. K., M. Zhang, W. S. Head, L. S. Satin & D. W. Piston (2008) Gap junction coupling and calcium waves in the pancreatic islet. *Biophys J*, 95, 5048-61.
- Berg, J. M., J. L. Tymoczko & L. Stryer. 2002. Each Organ Has a Unique Metabolic Profile. W H Freeman.
- Berger, M., D. W. Scheel, H. Macias, T. Miyatsuka, H. Kim, P. Hoang, G. M. Ku, G. Honig, A. Liou, Y. Tang, J. B. Regard, P. Sharifnia, L. Yu, J. Wang, S. R. Coughlin, B. R. Conklin, E. S. Deneris, L. H. Tecott & M. S. German (2015) Galphai/o-coupled receptor signaling restricts pancreatic beta-cell expansion. *Proc Natl Acad Sci U S A*, 112, 2888-93.
- Bernardo, A. S., C. W. Hay & K. Docherty (2008) Pancreatic transcription factors and their role in the birth, life and survival of the pancreatic beta cell. *Mol Cell Endocrinol*, 294, 1-9.
- Biden, T. J., B. Peter-Riesch, W. Schlegel & C. B. Wollheim (1987) Ca<sup>2+</sup>-mediated generation of inositol 1,4,5-triphosphate and inositol 1,3,4,5-tetrakisphosphate in pancreatic islets. Studies with K<sup>+</sup>, glucose, and carbamylcholine. *J Biol Chem*, 262, 3567-71.
- Bonner-Weir, S. & L. Orci (1982) New perspectives on the microvasculature of the islets of Langerhans in the rat. *Diabetes*, 31, 883-9.

- Borden, P., J. Houtz, S. D. Leach & R. Kuruvilla (2013) Sympathetic innervation during development is necessary for pancreatic islet architecture and functional maturation. *Cell Rep*, 4, 287-301.
- Brissova, M., A. Shostak, M. Shiota, P. O. Wiebe, G. Poffenberger, J. Kantz, Z. Chen, C. Carr, W. G. Jerome, J. Chen, H. S. Baldwin, W. Nicholson, D. M. Bader, T. Jetton, M. Gannon & A. C. Powers (2006) Pancreatic islet production of vascular endothelial growth factor--a is essential for islet vascularization, revascularization, and function. *Diabetes*, 55, 2974-85.
- Brissova, M., Aamodt, K., Brahmachary, P., Prasad, N., Hong, J.Y., Dai, C., Mellati, M., Shostak, A., Poffenberger, G., Aramandla, R., *et al.* (2014). Islet microenvironment, modulated by vascular endothelial growth factor-A signaling, promotes beta cell regeneration. *Cell metabolism* 19, 498-511.
- Brissova, M., Shostak, A., Fligner, C.L., Revetta, F.L., Washington, M.K., Powers, A.C., and Hull, R.L. (2015). Human Islets Have Fewer Blood Vessels than Mouse Islets and the Density of Islet Vascular Structures Is Increased in Type 2 Diabetes. *The journal of histochemistry and cytochemistry : official journal of the Histochemistry Society* 63, 637-645.
- Brouwers, B., de Faudeur, G., Osipovich, A.B., Goyvaerts, L., Lemaire, K., Boesmans, L., Cauwelier, E.J., Granvik, M., Pruniau, V.P., Van Lommel, L., *et al.* (2014). Impaired islet function in commonly used transgenic mouse lines due to human growth hormone minigene expression. *Cell metabolism* 20, 979-990.
- Bryzgalova G, Gao H, Ahren B, Zierath JR, Galuska D, Steiler TL, Dahlman-Wright K, Nilsson S, Gustafsson JA, Efendic S, Khan A. Evidence that oestrogen receptor-

- alpha plays an important role in the regulation of glucose homeostasis in mice: insulin sensitivity in the liver. *Diabetologia*. 2006;49:588–597.
- Bryzgalova G, Lundholm L, Portwood N, et al. Mechanisms of antidiabetogenic and body weight-lowering effects of estrogen in high-fat diet-fed mice. *Am J Physiol Endocrinol Metab*. 2008;295:E904–E912.
- Bunn, H. F. (1971) Differences in the interaction of 2,3-diphosphoglycerate with certain mammalian hemoglobins. *Science*, 172, 1049-50.
- Cai, Q., Brissova, M., Reinert, R.B., Pan, F.C., Brahmachary, P., Jeansson, M., Shostak, A., Radhika, A., Poffenberger, G., Quaggin, S.E., *et al.* (2012). Enhanced expression of Vegf-a in beta cells increases endothelial cell number but impairs islet morphogenesis and beta cell proliferation. *Developmental biology* 367, 40-54.
- Cabrera, O., D. M. Berman, et al. (2006). The unique cytoarchitecture of human pancreatic islets has implications for islet cell function. *Proc Natl Acad Sci U S A* 103(7): 2334-9.
- Carr, R. D., M. O. Larsen, M. S. Winzell, K. Jelic, O. Lindgren, C. F. Deacon & B. Ahren (2008) Incretin and islet hormonal responses to fat and protein ingestion in healthy men. *Am J Physiol Endocrinol Metab*, 295, E779-84.
- Chinnadurai, S., Fannesbeck, C., Snyder, K.M., Sathe, N.A., Morad, A., Likis, F.E., and McPheeters, M.L. (2016). Pharmacologic Interventions for Infantile Hemangioma: A Meta-analysis. *Pediatrics* 137, e20153896.
- Chowdhury, T. A., S. Shaho & A. Moolla (2014) Complications of diabetes: progress, but significant challenges ahead. *Ann Transl Med*, 2.



- Claffey, K.P., Wilkison, W.O., and Spiegelman, B.M. (1992). Vascular endothelial growth factor. Regulation by cell differentiation and activated second messenger pathways. *The Journal of biological chemistry* 267, 16317-16322.
- Contreras, J. L., Smyth, C. A., Bilbao, G., Young, C. J., Thompson, J. A., and Eckhoff, D. E. (2002). 17 $\beta$ -Estradiol protects isolated human pancreatic islets against proinflammatory cytokine-induced cell death: molecular mechanisms and islet functionality<sup>1</sup>. *Experimental Transplantation*, 74(9), 1252-1259
- Daaka, Y., L. M. Luttrell & R. J. Lefkowitz (1997) Switching of the coupling of the beta2-adrenergic receptor to different G proteins by protein kinase A. *Nature*, 390, 88-91.
- Davare, M. A., V. Avdonin, D. D. Hall, E. M. Peden, A. Burette, R. J. Weinberg, M. C. Horne, T. Hoshi & J. W. Hell (2001) A beta2 adrenergic receptor signaling complex assembled with the Ca<sup>2+</sup> channel Cav1.2. *Science*, 293, 98-101.
- Deutsch, G., J. Jung, M. Zheng, J. Lora & K. S. Zaret (2001) A bipotential precursor population for pancreas and liver within the embryonic endoderm. *Development*, 128, 871-81.
- D'Hoker, J., De Leu, N., Heremans, Y., Baeyens, L., Minami, K., Ying, C., Lavens, A., Chintinne, M., Stange, G., Magenheimer, J., *et al.* (2013). Conditional hypovascularization and hypoxia in islets do not overtly influence adult beta-cell mass or function. *Diabetes* 62, 4165-4173.
- Easterling, T.R. (2014). Pharmacological management of hypertension in pregnancy. *Seminars in perinatology* 38, 487-495.

- Eberhard, D., Kragl, M., and Lammert, E. (2010). 'Giving and taking': endothelial and beta-cells in the islets of Langerhans. *Trends in endocrinology and metabolism: TEM* 21, 457-463.
- Edlund, H. (1998). Transcribing pancreas. *Diabetes* 47(12): 1817-23.
- Edlund, H. (1999). Pancreas: how to get there from the gut? *Curr Opin Cell Biol* 11(6): 663-8.
- Elias, I., S. Franckhauser, T. Ferre, L. Vila, S. Tafuro, S. Munoz, C. Roca, D. Ramos, A. Pujol, E. Riu, J. Ruberte & F. Bosch (2012) Adipose tissue overexpression of vascular endothelial growth factor protects against diet-induced obesity and insulin resistance. *Diabetes*, 61, 1801-13.
- Ernst, S., C. Demirci, S. Valle, S. Velazquez-Garcia & A. Garcia-Ocana (2011) Mechanisms in the adaptation of maternal beta-cells during pregnancy. *Diabetes Manag (Lond)*, 1, 239-248.
- Fan, W., Yanase, T., Nomura, M., Okabe, T., Goto, K., Sato, T., Kawano, H., and Nawata, H. (2005) Androgen receptor null male mice develop late-onset obesity caused by decreased energy expenditure and lipolytic activity but show normal insulin sensitivity with high adiponectin secretion. *Diabetes*, 54(4), 1000-1008.
- Fuller MD, Emrick MA, Sadilek M, Scheuer T, Catterall WA (2010) Molecular mechanism of calcium channel regulation in the fight-or-flight response. *Sci Signal* 3: ra70
- Gabbay, K. H. & W. J. Tze (1972) Inhibition of glucose-induced release of insulin by aldose reductase inhibitors. *Proc Natl Acad Sci U S A*, 69, 1435-9.

- Gannon, M., Kulkarni, R.N., Tse, H.M., and Mauvais-Jarvis, F. (2018). Sex differences underlying pancreatic islet biology and its dysfunction. *Molecular Metabolism*, S2212-8778(18)30520-9.
- Gepts, W. & P. M. Lecompte (1981) The pancreatic islets in diabetes. *Am J Med*, 70, 105-15.
- Gittes, G. K. (2009) Developmental biology of the pancreas: a comprehensive review. *Dev Biol*, 326, 4-35.
- Goodner, C.J., Walike, B.C., Koerker, D.J., Ensink, J.W., Brown, A.C., Chideckel, E.W., Palmer, J. & Kalnasy, L. (1977) Insulin, glucagon, and glucose exhibit synchronous, sustained oscillations in fasting monkeys. *Science* 195 (4274), 177-179.
- Goyvaerts, L., K. Lemaire, I. Arijs, J. Auffret, M. Granvik, L. Van Lommel, N. Binart, P. in't Veld, F. Schuit & A. Schraenen (2015) Prolactin receptors and placental lactogen drive male mouse pancreatic islets to pregnancy-related mRNA changes. *PLoS One*, 10, e0121868.
- Greenwood, A. L., S. Li, K. Jones & D. A. Melton (2007) Notch signaling reveals developmental plasticity of Pax4(+) pancreatic endocrine progenitors and shunts them to a duct fate. *Mech Dev*, 124, 97-107.
- Gu, C., G. H. Stein, N. Pan, S. Goebbels, H. Hörnberg, K. A. Nave, P. Herrera, P. White, K. H. Kaestner, L. Sussel & J. E. Lee (2010) Pancreatic  $\beta$  cells require NeuroD to achieve and maintain functional maturity. *Cell Metab*, 11, 298-310.

- Gu, G., Dubauskaite, J., and Melton, D.A. (2002). Direct evidence for the pancreatic lineage: NGN3+ cells are islet progenitors and are distinct from duct progenitors. *Development* 129, 2447-2457.
- Guariguata, L., D. R. Whiting, I. Hambleton, J. Beagley, U. Linnenkamp & J. E. Shaw (2014) Global estimates of diabetes prevalence for 2013 and projections for 2035. *Diabetes Res Clin Pract*, 103, 137-49.
- Guillaume, M., S. Handgraaf, A. Fabre, I. Raymond-Letron, E. Riant, A. Montagner, A. Vinel, M. Buscato, N. Smirnova, C. Fontaine, H. Guillou, J. F. Arnal & P. Gourdy (2017) Selective Activation of Estrogen Receptor alpha Activation Function-1 Is Sufficient to Prevent Obesity, Steatosis, and Insulin Resistance in Mouse. *Am J Pathol*, 187, 1273-1287.
- Guo T, Wang W, Zhang H, Liu Y, Chen P, Ma K, et al. (2011) ISL1 Promotes Pancreatic Islet Cell Proliferation. *PLoS ONE* 6(8): e22387.
- Guo, C., Z. Zhang, P. Zhang, J. Makita, H. Kawada, K. Blessing & P. F. Kador (2014) Novel transgenic mouse models develop retinal changes associated with early diabetic retinopathy similar to those observed in rats with diabetes mellitus. *Exp Eye Res*, 119, 77-87.
- Gustavsson, N., Y. Lao, A. Maximov, J. C. Chuang, E. Kostromina, J. J. Repa, C. Li, G. K. Radda, T. C. Südhof & W. Han. 2008. Impaired insulin secretion and glucose intolerance in synaptotagmin-7 null mutant mice. In *Proc Natl Acad Sci U S A*, 3992-7.
- Gutierrez, G.D., Gromada, J., and Sussel, L. (2017). Heterogeneity of the Pancreatic Beta Cell. *Front Genet.* 8:22.

- Guz, Y., Montminy, M.R., Stein, R., Leonard, J., Gamer, L.W., Wright, C.V., and Teitelman, G. (1995). Expression of murine STF-1, a putative insulin gene transcription factor, in beta cells of pancreas, duodenal epithelium and pancreatic exocrine and endocrine progenitors during ontogeny. *Development* 121, 11-18.
- Halban, P. A., C. B. Wollheim, B. Blondel, P. Meda, E. N. Niesor & D. H. Mintz (1982) The possible importance of contact between pancreatic islet cells for the control of insulin release. *Endocrinology*, 111, 86-94.
- Hall, D. D., J. A. Feekes, A. S. Arachchige Don, M. Shi, J. Hamid, L. Chen, S. Strack, G. W. Zamponi, M. C. Horne & J. W. Hell (2006) Binding of protein phosphatase 2A to the L-type calcium channel Cav1.2 next to Ser1928, its main PKA site, is critical for Ser1928 dephosphorylation. *Biochemistry*, 45, 3448-59.
- Hang, Y. and Stein, R. (2011) MafA and MafB activity in pancreatic  $\beta$  cells. *Trends Endocrinol Metab.* 22(9): 364-373.
- Hansen, C. A., A. G. Schroering & J. D. Robishaw (1995) Subunit expression of signal transducing G proteins in cardiac tissue: implications for phospholipase C-beta regulation. *J Mol Cell Cardiol*, 27, 471-84.
- Hara, M., X. Wang, T. Kawamura, V. P. Bindokas, R. F. Dizon, S. Y. Alcoser, M. A. Magnuson & G. I. Bell (2003) Transgenic mice with green fluorescent protein-labeled pancreatic beta -cells. *Am J Physiol Endocrinol Metab*, 284, E177-83.
- Hatlapatka, K., Willenborg, M., and Rustenbeck, I. (2009). Plasma membrane depolarization as a determinant of the first phase of insulin secretion. *American journal of physiology Endocrinology and metabolism* 297, E315-322.

- Hell JW, Westenbroek RE, Warner C, Ahlijanian MK, Prystay W, Gilbert MM, Snutch TP, Catterall WA (1993) Identification and differential subcellular localization of the neuronal class C and class D L-type calcium channel  $\alpha 1$  subunits. *J Cell Biol* 123: 949–962
- Herrera, P. L., J. Huarte, F. Sanvito, P. Meda, L. Orci & J. D. Vassalli (1991) Embryogenesis of the murine endocrine pancreas; early expression of pancreatic polypeptide gene. *Development*, 113, 1257-65.
- Henderson, J.R., and Moss, M.C. (1985). A morphometric study of the endocrine and exocrine capillaries of the pancreas. *Q J Exp Physiol* 70, 347-356.
- Hesselbarth, N., C. Pettinelli, M. Gericke, C. Berger, A. Kunath, M. Stumvoll, M. Bluher & N. Kloting (2015) Tamoxifen affects glucose and lipid metabolism parameters, causes browning of subcutaneous adipose tissue and transient body composition changes in C57BL/6NTac mice. *Biochem Biophys Res Commun*, 464, 724-9.
- Hingorani, S.R., Petricoin, E.F., Maitra, A., Rajapakse, V., King, C., Jacobetz, M.A., Ross, S., Conrads, T.P., Veenstra, T.D., Hitt, B.A., *et al.* (2003). Preinvasive and invasive ductal pancreatic cancer and its early detection in the mouse. *Cancer cell* 4, 437-450.
- Hinoi, E., Gao, N., Jung, D.Y., Yadav, V., Yoshizawa, T., Myers, M.G., Jr., Chua, S.C., Jr., Kim, J.K., Kaestner, K.H., and Karsenty, G. (2008). The sympathetic tone mediates leptin's inhibition of insulin secretion by modulating osteocalcin bioactivity. *The Journal of cell biology* 183, 1235-1242.
- Hogan, M.F., and Hull, R.L. (2017). The islet endothelial cell: a novel contributor to beta cell secretory dysfunction in diabetes. *Diabetologia* 60, 952-959.

- Houtz, J., P. Borden, A. Ceasrine, L. Minichiello & R. Kuruvilla (2016) Neurotrophin Signaling Is Required for Glucose-Induced Insulin Secretion. *Dev Cell*, 39, 329-345.
- Huang, S. & Czech, M.P. (2007) The GLUT4 Glucose Transporter. *Cell Metabolism* 5(4), 237-252.
- Iversen, J. (1973) Adrenergic Receptors and the Secretion of Glucagon and Insulin from the Isolated, Perfused Canine Pancreas. *J Clin Invest*, 52, 2102-16.
- Jansson, L., and Hellerstrom, C. (1983). Stimulation by glucose of the blood flow to the pancreatic islets of the rat. *Diabetologia* 25, 45-50.
- Jing, X., D. Q. Li, C. S. Olofsson, A. Salehi, V. V. Surve, J. Caballero, R. Ivarsson, I. Lundquist, A. Pereverzev, T. Schneider, P. Rorsman & E. Renstrom (2005) CaV2.3 calcium channels control second-phase insulin release. *J Clin Invest*, 115, 146-54.
- Jo, J., G. Kilimnik, A. Kim, C. Guo, V. Periwal & M. Hara. 2011. Formation of Pancreatic Islets Involves Coordinated Expansion of Small Islets and Fission of Large Interconnected Islet-like Structures. In *Biophys J*, 565-74.
- Johansson, A., Lau, J., Sandberg, M., Borg, L.A., Magnusson, P.U., and Carlsson, P.O. (2009). Endothelial cell signalling supports pancreatic beta cell function in the rat. *Diabetologia* 52, 2385-2394.
- Johansson, M., Andersson, A., Carlsson, P.O., and Jansson, L. (2006a). Perinatal development of the pancreatic islet microvasculature in rats. *Journal of anatomy* 208, 191-196.

- Johansson, M., Mattsson, G., Andersson, A., Jansson, L., and Carlsson, P.O. (2006b). Islet endothelial cells and pancreatic beta-cell proliferation: studies in vitro and during pregnancy in adult rats. *Endocrinology* 147, 2315-2324.
- Johnson JH, Newgard CB, Milburn JL, Lodish HF, Thorens B (1990) The high  $K_m$  glucose transporter of islets of Langerhans is functionally similar to the low affinity transporter of liver and has identical primary sequence. *J Biol Chem* 265:6548–6551
- Jones ME, Thorburn AW, Britt KL, Hewitt KN, Wreford NG, Proietto J, Oz OK, Leury BJ, Robertson KM, Yao S, Simpson ER (2000) Aromatase-deficient (ArKO) mice have a phenotype of increased adiposity. *Proc Natl Acad Sci*, 97:12735–12740
- Jordan, V.C (2001) Selective Estrogen Receptor Modulation: A Personal Perspective. *Cancer Research*, 61, 5683-5687.
- Jordan, V.C (2006) Tamoxifen (ICI46,474) as a targeted therapy to treat and prevent breast cancer. *British Journal of Pharmacology*, 147, S269-S276.
- Kaido, T., Yebra, M., Cirulli, V., and Montgomery, A.M. (2004). Regulation of human beta-cell adhesion, motility, and insulin secretion by collagen IV and its receptor alpha1beta1. *The Journal of biological chemistry* 279, 53762-53769.
- Kajimura, D., Hinoi, E., Ferron, M., Kode, A., Riley, K.J., Zhou, B., Guo, X.E., and Karsenty, G. (2011). Genetic determination of the cellular basis of the sympathetic regulation of bone mass accrual. *J Exp Med* 208, 841-851.
- Kang et al., 2010 L. Kang, X. Zhang, Y. Xie, Y. Tu, D. Wang, Z. Liu, Z.Y. (2010) Wang Involvement of estrogen receptor variant ER-alpha36, not GPR30, in nongenomic estrogen signaling *Mol. Endocrinol.*, 24, 709-721



- Kautzky-Willer, A., Harreiter, J., and Pacini, G. (2016). Sex and Gender Differences in Risk, Pathophysiology and Complications of Type 2 Diabetes Mellitus. *Endocrine reviews* 37, 278-316.
- Kim, J., Oh, W.J., Gaiano, N., Yoshida, Y., and Gu, C. (2011). Semaphorin 3E-Plexin-D1 signaling regulates VEGF function in developmental angiogenesis via a feedback mechanism. *Genes & development* 25, 1399-1411.
- Klein, S. L., L. Schiebinger, M. L. Stefanick, L. Cahill, J. Danska, G. J. d. Vries, M. R. Kibbe, M. M. McCarthy, J. S. Mogil, T. K. Woodruff & I. Zucker (2015) Opinion: Sex inclusion in basic research drives discovery.
- Konstantinova, I. & E. Lammert (2004) Microvascular development: learning from pancreatic islets. *Bioessays*, 26, 1069-75.
- Konstantinova, I., G. Nikolova, M. Ohara-Imaizumi, P. Meda, T. Kucera, K. Zarbalis, W. Wurst, S. Nagamatsu & E. Lammert (2007) EphA-Ephrin-A-mediated beta cell communication regulates insulin secretion from pancreatic islets. *Cell*, 129, 359-70.
- Lacey, R. J., N. S. Berrow, N. J. London, S. P. Lake, R. F. James, J. H. Scarpello & N. G. Morgan (1990) Differential effects of beta-adrenergic agonists on insulin secretion from pancreatic islets isolated from rat and man. *J Mol Endocrinol*, 5, 49-54.
- Lacey, R. J., N. S. Berrow, J. H. Scarpello & N. G. Morgan (1991) Selective stimulation of glucagon secretion by beta 2-adrenoceptors in isolated islets of Langerhans of the rat. *Br J Pharmacol*, 103, 1824-8.
- Lacey, R.J., Cable, H.C., James, R.F., London, N.J., Scarpello, J.H., and Morgan, N.G. (1993). Concentration-dependent effects of adrenaline on the profile of insulin

secretion from isolated human islets of Langerhans. *The Journal of endocrinology* 138, 555-563.

Laughlin, M. R. (2014) Normal roles for dietary fructose in carbohydrate metabolism. *Nutrients*, 6, 3117-29.

Lavine, J.A., Kibbe, C.R., Baan, M., Sirinvaravong, S., Umhoefer, H.M., Engler, K.A., Meske, L.M., Sacotte, K.A., Erhardt, D.P., and Davis, D.B. (2015) Cholecystokinin expression in the  $\beta$ -cell leads to increased  $\beta$ -cell area in aged mice and protects from streptozotocin-induced diabetes and apoptosis. *Am J Physiol Endocrinol Metab*, 309(10), E819-28.

Lee, J.S., Jang, D.J., Lee, N., Ko, H.G., Kim, H., Kim, Y.S., Kim, B., Son, J., Kim, S.H., Chung, H., *et al.* (2009). Induction of neuronal vascular endothelial growth factor expression by cAMP in the dentate gyrus of the hippocampus is required for antidepressant-like behaviors. *The Journal of neuroscience : the official journal of the Society for Neuroscience* 29, 8493-8505.

Li, X., Zhang, L., Meshinchi, S., Dias-Leme, C., Raffin, D., Johnson, J.D., Treutelaar, M.K., and Burant, C.F. (2006). Islet microvasculature in islet hyperplasia and failure in a model of type 2 diabetes. *Diabetes* 55, 2965-2973.

Lima, J. J., H. Feng, L. Duckworth, J. Wang, J. E. Sylvester, N. Kissoon & H. Garg (2007) Association analyses of adrenergic receptor polymorphisms with obesity and metabolic alterations. *Metabolism*, 56, 757-65.

Liu, S., G. Kilic, M. S. Meyers, G. Navarro, Y. Wang, J. Oberholzer & F. Mauvais-Jarvis (2013) Oestrogens improve human pancreatic islet transplantation in a mouse model of insulin deficient diabetes. *Diabetologia*, 56, 370-81.

- Liu, S., Le May, C., Wong, W. P., Ward, R. D., Clegg, D. J., Marcelli, M., Korach, K. S., and Mauvais-Jarvis, F. (2009) Importance of extranuclear estrogen receptor-alpha and membrane G protein-coupled estrogen receptor in pancreatic islet survival. *Diabetes* 58, 2292-2302
- MacDonald, P.E., Joseph, J.W., and Rorsman, P. (2005). Glucose-sensing mechanisms in pancreatic beta-cells. *Philosophical transactions of the Royal Society of London Series B, Biological sciences* 360, 2211-2225.
- Magenheim, J., O. Ilovich, A. Lazarus, A. Klochender, O. Ziv, R. Werman, A. Hija, O. Cleaver, E. Mishani, E. Keshet & Y. Dor (2011) Blood vessels restrain pancreas branching, differentiation and growth. *Development*, 138, 4743-52.
- Manrique C, Lastra G, Habibi J, Mugerfeld I, Garro M, Sowers JR. Loss of estrogen receptor alpha signaling leads to insulin resistance and obesity in young and adult female mice. *Cardiorenal Med* (2012) 2(3):200–10
- Marchese, E., Rodeghier, C., Monson, R.S., McCracken, B., Shi, T., Schrock, W. *et al.* (2015) Enumerating beta-cells in whole human islets: sex differences and associations with clinical outcomes after islet transplantation. *Diabetes Care*, 38 (11), e176–7
- Marchetti, B., Morale, M.C., Paradis, P., and Bouvier, M. (1994). Characterization, expression, and hormonal control of a thymic beta 2-adrenergic receptor. *The American journal of physiology* 267, E718-731.

- Masuo, K., T. Katsuya, Y. Fu, H. Rakugi, T. Ogihara & M. L. Tuck (2005) Beta2- and beta3-adrenergic receptor polymorphisms are related to the onset of weight gain and blood pressure elevation over 5 years. *Circulation*, 111, 3429-34.
- Matsumoto, M., Miki, T., Shibasaki, T., Kawaguchi, M., Shinozaki, H., Nio, J., Saraya, A., Koseki, H., Miyazaki, M., Iwanaga, T., *et al.* (2004). Noc2 is essential in normal regulation of exocytosis in endocrine and exocrine cells. *Proceedings of the National Academy of Sciences of the United States of America* 101, 8313-8318.
- Matsunaga, K., Taoka, M., Isobe, T., and Izumi, T. (2017). Rab2a and Rab27a cooperatively regulate the transition from granule maturation to exocytosis through the dual effector Noc2. *Journal of cell science* 130, 541-550.
- Mauvais-Jarvis, F. (2015) Sex differences in metabolic homeostasis, diabetes, and obesity. *Biol Sex Differ*, 6, 14.
- McCarthy, M.M., Arnold, A.P., Ball, G.F., Blaustein, J.D., and De Vries, G.J. (2012). Sex differences in the brain: the not so inconvenient truth. *The Journal of neuroscience : the official journal of the Society for Neuroscience* 32, 2241-2247.
- Miki, T., K. Minami, H. Shinozaki, K. Matsumura, A. Saraya, H. Ikeda, Y. Yamada, J. J. Holst & S. Seino (2005) Distinct effects of glucose-dependent insulinotropic polypeptide and glucagon-like peptide-1 on insulin secretion and gut motility. *Diabetes*, 54, 1056-63.
- Mizuno, K., T. Fujita, H. Gomi & T. Izumi (2016) Granophilin exclusively mediates functional granule docking to the plasma membrane. *Sci Rep*, 6, 23909.
- Molinoff, P.B. (1984). Alpha- and beta-adrenergic receptor subtypes properties, distribution and regulation. *Drugs* 28 Suppl 2, 1-15.

- Motulsky HJ, Michel MC. Neuropeptide Y mobilizes Ca<sup>2+</sup> and inhibits adenylate cyclase in human erythroleukemia cells. *Am J Physiol.* 1988;255:E880–885.
- Mukouyama, Y. S., D. Shin, S. Britsch, M. Taniguchi & D. J. Anderson (2002) Sensory nerves determine the pattern of arterial differentiation and blood vessel branching in the skin. *Cell*, 109, 693-705.
- Murakami, T., T. Miyake, M. Tsubouchi, Y. Tsubouchi, A. Ohtsuka & T. Fujita (1997) Blood flow patterns in the rat pancreas: a simulative demonstration by injection replication and scanning electron microscopy. *Microsc Res Tech*, 37, 497-508.
- Murtaugh, L. C. (2007) Pancreas and beta-cell development: from the actual to the possible. *Development*, 134, 427-38.
- Navarro, G., W. Xu, D. A. Jacobson, B. Wicksteed, C. Allard, G. Zhang, K. De Gendt, S. H. Kim, H. Wu, H. Zhang, G. Verhoeven, J. A. Katzenellenbogen & F. Mauvais-Jarvis (2016) Extranuclear Actions of the Androgen Receptor Enhance Glucose-Stimulated Insulin Secretion in the Male. *Cell Metab*, 23, 837-51.
- Nelson, D. L. & M. M. Cox. 2008. *Lehninger Principles of Biochemistry*.
- Nevins A.K, Thurmond D.C. 2003. Glucose regulates the cortical actin network through modulation of Cdc42 cycling to stimulate insulin secretion. *Am. J. Physiol. Cell Physiol.* 285:C698–C710.
- Nikolova, G., Jabs, N., Konstantinova, I., Domogatskaya, A., Tryggvason, K., Sorokin, L., Fassler, R., Gu, G., Gerber, H.P., Ferrara, N., *et al.* (2006). The vascular basement membrane: a niche for insulin gene expression and Beta cell proliferation. *Developmental cell* 10, 397-405.

- Nikolova, G., Strilic, B., and Lammert, E. (2007). The vascular niche and its basement membrane. *Trends in cell biology* 17, 19-25.
- Obermüller S, Calegari F, King A, Lindqvist A, Lundquist I, Salehi A, et al. (2010) Defective Secretion of Islet Hormones in Chromogranin-B Deficient Mice. *PLoS ONE* 5(1): e8936
- Olerud, J., Mokhtari, D., Johansson, M., Christoffersson, G., Lawler, J., Welsh, N., and Carlsson, P.O. (2011). Thrombospondin-1: an islet endothelial cell signal of importance for beta-cell function. *Diabetes* 60, 1946-1954.
- Olofsson, C. S., S. O. Gopel, S. Barg, J. Galvanovskis, X. Ma, A. Salehi, P. Rorsman & L. Eliasson (2002) Fast insulin secretion reflects exocytosis of docked granules in mouse pancreatic B-cells. *Pflugers Arch*, 444, 43-51.
- Olofsson, C. S., J. Hakansson, A. Salehi, M. Bengtsson, J. Galvanovskis, C. Partridge, M. SorhedeWinzell, X. Xian, L. Eliasson, I. Lundquist, H. Semb & P. Rorsman (2009) Impaired insulin exocytosis in neural cell adhesion molecule-/- mice due to defective reorganization of the submembrane F-actin network. *Endocrinology*, 150, 3067-75.
- Palmer, B. F. & D. J. Clegg (2015) The sexual dimorphism of obesity. *Mol Cell Endocrinol*, 402, 113-9.
- Parati, G., and Esler, M. (2012). The human sympathetic nervous system: its relevance in hypertension and heart failure. *European heart journal* 33, 1058-1066.
- Park CJ, Zhao Z, Glidewell-Kenney C, et al. Genetic rescue of nonclassical ER $\alpha$  signaling normalizes energy balance in obese Era-null mutant mice. *Journal of Clinical Investigation*. 2011;121(2):604–612.

- Park, H. S., E. S. Shin & J. E. Lee (2008) Genotypes and haplotypes of beta2-adrenergic receptor and parameters of the metabolic syndrome in Korean adolescents. *Metabolism*, 57, 1064-70.
- Parton, R.G., and Simons, K. (2007). The multiple faces of caveolae. *Nature reviews Molecular cell biology* 8, 185-194.
- Patriarchi, T., H. Qian, V. Di Biase, Z. A. Malik, D. Chowdhury, J. L. Price, E. A. Hammes, O. R. Buonarati, R. E. Westenbroek, W. A. Catterall, F. Hofmann, Y. K. Xiang, G. G. Murphy, C. Chen, M. F. Navedo & J. W. Hell. 2016. Phosphorylation of Cav1.2 on S1928 uncouples the L-type Ca<sup>2+</sup> channel from the  $\beta$ 2 adrenergic receptor. In *EMBO J*, 1330-45.
- Peters, S.A., Huxley, R.R., Sattar, N., and Woodward, M. (2015). Sex Differences in the Excess Risk of Cardiovascular Diseases Associated with Type 2 Diabetes: Potential Explanations and Clinical Implications. *Current cardiovascular risk reports* 9, 36.
- Perez, Dianne M. (2006). The adrenergic receptors in the 21st century. Totowa, New Jersey: Humana Press. pp. 54, 129–134.
- Pierreux, C. E., S. Cordi, A. C. Hick, Y. Achouri, C. Ruiz de Almodovar, P. P. Prevot, P. J. Courtoy, P. Carmeliet & F. P. Lemaigre (2010) Epithelial: Endothelial cross-talk regulates exocrine differentiation in developing pancreas. *Dev Biol*, 347, 216-27.
- Pollreisz, A. & U. Schmidt-Erfurth (2010) Diabetic Cataract—Pathogenesis, Epidemiology and Treatment. *Journal of Ophthalmology*, 2010, 8.
- Qiu, W., Zhang, Y., Feng, Y., Li, L., Yang, L., & Xu, C. (2017) Deciphering Pancreatic Islet  $\beta$  cell and  $\alpha$  cell maturation pathways and characteristic features and the single-cell level. *Cell Metabolism*. 25, 1194-1205.

- Reinert, R.B., Brissova, M., Shostak, A., Pan, F.C., Poffenberger, G., Cai, Q., Hundemer, G.L., Kantz, J., Thompson, C.S., Dai, C., *et al.* (2013). Vascular endothelial growth factor- $\alpha$  and islet vascularization are necessary in developing, but not adult, pancreatic islets. *Diabetes* 62, 4154-4164.
- Reinert, R.B., Cai, Q., Hong, J.Y., Plank, J.L., Aamodt, K., Prasad, N., Aramandla, R., Dai, C., Levy, S.E., Pozzi, A., *et al.* (2014). Vascular endothelial growth factor coordinates islet innervation via vascular scaffolding. *Development* 141, 1480-1491.
- Ribas V, Drew BG, Le JA, et al. Myeloid-specific estrogen receptor  $\alpha$  deficiency impairs metabolic homeostasis and accelerates atherosclerotic lesion development. *Proc Natl Acad Sci USA*. 2011;108:16457–16462.
- Ribes, G., D. Hillaire-Buys, R. Gross, J. P. Blayac & M. M. Loubatieres-Mariani (1989) Involvement of a central nervous pathway in yohimbine-induced insulin secretion. *Eur J Pharmacol*, 162, 207-14.
- Rocheleau, J. V., M. S. Remedi, B. Granada, W. S. Head, J. C. Koster, C. G. Nichols & D. W. Piston (2006) Critical role of gap junction coupled KATP channel activity for regulated insulin secretion. *PLoS Biol*, 4, e26.
- Rogers, W. A. & A. J. Ballantyne (2008) Exclusion of women from clinical research: myth or reality? *Mayo Clin Proc*, 83, 536-42.
- Rorsman, P., and Ashcroft, F.M. (2018). Pancreatic beta-Cell Electrical Activity and Insulin Secretion: Of Mice and Men. *Physiological reviews* 98, 117-214.



- Rybin, V. O., E. Pak, S. Alcott & S. F. Steinberg (2003) Developmental changes in beta2-adrenergic receptor signaling in ventricular myocytes: the role of Gi proteins and caveolae microdomains. *Mol Pharmacol*, 63, 1338-48.
- Sand, F. W., A. Hornblad, J. K. Johansson, C. Loren, J. Edsbacke, A. Stahlberg, J. Magenheimer, O. Ilovich, E. Mishani, Y. Dor, U. Ahlgren & H. Semb (2011) Growth-limiting role of endothelial cells in endoderm development. *Dev Biol*, 352, 267-77.
- Santulli, G., A. Lombardi, D. Sorriento, A. Anastasio, C. Del Giudice, P. Formisano, F. Beguinot, B. Trimarco, C. Miele & G. Iaccarino (2012) Age-related impairment in insulin release: the essential role of beta(2)-adrenergic receptor. *Diabetes*, 61, 692-701.
- Sasson, S. and Notides, A.C (1988) Mechanism of the estrogen receptor interaction with 4-hydroxytamoxifen. *Mol Endocrinology*, 4, 307-312.
- Scaglia, L., F. E. Smith & S. Bonner-Weir (1995) Apoptosis contributes to the involution of beta cell mass in the post partum rat pancreas. *Endocrinology*, 136, 5461-8.
- Schulla, V., E. Renstrom, R. Feil, S. Feil, I. Franklin, A. Gjinovci, X. J. Jing, D. Laux, I. Lundquist, M. A. Magnuson, S. Obermuller, C. S. Olofsson, A. Salehi, A. Wendt, N. Klugbauer, C. B. Wollheim, P. Rorsman & F. Hofmann (2003) Impaired insulin secretion and glucose tolerance in beta cell-selective Ca(v)1.2 Ca<sup>2+</sup> channel null mice. *Embo j*, 22, 3844-54.
- Sharma, A.M., Pischon, T., Engeli, S., and Scholze, J. (2001). Choice of drug treatment for obesity-related hypertension: where is the evidence? *Journal of hypertension* 19, 667-674.

- Shen, Q., S. K. Goderie, L. Jin, N. Karanth, Y. Sun, N. Abramova, P. Vincent, K. Pumiglia & S. Temple (2004) Endothelial cells stimulate self-renewal and expand neurogenesis of neural stem cells. *Science*, 304, 1338-40.
- Shibasaki, T., Sunaga, Y., and Seino, S. (2004). Integration of ATP, cAMP, and Ca<sup>2+</sup> signals in insulin granule exocytosis. *Diabetes 53 Suppl 3*, S59-62.
- Shulman, G. I. (2014) Ectopic fat in insulin resistance, dyslipidemia, and cardiometabolic disease. *N Engl J Med*, 371, 1131-41.
- Simpson, E.R., Misso, M., Hewitt, K.N., Hill, R.A., Boon, W.C., Jones, M.E., Kovacic, A., Zhou, J., & Clyne, C.D (2005) Estrogen - the good, the bad, and the unexpected. *Endocr Rev*, 26(3), 322-30.
- Skoglund, G., I. Lundquist & B. Ahren (1987) Alpha 1- and alpha 2-adrenoceptor activation increases plasma glucagon levels in the mouse. *Eur J Pharmacol*, 143, 83-8.
- Song, J., Xu, Y., Hu, X., Choi, B., and Tong, Q. (2010). Brain expression of Cre recombinase driven by pancreas-specific promoters. *Genesis* 48, 628-634.
- Sorenson, R. L. & T. C. Brelje (1997) Adaptation of islets of Langerhans to pregnancy: beta-cell growth, enhanced insulin secretion and the role of lactogenic hormones. *Horm Metab Res*, 29, 301-7.
- Soriano S, Ropero AB, Alonso-Magdalena P, et al. Rapid regulation of K(ATP) channel activity by 17beta-estradiol in pancreatic beta-cells involves the estrogen receptor beta and the atrial natriuretic peptide receptor. *Mol Endocrinol* 2009;23:1973–1982
- Steiner, D. J., A. Kim, K. Miller & M. Hara (2010) Pancreatic islet plasticity: interspecies comparison of islet architecture and composition. *Islets*, 2, 135-45.

- Tanko, L. B., Y. Z. Bagger, P. Alexandersen, P. J. Larsen & C. Christiansen (2003) Central and peripheral fat mass have contrasting effect on the progression of aortic calcification in postmenopausal women. *Eur Heart J*, 24, 1531-7.
- Thorens B, Sarkar HK, Kaback HR, Lodish HF (1988) Cloning and functional expression in bacteria of a novel glucose transporter present in liver, intestine, kidney, and beta-pancreatic islet cells. *Cell* 55:281–290
- Tomas, A., B. Yermen, L. Min, J. E. Pessin & P. A. Halban (2006) Regulation of pancreatic beta-cell insulin secretion by actin cytoskeleton remodelling: role of gelsolin and cooperation with the MAPK signalling pathway. *J Cell Sci*, 119, 2156-67.
- Tozzi, M. G., M. Camici, L. Mascia, F. Sgarrella & P. L. Ipata (2006) Pentose phosphates in nucleoside interconversion and catabolism. *Febs j*, 273, 1089-101.
- Van Pelt, R. E., E. M. Evans, K. B. Schechtman, A. A. Ehsani & W. M. Kohrt (2002) Contributions of total and regional fat mass to risk for cardiovascular disease in older women. *Am J Physiol Endocrinol Metab*, 282, E1023-8.
- Varlamov, O., Bethea, C.L., and Roberts, C.T., Jr. (2014). Sex-specific differences in lipid and glucose metabolism. *Frontiers in endocrinology* 5, 241.
- Vetterlein, F., A. Petho & G. Schmidt (1987) Morphometric investigation of the microvascular system of pancreatic exocrine and endocrine tissue in the rat. *Microvasc Res*, 34, 231-8.
- Wade, G. N. & H. W. Heller (1993) Tamoxifen mimics the effects of estradiol on food intake, body weight, and body composition in rats. *Am J Physiol*, 264, R1219-23.

- Wamelink, M. M., E. A. Struys & C. Jakobs (2008) The biochemistry, metabolism and inherited defects of the pentose phosphate pathway: a review. *J Inherit Metab Dis*, 31, 703-17.
- Wang, Q. A., C. Tao, R. K. Gupta & P. E. Scherer (2013) Tracking adipogenesis during white adipose tissue development, expansion and regeneration. *Nat Med*, 19, 1338-44.
- Wenzel-Seifert, K. & R. Seifert (2000) Molecular analysis of beta(2)-adrenoceptor coupling to G(s)-, G(i)-, and G(q)-proteins. *Mol Pharmacol*, 58, 954-66.
- Wheeler, M.B., Sheu, L., Ghai, M., Bouquillon, A., Grondin, G., Weller, U., Beaudoin, A.R., Bennett, M.K., Trimble, W.S., and Gaisano, H.Y. (1996). Characterization of SNARE protein expression in beta cell lines and pancreatic islets. *Endocrinology* 137, 1340-1348.
- Wong WP, Tiano JP, Liu S, Hewitt SC, Le May C, Katzenellenbogen JA, Katzenellenbogen BS, Korach KS, Mauvais-Jarvis F (2010). Extranuclear estrogen receptor- $\alpha$  stimulates NeuroD1 binding to the insulin promoter and favors insulin synthesis. *Proc Natl Acad Sci USA* 107, 13057-13062
- Wu, D., Zhau, H.E., Huang, W.C., Iqbal, S., Habib, F.K., Sartor, O., Cvitanovic, L., Marshall, F.F., Xu, Z., and Chung, L.W. (2007). cAMP-responsive element-binding protein regulates vascular endothelial growth factor expression: implication in human prostate cancer bone metastasis. *Oncogene* 26, 5070-5077.
- Xiao, C., J. Hsieh, K. Adeli & G. F. Lewis (2011) Gut-liver interaction in triglyceride-rich lipoprotein metabolism. *Am J Physiol Endocrinol Metab*, 301, E429-46.

- Xu, W., T. Niu, B. Xu, G. Navarro, M. J. Schipma & F. Mauvais-Jarvis (2017) Androgen receptor-deficient islet beta-cells exhibit alteration in genetic markers of insulin secretion and inflammation. A transcriptome analysis in the male mouse. *J Diabetes Complications*, 31, 787-795.
- Xu Y, Nedungadi TP, Zhu L, Sobhani N, Irani BG, Davis KE, Zhang X, Zou F, Gent LM, Hahner LD, Khan SA, Elias CF, Elmquist JK, Clegg DJ. Distinct hypothalamic neurons mediate estrogenic effects on energy homeostasis and reproduction. *Cell metabolism*. 2011;14:453–65.
- Yang, S. N., O. Larsson, R. Branstrom, A. M. Bertorello, B. Leibiger, I. B. Leibiger, T. Moede, M. Kohler, B. Meister & P. O. Berggren (1999) Syntaxin 1 interacts with the L(D) subtype of voltage-gated Ca(2+) channels in pancreatic beta cells. *Proc Natl Acad Sci U S A*, 96, 10164-9.
- Yao, Q., Wang, B., An, X., Zhang, J., and Ding, L. (2018) Testosterone level and risk of type 2 diabetes in men: a systematic review and meta-analysis. *Endocr Connect*, 7(1), 220-231.
- Yie, S.M., and Brown, G.M. (1995). Effects of sex hormones on the pineal response to isoproterenol and on pineal beta-adrenergic receptors. *Neuroendocrinology* 62, 93-100.
- Yu, I. C., H. Y. Lin, N. C. Liu, J. D. Sparks, S. Yeh, L. Y. Fang, L. Chen & C. Chang (2013) Neuronal androgen receptor regulates insulin sensitivity via suppression of hypothalamic NF-kappaB-mediated PTP1B expression. *Diabetes*, 62, 411-23.

Zhang, M., P. Goforth, R. Bertram, A. Sherman & L. Satin (2003) The  $\text{Ca}^{2+}$  dynamics of isolated mouse beta-cells and islets: implications for mathematical models. *Biophys J*, 84, 2852-70.

# ALEXIS M. CEASRINE

Phone: (401) 741-0969  
aceasrine@gmail.com

## EDUCATION

---

- PhD** Johns Hopkins University October 2018  
Cell, Molecular, Developmental Biology and Biophysics (CMDB)  
Dissertation: “Adrenergic Signaling in Pancreatic Islet Development”  
Advisor: Dr. Rejji Kuruvilla
- BS** Hofstra University, Cell and Molecular Biology May 2013  
GPA 3.78/4.0  
Minor in Forensic Science

## RESEARCH EXPERIENCE

---

- Dissertation**, Johns Hopkins University, Baltimore, MD 2013 to 2018
- Hofstra University**, Hempstead, NY 2011 to 2013  
**Undergraduate Research Assistant**  
Molecular Biology, Dr. Maureen Krauss
- National Institute of Standard and Technology (NIST)**, Gaithersburg, MD 2012  
**Department of Homeland Security (DHS) Guest Researcher**  
Chemistry, Dr. Pamela Chu

## HONORS AND AWARDS

---

- Keystone Symposia Scholarship** 2017  
Research-based scholarship to attend “Sex and Gender Factors  
Affecting Metabolic Homeostasis, Diabetes, and Obesity” Keystone  
Conference
- Best Poster Award** 2016  
Research and presentation-based poster award at  
Johns Hopkins University Biology Department Retreat
- Victor Corces Teaching Award** 2015  
Undergraduate Cell Biology Lab

## PUBLICATIONS

---

**Ceasrine, A.M.**, Ruiz-Otero, N., Lin, E.E., Lumelsky, D.N., Boehm, E.D., Kuruvilla, R. Tamoxifen improves glucose tolerance in a delivery, sex, and strain-dependent manner in mice. *Endocrinology*. 2019 Feb.

**Ceasrine, A.M.**, Lin, E.E., Lumelsky, D.N., Iyer, R., Kuruvilla R. *Adrb2* controls glucose homeostasis by developmental regulation of pancreatic islet vasculature. *Elife*. 2018 Oct 10;7.

Leung, W ... DiAngelo, J.R., ... **Ceasrine, A.M.**, ... Elgin, S.C.R. Retrotransposons are the major contributors to the expansion of the *Drosophila ananassae* Muller F element. *G3: Genes|Genomes|Genetics*. (This paper from the Genomics Education Partnership has 272 co-authors; 237 of them participated as students.) 2017;7(8):2439-2460.

Houtz, J., Borden, P., **Ceasrine, A.**, Minichiello, L., Kuruvilla, R. Neurotrophin Signaling Is Required for Glucose-Induced Insulin Secretion. *Dev Cell*. 2016 Nov 7;39(3):329-345. *Image chosen for cover of this issue.*

Wang, G., Rajpurohit, S.K., Delaspre, F., Walker, S.L., White, D.T., **Ceasrine, A.**, Kuruvilla, R., Li, R.J., Shim, J.S., Liu, J.O., Parsons, M.J., Mumm, J.S. First quantitative high-throughput screen in zebrafish identifies novel pathways for increasing pancreatic  $\beta$ -cell mass. *Elife*. 2015 Jul 28;4.

Otis, J.P., Zeituni, E.M., Thierer, J.H., Anderson, J.L., Brown, A.C., Boehm, E.D., Cerchione, D.M., **Ceasrine, A.M.**, Avraham-Davidi, I., Tempelhof, H., Yaniv, K., Farber, S.A.. Zebrafish as a model for apolipoprotein biology: comprehensive expression analysis and a role for ApoA-IV in regulating food intake. *Dis Model Mech*. 2015 Mar;8(3):295-309.

## CONFERENCES

---

**Ceasrine, A.M.**, Lin, E.E., Lumelsky, D., and Kuruvilla, R. Adrenergic Signaling in the Developing Pancreas. Oral presentation at Johns Hopkins University CMDB Retreat, 2017.

**Ceasrine, A.M.**, Lin, E.E., Lumelsky, D., and Kuruvilla, R. Developmental  $\beta$ -adrenergic signaling is essential for islet vascularization and function. Poster presentation at Keystone Symposium for Sex and Gender Factors Affecting Metabolic Homeostasis, Diabetes and Obesity, 2017.

**Ceasrine, A.M.**, Lin, E.E., Lumelsky, D., and Kuruvilla, R. Developmental  $\beta$ -adrenergic signaling is essential for islet vascularization and function. Poster presentation at Johns Hopkins University CMDB Retreat, 2016.

**Ceasrine, AM**, Miller, J.S., Dreslinkski, T., Krause, M.K., and Lefurgy, S.T. Molecular Genetic Basis for the Octopine Dehydrogenase Polymorphism in Atlantic Bay Scallops *Argopecten irradians*. Poster presentation at the Aquaculture 2013 Conference.



## PROFESSIONAL SERVICE

---

### Peer-Reviewed Articles for:

- Scientific Reports

## TEACHING AND MENTORING EXPERIENCE

---

### Teaching

#### Johns Hopkins University, Baltimore, MD

**Teaching Assistant**, Graduate Developmental Biology 2017 and 2018

**Tutor**, Graduate Developmental Biology 2018

**Teaching Assistant**, Undergraduate Biology lecture and lab courses 2015-2017

**Teaching Assistant**, High-school/incoming students Summer 2016

#### Hofstra University, Hempstead, NY

**Tutor**, Cell Biology 2012

**Teaching Assistant**, Undergraduate Cell Biology and Genetics 2011

### Mentoring

#### Students Advised

Nelmari Ruiz Otero\*, Ph.D. Candidate, Fall 2015

Haolong Zhu, Ph.D. Candidate, Fall 2018

Joselyn Yamamoto, Ph.D. Candidate, Winter 2019

David Lumelsky\*, Undergraduate Biology Major, 2016-2018

Chinar Berry, Undergraduate Biology Major, 2015-2016

Joan Ndungu, Research Experience for Undergraduates (REU) student, Summer 2017

Carlea Williams-Locks, NIDDK STEP-UP High School Student, Summer 2016

Radhika Iyer\*, High School Student, Summer 2016

\*co-author on one or more manuscripts

## SERVICE

---

**Biology Graduate Class of 2013 Representative**, Johns Hopkins University  
2013-2018

**Mentoring to Inspire Diversity in Science (MInDS) Mentor**  
2015, 2017, 2018

**STEM Achievement in Baltimore Elementary Schools (SABES) Mentor**  
2017

**BioEYES volunteer**, USA Science & Engineering Festival  
2014, 2016

## REFERENCES

---

1. **Rejji Kuruvilla, Ph.D.** – Thesis Advisor  
Associate Professor of Biology  
Department of Biology  
Johns Hopkins University  
Phone: (410) 516-2366  
E-mail: [rkuruvilla@jhu.edu](mailto:rkuruvilla@jhu.edu)
2. **Samer Hattar, Ph.D.** – Thesis committee member  
Senior Investigator and Chief of the Section on Light and Circadian Rhythms  
National Institute of Mental Health  
Phone: (301) 435-1887  
E-mail: [samer.hattar@nih.gov](mailto:samer.hattar@nih.gov)
3. **Michael Parsons, Ph.D.** – Thesis committee member  
Associate Professor of Developmental and Cell Biology  
Department of Developmental and Cell Biology  
University of California Irvine  
Phone: (949) 824-8728  
E-mail: [mparson1@uci.edu](mailto:mparson1@uci.edu)
4. **Mark Van Doren, Ph.D.** – Thesis committee member  
Professor of Biology  
Department of Biology  
Johns Hopkins University  
Phone: (410) 516-4830  
E-mail: [vandoren@jhu.edu](mailto:vandoren@jhu.edu)